12-2015

# Normal Glycolytic Enzyme Activity is Critical for Hypoxia Inducible Factor-1a Activity and Provides Novel Targets for Inhibiting Tumor Growth

Geoffrey Grandjean PhD

# NORMAL GLYCOLYTIC ENZYME ACTIVITY IS CRITICAL FOR HYPOXIA INDUCIBLE FACTOR-1α ACTIVITY AND PROVIDES NOVEL TARGETS FOR INHIBITING TUMOR GROWTH

A

DISSERTATION

Presented to the Faculty of

The University of Texas

Health Science Center at Houston

and

The University of Texas

M. D. Anderson Cancer Center

Graduate School of Biomedical Sciences

in Partial Fulfillment

of the Requirements

for the Degree of

DOCTOR OF PHILOSOPHY

By

Geoffrey Grandjean B.S.

December 2015

**Acknowledgements**

Many thanks to all of the members of the Powis Lab through the years who have taught me and helped to shape me as a scientist. To members of both my advisory and supervisory committees for their insight and input into this project as well as the hardworking scientists and physicians of both the University of Texas MD Anderson Cancer Center and the Sanford Burnham Prebys Medical Discovery Institute.

Normal Glycolytic Enzyme Activity is Critical for Hypoxia Inducible Factor-1α Activity and Provides Novel Targets for Inhibiting Tumor Growth

By Geoffrey Grandjean

Advisory Professor: Garth Powis, D. Phil

Unique to proliferating cancer cells is the observation that their increased need for energy is provided by a high rate of glycolysis followed by lactic acid fermentation in a process known as the Warburg Effect, a process many times less efficient than oxidative phosphorylation employed by normal cells to satisfy a similar energy demand [1]. This high rate of glycolysis occurs regardless of the concentration of oxygen in the cell and is typically at rates significantly higher than those found in normal cells of the same tissue type. Unlike the case of proliferating cancer cells in culture, the internal environment of most solid tumors is hypoxic due to an inadequate or disorganized blood supply leading to even greater increases in glycolytic rates and, therefore, lactic acid production [2]. The regulation of glycolytic enzyme expression by the hypoxia-inducible factor 1 alpha (HIF-1α) transcription factor in states of low oxygen stress is a well described phenomenon [3, 4]. Through the use of a high throughput siRNA screen using an siRNA library targeting all the known open reading frames of the human genome (Dharmacon, Inc.), novel regulators of HIF-1α were identified including many enzymes involved in the glycolytic pathway. Here, I describe a novel relationship between glycolysis and its regulation of HIF-1α activity. Our studies have shown that of the 40 enzymes of glycolysis involving 11 enzymatic steps and various enzyme isoforms, siRNA knockdown of Aldolase A (ALDOA) produces the maximum inhibition of HIF-1α activity *in vitro* – a finding that I have subsequently confirmed in a murine *in vivo* model. Further study indicated that this is mediated through a mechanism involving AMPK, a sensor of low ATP levels, and the subsequent dissociation of HIF-1α and p300, a critical co-activator of HIF-1α. ALDOA was chosen as the molecular target

for a drug discovery effort because it produced maximum inhibition of cancer growth and would serve as a dual glycolysis and HIF-1α inhibitor, thus blocking two important cancer cell survival mechanisms at the same time.

Tumor hypoxia is a pervasive problem in regards to treatment options as hypoxic tumor cells are resistant to traditional chemo and radiotherapies. Thus, the overreaching goal of this research is to identify viable dual inhibitors of energy production and specific stress survival pathways to be used as a combinatorial therapy for patients in which tumor hypoxia has rendered standard therapeutic tools ineffective.

**Table of Contents:**

**List of Illustrations :**

**Introduction :**



**Chapter 1:**

**List of Tables:**

**List of Abbreviations:**

**°C** Degrees Celsius

**2-DG** 2-Deoxyglucose

**3-PG** 3-Phosphoglycerate

**ADP** Adenosine Diphosphate

**ALDOA** Aldolase A

**ALDOB** Aldolase B

**ALDOC** Aldolase C

**AMPK** 5' Adenosine Monophosphate-Activated Protein Kinase

**Arg** Arginine

**Asp** Aspartic Acid

**ATCC** American Type Culture Collection

**ATP** Adenosine Triphosphate

**BPG** 1,3-Bisphosphoglycerate

**cAMP** Cyclic Adenosine Monophosphate

**CBP** CREB Binding Protein

**cLogP** Partition Coefficient

**CMV** Cytomegalovirus

**$CO_2$** Carbon Dioxide

**COPB2** Coatomer Subunit Beta 2

**COX** Cyclooxygenase

**CREB** cAMP Response Element-Binding Protein

**DAP** Dihydroxyacetone Phosphate

**DHAP** Dihydroxyacetone Phosphate

**DMEM** Dulbecco's Modified Eagle's Medium

**DMSO** Dimethylsulfoxide

**DNA** Deoxyribonucleic Acid

**Doxy** Doxycycline

**DTT** Dithiothreitol

**ECAR** Extra Cellular Acidification Rate

**EDTA** Ethylenediaminetetraacetic Acid

**EMSA** Electrophoretic Mobility Shift Assay

**EP300** Adenovirus Early Region 1A Binding Protein p300

**Ex/Em** Excitation / Emission

**F-6-P** Fructose-6-Phosphate

**F-Actin** Filamentous Actin

**FBP** Fructose 1,6-Bisphosphate

**FBS** Fetal Bovine Serum

**FDA** Food and Drug Administration

**FDG-PET** Fluorodeoxyglucose Positron Emission Tomography

**FI** Fluorescence Intensity

**FIH** Factor Inhibiting HIF

**G418** Geneticin Aminoglycoside Antibiotic

**GAP** D-Glyceraldehyde-3-Phosphate

**GAPDH** Glyceraldehyde 3-Phosphate Dehydrogenase

**GDH** Glycerophosphate Dehydrogenase

**Glu** Glutamic Acid

**GLUT-1** Glucose Transporter 1

**GOLD** Genetic Optimization of Ligand Docking

**GP** L-a-Glycerol Phosphate

**$H_2O$** Water

**HIF** Hypoxia Inducible Factor

**HK** Hexokinase

**HRE** Hypoxia Responsive Element

**IgG** Immunoglobulin G

**$K_{cat}$** Number of substrate molecule each enzyme site converts to product per unit time

**KIF11** Kinesin Family Member 11

**KRAS** Kirsten rat sarcoma

**Luc** Luciferase

**M** Molar

**MAPK** Mitogen Activated Protein Kinase

**$MgSO_4$** Magnesium Sulfate

**mM** Millimolar

**mRNA** Messenger Ribo Nucleic Acid

**Mut** Mutant

**NAD** Nicotinamide Adenine Dinucleotide (oxidized)

**NADH** Nicotinamide Adenine Dinucleotide (reduced)

**ND** Not Determined

**nM** Nanomolar

**NOD-SCID** Nonobese diabetic/severe combined immunodeficiency

**NSCLC** Non-Small Cell Lung Cancer

**$O_2$** Oxygen

**OCR** Oxygen Consumption Rate

**P300** Adenovirus Early Region 1A Binding Protein p300

**P53** Tumor Protein p53

**PBS** Phosphate Buffered Saline

**PCAF** p300/CBP Associated Factor

**PDB** Protein Data Bank

**PDK1** Pyruvate Dehydrogenase Lipoamide Kinase Isozyme 1, Mitochondrial

**PEP** Phosphoenolpyruvate

**PGK1** Phosphoglycerate Kinase 1

**PGK2** Phosphoglycerate Kinase 2

**PH Domain** Pleckstrin Homology Domain

**PI-3-K** Phosphoinositide 3-kinase

**PLK1** Polo-Like Kinase1

**PTEN** Phosphatase and Tensin Homolog

**PVDF** Polyvinylidene Fluoride

**pVHL** Von Hippel–Lindau Tumor Suppressor

**SAR** Structure Activity Relationship

**SD** Standard Deviation

**SDS-PAGE** Sodium Dodecyl Sulfate-Polyacrylamide Gel Electrophoresis

**Ser** Serine

**shRNA** Short-Hairpin Ribonucleic Acid

**siRNA** Short-Interfering Ribonucleic Acid

**SSD** Sum of Standard Deviations

**TCA** Tricarboxylic Acid

**TCEP** Tris(2-carboxyethyl)phosphine

**TCGA** The Cancer Genome Atlas

**Thr** Threonine

**VEGF** Vascular Endothelial Growth Factor

**WASP** Neuronal Wiskott–Aldrich Syndrome Protein

**WT** Wild-Type

**Y** Tyrosine

**µg** Microgram

**µL** Microliter

**µM** Micromolar

## Introduction

The targeted, preferential killing of cancer cells without non-specific toxicity to normal cells in the body is one of the most critical and difficult challenges in cancer chemotherapy. In order to create effective, non-toxic anticancer agents it is essential to gain a comprehensive understanding about the biological and biochemical processes that differ between these cancerous and normal cell populations. As technology and laboratory techniques have evolved over the years, tremendous progress has been achieved in the understanding of signaling molecules, specific genes, and proteins that are involved in cancer development and progression and with this progress has come a better appreciation for the need for these targeted therapies. With every discovery, however, comes a greater understanding about the complexities inherent to this disease. The high level of heterogeneity commonly found among the cells of a single tumor serves as a confounder as the wide range of genetic and epigenetic alterations can be so diverse that often the use of a single agent is impossible. For this reason, a range of target specific agents is often used in a cocktail of therapies to eliminate a wider range of malignant cells. Alternatively, the identification and subsequent exploitation of a fundamental difference between normal and cancer cells could lead to a level of therapeutic selectivity not previously described by allowing for remedial discrimination between malignant cells and those associated with a patient's healthy tissue.

## Glycolysis and Cancer

Aerobic glycolysis occurs by the Embden-Myerhoff-Parnas pathway, a series of cytoplasmic enzymatic steps converting glucose to pyruvate (generating 2 ATP per molecule of glucose). Pyruvate is metabolized by the mitochondrial tricarboxylic acid (TCA) cycle generating NADH, which fuels oxidative phosphorylation (thus producing 36 ATP for one molecule of glucose). In the first phase of glycolysis, molecular glucose undergoes a series of phosphorylations and isomerizations in preparation for its cleavage into two triose molecules. In the second phase of

glycolysis, glyceraldehyde 3-phosphate undergoes a series of energy-releasing processes to not only recover ATP that is invested early in the glycolytic process, thus providing chemical motive for further execution of the cascade, but also the generation of ATP through substrate-level phosphorylation [5] (**Figure 1**). Cancer cells rely heavily on glycolysis and, under aerobic conditions, it can provide over 60% of the cancer cells' ATP compared to just 10% in normal cells. Warburg attributed this effect to defective mitochondrial oxidative phosphorylation in cancer cells [6], but subsequently it was shown that cancer cells have normal oxidative phosphorylation [2, 5, 7, 8]. More recently it has been shown that many actively dividing cells have high rates of glycolysis, and in most cases neither ATP nor NADH is limiting for cell growth [2]. It is now recognized that glycolysis is also a critical source of metabolic intermediates for the rapid synthesis of amino acids, nucleosides and lipids of the cellular biomass. High levels of aerobic glycolysis have been measured in a wide range of tumor types regardless of the tissue type from which they originated, as compared to their normal tissue counterparts which do not utilize aerobic glycolysis to satisfy their energy demands. This suggests that a characteristic of cancer cells, in combination with unrestrained growth, is that they revert to a metabolic phenotype, namely increased glycolysis, which provides proliferative advantages to rapidly dividing cells. This increased glycolysis in cancer cells is commonly referred to as the Warburg effect.

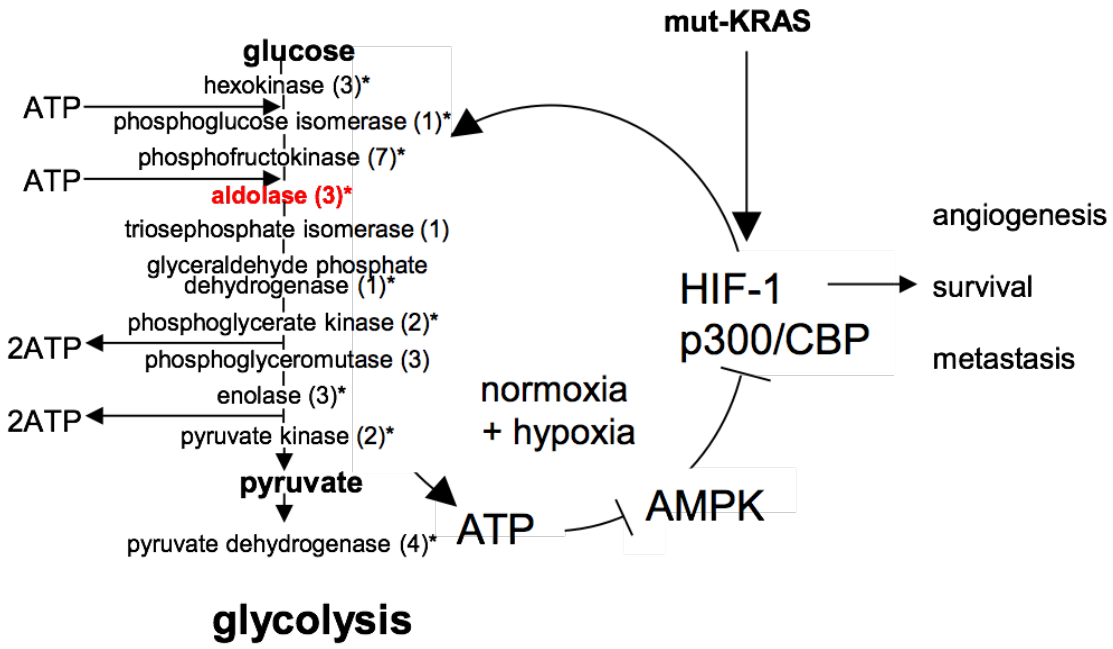


**Figure 1. The Glycolysis/HIF-1 Feed Forward Cycle in Cancer.**

In upper glycolysis glucose is phosphorylated and isomerized to enable its cleavage into two trioses:

**1** – Glucose is phosphorylated at the 6 carbon through the use of ATP by the transferase class enzyme Hexokinase. This regulatory step is negatively regulated by the accumulation of the product, glucose-6-phosphate.

**2** – Glucose-6-phosphate is then converted to Fructose-6-phosphate (F-6-P) by Phosphoglucoisomerase

**3** – Fructose-6-phosphate is phosphorylated at the 1 carbon position, again through the use of ATP, by the transferase class enzyme Phosphofructokinase to yield Fructose-1,6,bisphosphate (FBP). This is often considered the primary control step in glycolysis as it is the committed step of the process due to its large delta G value.

**4 – FBP is then cleaved into two, three carbon molecules – Dihydroxyacetone phosphate (DHAP) and Glyceraldehyde-3-phosphate – by the lyase class enzyme Aldolase (Aldolase A [ALDOA]) is our primary target for inhibition shown in red).**

**5** – DHAP produced in step 4 is converted to Glyceraldehyde-3-phosphate by Triose phosphate isomerase to satisfy the needs of the first step of lower glycolysis.

In lower glycolysis, glyceraldehyde 3-phosphate undergoes two major energy-releasing electron rearrangements.

**6** – Glyceraldehyde-3-phosphate is phosphorylated at the 1 carbon position by Glyceraldehyde-3-phosphate dehydrogenase to yield 1,3-Bisphosoglycerate (BPG).

**7** – Phosphoglycerate kinase phosphorylates ADP to yield ATP and 3-phosphoglycerate (3-PG).

**8** – 3-PG is converted to 2-phosophoglycerate by Phosphoglycerate mutase.

**9** – 2-phosphoglycerate is then converted to phosphoenolpyruvate (PEP) by Enolase. $H_2O$, potassium and magnesium are all released as a result.

**10** – Pyruvate kinase uses PEP to phosphorylate ADP and yield pyruvate. High levels of ATP, Acetyl-CoA, Alanine and cAMP can all negatively regulate this step.

In parenthesis are number of isoenzymes, * indicates proteins induced by HIF-1.

**Anaerobic Glycolysis**

In conditions of limited oxygen as found in most solid tumors (<1% $O_2$ compared to 3–15% $O_2$ found in normal tissues), pyruvate is converted to lactate by a process known as anaerobic glycolysis, and the lactate is then mostly secreted from the cell, although recent work suggests that in the heterogeneous tumor environment, some cells can use lactate as a source of fuel for mitochondrial oxidative phosphorylation [9]. There are 11 enzymatic steps to glycolysis with 40 possible contributing isoenzymes. Glycolysis has to be supplemented by an increase in cellular glucose uptake through GLUT transporters that are also upregulated in cancer [10, 11], forming the basis for $^{18}$F-deoxyglucose positron emission tomography (FDG-PET) measurement of glucose uptake by patient tumors as an indicator of response to therapy [12, 13]. Activation of oncogenes, or loss of tumor suppressors can lead to upregulated glycolysis and glucose transport in cancer. These include PI-3-kinase, oncogenic protein tyrosine kinases that act through PI-3-kinase, and loss of the tumor suppressor PTEN, that all lead to downstream activation of AKT that maintains hexokinase function and localizes glucose transporters to the cell surface [14, 15]. Myc activates the transcription of several glycolytic enzymes [1, 16, 17] as does mutant KRAS [18, 19]. Inactivation of the tumor suppressor p53 causes a shift of energy metabolism to glycolysis through down regulation of mitochondrial respiration as a result of cytochrome C oxidase (COX) deficiency [20].

**Tumor Hypoxia as an Inducer of Glycolysis**

Hypoxic regions present in all solid tumors occur due to decreased blood flow and disorganized tumor vasculature and provide a stressful environment favoring tumor growth [21-23]. A cancer cell's response to hypoxia is mediated by the hypoxia inducible transcription factors HIF-1 and 2 [24, 25], which together increase expression of numerous survival genes. Among them are genes that encode vascular endothelial growth factor (VEGF) (by HIF -1 and HIF-2 [26-28]), glycolytic enzymes (by HIF-1 only [29]) and induction of the expression of GLUT-1 glucose

transporter [10, 17]. At the same time there is inhibition of mitochondrial aerobic respiration through induction of pyruvate-dehydrogenase kinase-1 (PDK1) [30]. Additionally, it has been shown that the ability of mutant KRAS, found in more than 97% of pancreatic cancer, to increase glycolysis is mediated through expression of HIF-1α, which is detectable in pancreatic cancer cell lines even under aerobic conditions [18, 19, 31].

**Inhibitors of glycolysis as cancer drugs**

A number of attempts have been made to develop inhibitors of enzymes of glycolysis as potential anticancer agents [32-37]. These have typically been simple small molecule analogs of substrates of glycolytic enzymes and include 2-deoxyglucose a competitive inhibitor of glucose utilization [38, 39] which has, historically, shown minimal clinical activity at doses that can be safely administered to patients [40], 5-thioglucose and 3-bromopyruvate as hexokinase (HK) inhibitors [41, 42] when infused in rabbits are severely hepatotoxic [43], and dichloroacetate, an inhibitor of PDK1 [44] which is known to cause toxic neuropathy in humans [45]. Overall the use of small molecule substrate analogs to inhibit glycolysis has yielded disappointing clinical effects, and in many cases considerable toxicity.

**HIF-1 as a Tumor Survival Factor and Cancer Drug Target**

HIF-1 and 2 are critical mediators of the hypoxic response and transactivate a large number of genes promoting a wide range of factors associated with cancer progression including angiogenesis, anaerobic metabolism and resistance to apoptosis [46] with HIF-1α preferentially inducing glycolytic enzyme genes [24, 29]. HIF-1 is a heterodimer comprised of an oxygen labile HIF-α subunit and a stable HIF-1β subunit. Under aerobic conditions HIF-1α is hydroxylated by the prolyl hydroxylase proteins and subsequently ubiquitinated by the von Hippel Lindau protein (pVHL) and targeted for proteasomal degradation [47]. During hypoxia, pVHL binding is

abrogated due to the lack of this hydroxylation. The resulting stabilization of HIF-1α causes its translocation to the nucleus where it heterodimerizes with HIF-1β and binds to a conserved DNA sequence known as the hypoxia responsive element (HRE), thus transactivating a variety of hypoxia-responsive genes [48]. Elevated levels of tumor HIF-1α have been associated with poor patient survival in multiple tumor types [49]. HIF-1α is thus an attractive target for cancer drug development and a number of inhibitors have been reported [50]. Recently the clinical trial of a first generation HIF-1α inhibitor, PX-478 was reported with promising results establishing the validity of HIF-1α as a drug target [51]. The mechanism by which PX-478 inhibits HIF-1α remains unclear and the off target side effects of PX-478 will likely limit its future development. However, HIF-1α remains a promising target for drug development and second-generation inhibitors with defined mechanisms of action and low toxicity are needed.

**ALDOA as a Cancer Drug Target**

It is known that malignant transformation results in a significant change in the expression of glycolytic isoenzymes and favors those isoenzymes that facilitate survival and uncontrolled proliferation. It has been found that the expression of ALDOA is significantly elevated relative to the two other isoforms, ALDOB and ALDOC, in a wide variety of human tumor types including pancreatic cancer [29]. ALDOA is also highly expressed in developing embryos suggesting it is adapted to the metabolic requirements of rapid cell proliferation [52, 53]. ALDOA has also been shown to have a $k_{cat}$ that is significantly higher than that of the other ALDO isoenzymes [54, 55]. Based on these findings it has been suggested that ALDOA could serve as a cancer drug target for inhibiting glycolysis [33, 56]. We have now shown a novel finding that ALDOA is the most important of the 40 isoenzymes of glycolysis responsible for maintaining HIF-1 activity. It is a doubly attractive target based on the finding that its inhibition leads to both an inherent reduction in cancer cell energy metabolism and HIF-1 activity. Aldolases have also been reported to bind to a number of non-glycolytic proteins including F-actin [57], WASP and N-WASP, activators of

Arp2/3 and actin polymerization [58] and the PH domain of phospholipase D2 [59]. Although the significance of this binding is not clear, the observations have also led to the suggestion that Aldolases could be a target for inhibiting cancer growth [60].

**Summary**

In this study, the identification of a novel feed-forward cycle of increased HIF-1α and increased glycolysis that is critical for tumor growth and survival, is paired with an understanding that the inhibition of the glycolysis/HIF-1 cycle is selective for hypoxic tumor cells due to the fact that normal aerobic dividing cells, despite using aerobic glycolysis do not express HIF-1. Inhibiting this cycle, thus, provides a novel way to target human malignancies. In pancreatic cancer where the glycolysis/HIF-1 cycle appears to be particularly prominent, the key activating event may be increased HIF-1α by mut-KRAS even in hypoxic conditions. This may be why KRAS signaling is significantly correlated with glycolysis in pancreatic cancer [61, 62]. Considering this fact and taking into account that it is overexpressed in pancreatic cancer and strongly associated with decreased patient survival, we have identified and validated the glycolysis enzyme ALDOA as a critical step in the glycolysis/HIF-1 cycle. By using ALDOA as a target for the design of pharmacological probes, we are able to attack, at the same time with a single agent, two critical cancer survival mechanisms: glycolysis and angiogenesis. ALDOA has a known crystal structure which allowed us to use molecular modeling for lead optimization, and co-crystallography for validation of ALDOA-inhibitor leads. Through the combination of virtual screening, high-throughput consideration of large small molecule libraries and subsequent validation of lead compounds in biological assays, we have identified low micromolar affinity inhibitors of ALDOA as tool compounds and as potential leads for preclinical development as novel anticancer agents. Further, we have identified a potential mechanism for inhibition of ALDOA leading to decreased HIF-1 activity through the AMPK inhibition of the HIF-1 co-activator p-300 allowing for the combination of novel target identification, elucidation of

biological mechanisms responsible for the critical nature of the target in the progression of human cancer, discovery of probe inhibitors and validation of their efficacy using both *in vitro* biochemical and *in vivo* anti-tumor experiments.

## Materials and Methods

### Cells and Culture Conditions

MIA PaCa-2, MDA-MB-231, and PANC1 cell lines were obtained from the American Type Culture Collection (ATCC) and grown in DMEM media; HT-29 cells were obtained from ATCC and cultured in McCoy's 5A media. DNA fingerprinting was conducted by the University of Texas M.D. Anderson Cancer Center Characterized Cell Line Core Service at the same time as total protein lysate preparation in order to confirm the identities of cells used in all experiments. All cell lines were routinely tested to be mycoplasma free using the e-Myco kit (Boca Scientific).

### Creation of Stable and Inducible Cell Lines

Following karyotype analysis, a 5X HRE repeat (hypoxia response element) sequence from the VEGF and EPO genes was cloned in front of firefly luciferase in the pGL3 Basic Vector. This HRE/luciferase sequence was then sub-cloned into the pcDNA3.1 vector with Neomycin resistance. The resulting plasmid was transfected into MIA PaCa-2 and PANC1 pancreatic carcinoma, MDA-MB-231 breast adenocarcinoma, and HT-29 colorectal adenocarcinoma cells and stable clones selected following long term culture in DMEM 10% FBS with G418 selective pressure using 300 µg/mL Geneticin (Invitrogen).The reporter plasmid was a gift of Dr. R. Gillies (Moffitt Cancer Center, Tampa, FL). Following selection, pools of stably transfected cells were generated and frozen for later use.

For conditional Aldolase A knockdown in an *in vivo* murine model, four sequences predicted to target ALDOA gene expression were selected from the Thermo Scientific Dharmacon shRNA library and each was inserted into a TRIPZ doxycycline inducible lentiviral vector (Open Biosystems). Each of the four HRE luciferase lines described above was transduced with shALDOA-expressing lentivirus, and stable lines were selected in puromycin in 96-well plates with one cell per well to generate clonal populations. After puromycin and G418-resistant clones were selected, shALDOA expression was induced using doxycycline in both normoxia and hypoxia (1% $O_2$) to assess ALDOA knockdown.

**siRNA Screening**

Cells underwent two consecutive passages in the absence of G418 selection before confirmation that the cells were mycoplasma negative. Optimization of ideal transfection reagent and reagent concentration was carried out using high-throughput optimization methods for reverse transfection (**Figure 2**). In the course of this process, 8 transfection reagents from various manufacturers (DharmaFECT 1, 2, 3, and 4 [Dharmacon], XtremeGENE [Roche], Lipofectamine RNAiMAX [Invitrogen], HiPerfect [Qiagen], or siPort NeoFX [Thermo Fisher Scientific]) were used in a range of concentrations per well and paired with one of nine negative (siGenome Scrambled Non-targeting control 1, 2, 3, 4 or 5 or siOnTargetPlus Non-targeting control 1, 2, 3, or 4 [Dharmacon]) or one of four positive controls (siPLK1 an inhibitor of the G2/M transition [63], siTOX an inducer of the interferon response [64], siCOPB2 an inhibitor of Golgi budding and vesicular trafficking [65], or siKIF11 an inhibitor of mitotic spindle formation [66]). Optimal combinations were identified by calculation of z'-factor ultimately yielding the combination of least toxic and most efficient transfection reagent, least toxic negative control siRNA and most effective positive control siRNA per cell line.

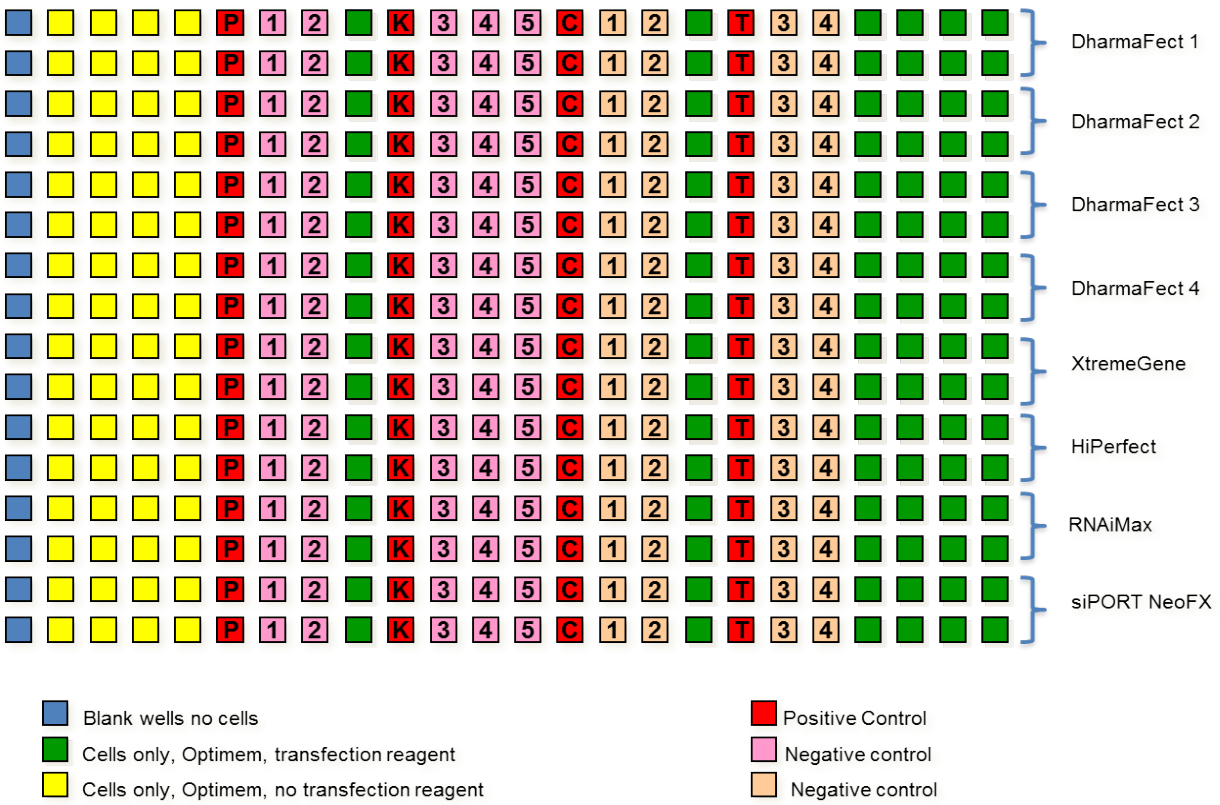


**Figure 2. siRNA Transfection Optimization Format**

The combination of 8 transfection reagents with nine positive and four negative control siRNAs allows for the identification of the optimal combination of reagents and controls per cell line when the z'-factor criteria was satisfied per the following equation:

**Z'-factor = 1-(3*(SSD/(Range)))**

SSD – sum of standard deviations in negative control and positive controls samples

Range – negative control average – positive control average

If the end value was greater than .7, the assay was considered robust enough to continue.

Following optimization, parallel screens were then carried out with a genome wide siRNA library (Dharmacon) in one of two different levels of oxygenation: normoxia or hypoxia. Optimization of cell number and $O_2$ level was conducted in order to identify the ideal conditions for hypoxia related experiments (**Figure 3**). To this end, 60–70% confluent cells were cultured in a hypoxia chamber (InVIVO$_2$ 400, Ruskinn) flushed with 1% $O_2$ and 5% $CO_2$ with balance of 94% nitrogen at 37 °C for 16 hours following 48 hours of transfection in air. Control cells were placed in a 5% $CO_2$ and 95% air incubator (20% $O_2$) at 37 °C for the duration of the experiment. All experiments were conducted in 384 well, white, clear-bottom, tissue culture treated plates (Falcon) in which 10 µl of 1x siRNA buffer containing 200 nM siRNA was complexed with 10 µl of OptiMEM transfection media containing 0.07 µl of XtremeGENE (Roche) for 30 minutes prior to the addition of a mixture of 30 µl of complete DMEM media (10% FBS) and 2000 cells. At the completion of experiments, cell viability was first measured using the cell proliferation reagent WST-1 (Roche) followed by the washing of the wells with PBS and subsequent analysis of HRE-luciferase expression and activity using an in-house luciferase assay buffer containing 25 mM Tricine, 0.5 mM EDTA-Na2, 0.54 mM Na-triphosphate, 16.3 mM MgSO4*7 H2O, 0.3% Triton X-100, 0.1% DTT, 10 mM ATP, and 2.7 mM Coenzyme A adjusted to pH 7.8 to yield a combined viability and HRE activity reading.

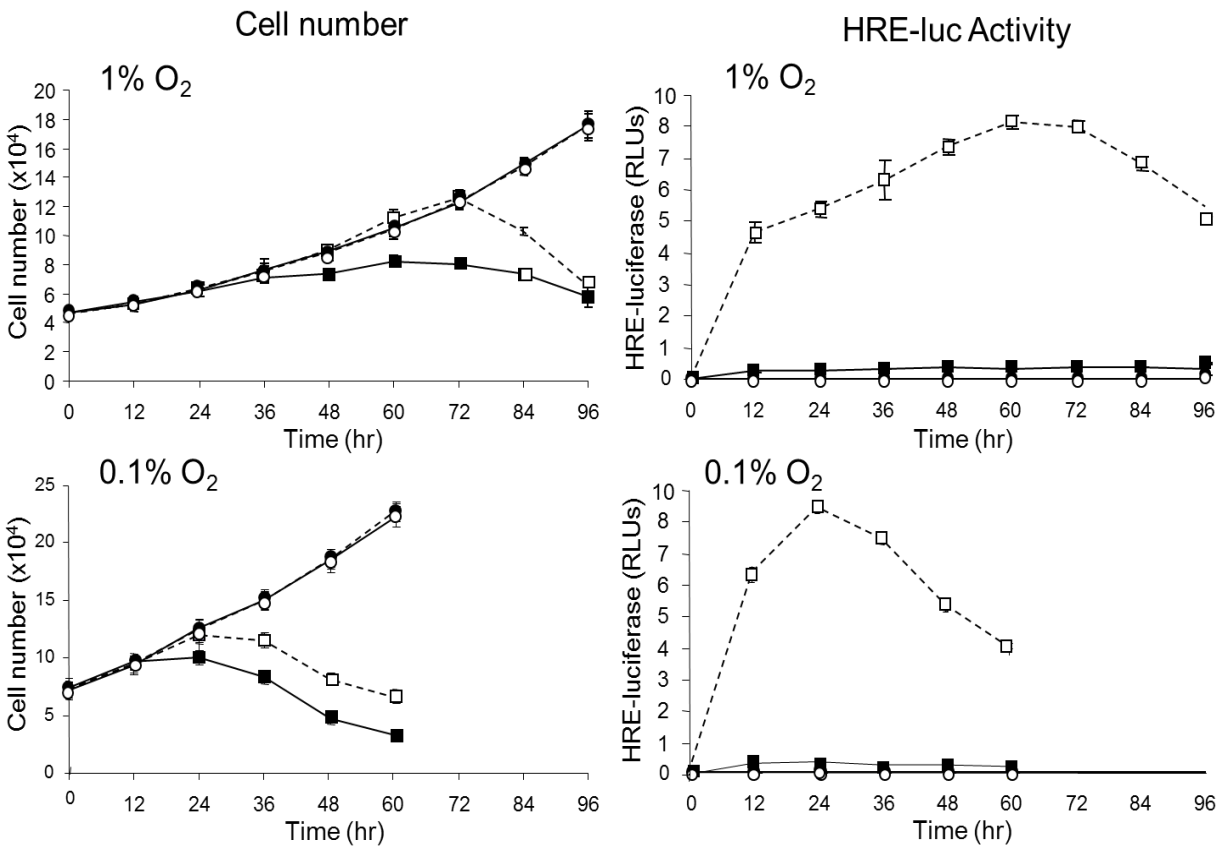


**Figure 3. Optimization of $O_2$ Conditions Based on Growth Rate and HRE-luciferase Activity in Hypoxia Based Experiments**

Growth rate (based on cell number) and HRE-luciferase activity was measured at 12 hour time points in order to identify optimal oxygen concentration conditions and duration of the exposure to hypoxia in order to have the highest possible baseline HRE-activity during the high throughput siRNA screen to find inhibitors of HIF-1 transcriptional activity. Values are the mean of 6 determinations. Bars are S.D.

**Individual siRNA Transfection**

After identifying initial glycolysis genetic hits, follow-up work in each of the 3 additional cell lines listed was conducted by de-convoluting pooled siRNA for selected targets from an alternative supplier for additional validation purposes. For transfection in a six well plate format, 300 µl of 1x siRNA buffer containing 200 nM siRNA was added to each well followed by 300 µl of OptiMEM with 2.5 µl of either DharmaFECT 4 (for MDA-MB-231 and PANC1 transfections), DharmaFECT 1 (for HT-29) or XtremeGENE (for MIA PaCa-2). Following 30 minutes of incubation at room temperature to allow for transfection reagent-siRNA complexing, 900 µl of complete media containing 100,000 cells was added per well yielding a final screening concentration of 40 nM siRNA. Per well siALDOA SMARTpool (Dharmacon, M-010376-01), individual siALDOA siRNAs (Qiagen GS226), siPGK1 SMARTpool (Dharmacon, M-006767-01), individual siPGK1 siRNAs (Qiagen, GS5230), siPGK2 SMARTpool (Dharmacon, M-006768-02), or individual siPGK2 siRNAs (Qiagen, GS5232) was added and knockdown efficiency was determined by Western blotting of cell lysates 96 hours post transfection. Dharmacon SMARTpool siRNAs for HIF-1α, AMPK, EP300, PLK-1 or the On-Target-Plus non-targeting pool #4 (OTP4) were included as controls. Total siRNA concentration was kept at 40 nM when siRNA combinations were used.

**Immunoblots and Immunoprecipitations**

Cells were washed twice with pre-chilled, ice-cold PBS before adding ice-cold lysis buffer containing 50 mmol/L HEPES (pH 7.5), 50 mmol/L NaCl, 0.2 mmol/L NaF, 0.2 mmol/L sodium orthovanadate, 1 mmol/L phenylmethylsulfonyl fluoride, 20 µg/mL aprotinin, 20 µg/mL leupeptin, 1% NP40, and 0.25% sodium deoxycholate. Following scraping, samples were vortexed frequently on ice for 20 minutes, followed by microcentrifugation at 14,000 rpm for 10 minutes. Cleared supernatants were collected, followed by protein quantification using the BCA reaction

kit (Pierce Biotechnology, Inc.) and 50 µg of cell lysate protein were boiled for 5 min with denaturing buffer containing 0.25 mol/L Tris (pH 6.8), 35% glycerol, 8% SDS, and 10% 2-mercaptoethanol, loaded on a 10% acrylamide/bisacrylamide gel, and separated by electrophoresis at 90 V for 1 hour and 20 minutes. Proteins were electrophoretically transferred to a methanol activated polyvinylidene fluoride (PVDF) membrane; pre-incubated with a blocking buffer of 5% milk; and incubated overnight with anti–phosphorylated Thr172 – AMPK or anti-AMPK (Cell Signaling 1:1000), anti-HIF-1α (BD Biosciences 1:500), anti-Aldolase A (AbNova 1:500), anti-Aldolase B or anti-Aldolase C (Novus Biologicals 1:1000), anti-phosphorylated Ser89-EP300 or anti-EP300 (Santa Cruz Biotechnology 1:1000) or anti-β-actin (Santa Cruz Biotechnology 1:2000). Donkey anti-rabbit, sheep anti-mouse (GE Healthcare), or donkey anti-goat (Santa Cruz Biotechnology) IgG horseradish peroxidase-coupled secondary antibody was used for detection where appropriate. Band density was measured using the densitometry functionality found within the Image-J open source image analysis program following ECL mediated image development on either Kodak X-Omat Blue ML films (Eastman Kodak) or the FluorChem M Imaging Platform (Protein Simple).

**Determination of Cellular ATP Concentration**

Cellular ATP was measured using an ATP Assay Kit (Abcam) according to the manufacturer's protocol and quantified by both colorimetric (λmax = 570 nm) and fluorometric (Ex/Em = 535/587 nm) methods, 96 hours post siRNA-transfection. Each experiment was performed in both biological and technical triplicates.

**Xenograft Analysis**

Approximately $10^7$ MDA-MB-231 HRE cells, MDA-MB-231 cells harboring shALDOA clones 8.8 and 9.7, and MDA-MB-231 HRE empty vector cells, all in log cell growth, were suspended

each in 0.2 mL PBS and injected subcutaneously into the mammary fat pads of female *NOD-SCID* mice. Groups contained five mice each. When the tumors reached 250 $mm^3$, chow containing doxycycline was substituted for control feed (Harlan Laboratories) in test groups. An additional group of five mice was fed doxycycline containing chow for one week prior to injection of the inducible cells to measure the possible inhibitory effect on initial tumorigenesis. Mice were euthanized when they became clinically moribund associated with the metastatic spread of the MDA-MB-231 tumor to liver and lung. Animal studies were approved by SBPMRI's Animal Care and Use Committee.

**Molecular modeling**

**Target Receptor and Chemical Database selection**

The crystal structure of Aldolase was obtained from the Protein Data Bank [67] (4ALD) and considered as the basis for virtual screening [68]. For the ligand set used in these virtual screens, we selected the 10,000 compound Myria Screen chemical library.

**Virtual Screening**

The virtual screens were performed using the GOLD (Genetic Optimization for Ligand Docking) software from CCDC [69]. GoldScore was chosen as the fitness function, and 29 residues within 6Å of 2FP (fructose 1,6-bisphosphate) were selected as defining the binding site.

Two successive GOLD screens were carried out: the first screen docked the entire MyriaScreen ligand set into a rigid structure in which no considerations were made as to flexibility of the structure. The resulting top 2000 ligands were then clustered based on structural MACCS (Molecular ACCess System) fingerprints using MOE fingerprint clustering. The second screen considered only the top 60 unique scoring ligands allowing for flexible side chains. Using the Tanimoto coefficient with chemical similarity and overlap considerations set to 60%, cluster

centers were retained. The resulting 60 unique ligands from this clustering were then minimized in MOE, and screened a second time in GOLD with full flexibility considerations made for the following Aldolase residues: Asp33, Ser38, Lys146, Arg148, Glu187, and Lys229. These residues were selected as flexible based on location relative to the binding site and propensity to form favorable interactions with the natural substrate, 2FP.

The results from the second screen were then individually visualized (using PyMOL) in their docked conformation (protein-ligand complex). Two main criterions were considered in the final selection process. First was the resulting orientation and configuration within the protein structure. We considered interactions that would increase the binding affinity (e.g. hydrogen bonds, static and aromatic effects). The second consideration was the distinctiveness in the molecular scaffold when compared to the other ligands at this stage. We placed the ligands into "classes" based upon the individuality of their underlying scaffold and how this scaffold was oriented in the binding site. Ligands that shared a similar scaffold and orientation were considered to be in the same class. Based on the combination of the two criteria, 22 ligands in total were recommended to be tested for biological activity.

**Aldolase Enzymatic Activity Assay**

A 96 well plate assay based on conversion of fructose 1,6-bisphosphate (F-1,6-BP) into glyceraldehyde 3-phosphate (GAP) and dihydroxyacetone phosphate (DHAP) measured in a coupled reaction with GAP dehydrogenase by the oxidation of NADH to NAD was used to measure the effect on Aldolase A cleavage activity using an adapted method previously described [70]. All enzymatic assays were conducted at 22º C in a final volume of 100 µl following the addition of recombinant Aldolase A protein (Novus Biologicals) to a reaction mixture containing substrate, 0.15 mM NADH, 50 mM Tris-acetate, 10 mM EDTA (pH 7.6), 100 mg/ml bovine serum albumin, and 2 mg/ml α-glycerophosphate dehydrogenase/triose phosphate isomerase. Enzymatic activity was measured by endpoint assay at 364 nm sampling at 30

second intervals. Initial attempts to verify ability of previously selected compounds from virtual screening methods to inhibit Aldolase activity was monitored by following this NADH-dependent coupled reaction at 340 nm proved to be incompatible with high throughput screening due to spectroscopic interference at 340 nm by compounds typically found in screening collections. To address this challenge we developed a robust fluorescence-based assay for ALDOA (**Figure 4**) and screened a collection of >65,000 compounds (**Table 1**) in 384-well format, identifying approximately 20 novel inhibitors with $EC_{50}$'s in the range of 1-20 μM, whose affinity compare favorably to that of Fru-1,6-P2 using the protocol outlined in **Figure 5**.

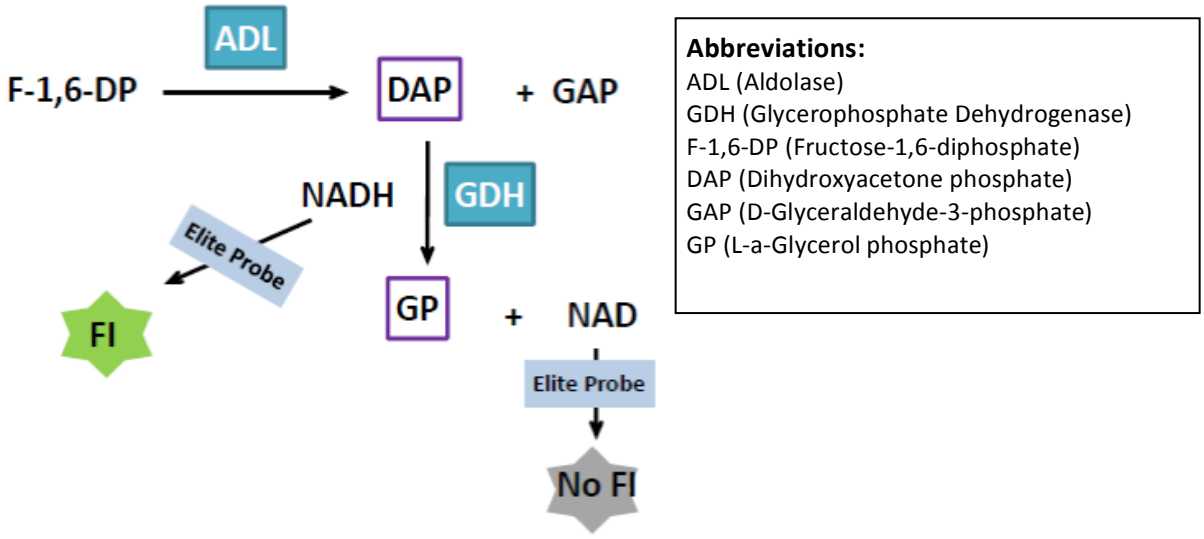


**Figure 4. Optimization of Fluorescence-based NADH Oxidation HTS Aldolase Assay**

Glyceraldehyde-3-phosphate dehydrogenase converts glyceraldehyde-3-phosphate (G-3-P) to 1,3-bisphosphoglycerate (1,3-BGP) through oxidative phosphorylation. NAD+ is reduced to NADH when a phosphate group is exchanged for a hydrogen on the carbonyl carbon of G-3-P thus converting G-3-P to 1,3-BGP. This assay uses glycerophosphate dehydrogenase to catalyze the conversion of dihydroxyacetone phosphate (the product of the ALDOA catalyzed reaction) to glyceraldehyde-3 phosphate in an NADH-dependent manner. Thus, the rate of change of fluorescence intensity is used to indirectly calculate the activity of ALDOA.

| Compound Collection | Total Compounds | # of Hits | Hit Rate |
|---|---|---|---|
| Kinase focused | 652 | 14 | 2.15 |
| NIH clinical | 674 | 4 | 0.59 |
| Lopac | 1,280 | 4 | 0.31 |
| Spectrum | 2,000 | 15 | 0.75 |
| Academic (UT Austin/Kansas) | 2,100 | 7 | 0.33 |
| NCI Diversity | 2,537 | 12 | 0.47 |
| Chembridge Fragment | 4,000 | 69 | 1.73 |
| Chembridge KINASet | 11,250 | 94 | 0.84 |
| Chemdiv Fragment | 12,800 | 70 | 0.55 |
| Chemdiv Diversity | 14,243 | 132 | 0.93 |
| Maybridge Diversity | 14,400 | 219 | 1.52 |
| **Total** | **65,936** | **640** | **0.97** |

**Table 1. Commercial and Academic Small Molecule Collections and Corresponding Hit Rates in High Throughput Small Molecule Inhibitor Screen**

Commercial and academic collections used in the high throughput small molecule inhibitor screen representing structurally diverse sets of compounds known to be biologically active and drug like:

- The kinase focused library was custom-selected by screening group at UT Austin and is comprised of 600+ compounds known to have inhibitory effects against more than 100 kinases.
- The Evotec NIH clinical collection is part of the NIH Molecular Libraries Small Molecule Repository which distributes samples for high throughput biological screening.
- Lopac$^{1280}$ from Sigma-Aldrich is a collection of 1280 pharmacologically active compounds including marketed drugs
- The Spectrum collection uniquely offers a combination of drug components, natural products, and other bioactive components which have been dropped from development for toxicological or other reasons.
- Academic collections were a result of deposited samples composed of unique molecules with diverse pharmacophores by chemists at both the University of Texas at Austin and University of Kansas.
- The NCI diversity set is a small library, ideal for beginning a screening campaign, consisting of a collection of chemically diverse synthetic small molecules selected from the full NCI screening collection to allow users to focus their cancer screening efforts on a small scale.
- The Chembridge Fragment and Kinase Sets are customizable collections of fragment compounds chosen based on satisfaction of the Astex Rule of Three in which the compound's molecular weight is <300, the number of hydrogen bond donors is ≤3, the number of hydrogen bond acceptors is ≤3 and ClogP is ≤3 [71] and *in silico* validated pharmacophores that may interact with ATP ligand sites of kinases.
- Fragments in the Chemdiv collection contain only C, H, N, O, S, P, F, Cl and Br atoms, are highly water soluble and feature diversity, low structural complexity and a high level of drug-likeness.
- Additional diversity found in the Maybridge collection has a high rate (95%+) of satisfying Lipinski's Rule of 5.

Hits were selected based on inhibition of Aldolase enzymatic activity by at least 30% relative to negative controls using a modified Elite NADH fluorescent probe coupled enzymatic activity assay.

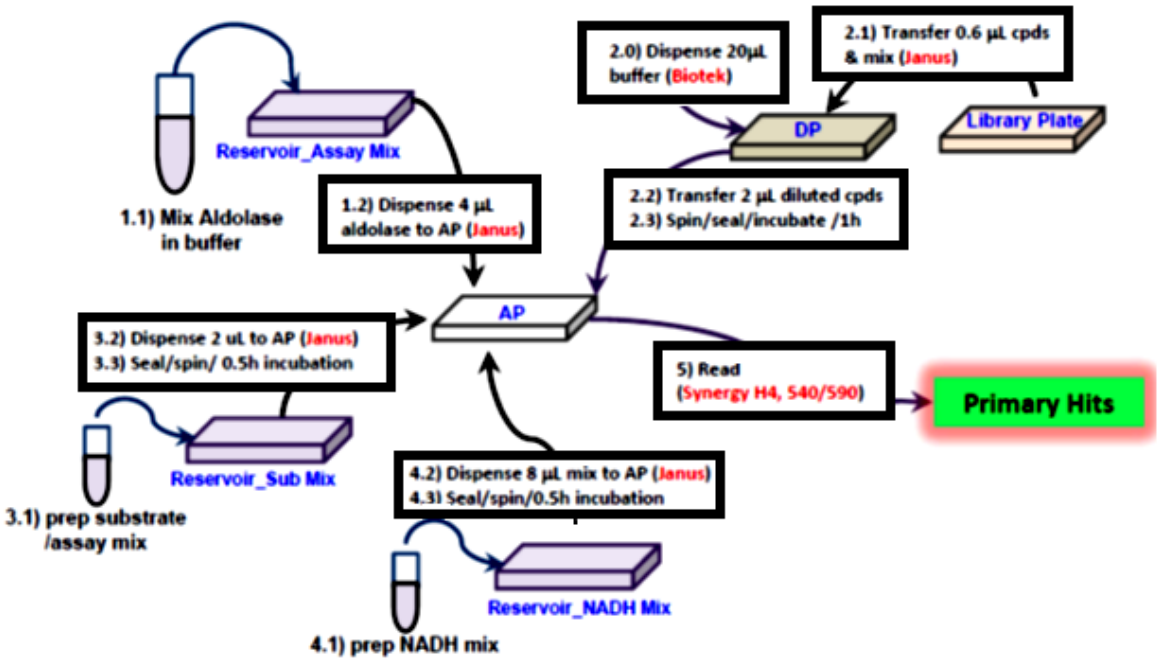


**Figure 5. High Throughput Small Molecule Screening Protocol:**

1. Prepare a 2x Aldolase A mixture (5 nM) in 1X assay buffer (1x PBS 0.01% TritonX-100, 0.1% BSA) and dispense 4 µl to the assay plate (AP)
2. Spin plate at 800 RPM for 1 minute to ensure that entire volume is at the bottom of each well
3. Dispense 30 µl water into dilution plate (DP) and add 0.6 µl of 10 mM compound solutions to make a 200 µM (4x) compound stock solution.
4. Directly transfer 2 µl of the compound stock to the assay plate.
5. Spin plate at 800 RPM for 1 minute, seal, and incubate at room temperature for 1 hour.
6. Prepare 4x substrate mixture (F(1,6)BP, Glyceraldehyde Dehydrogenase and NADH) in 2x assay buffer.
7. Dispense 2 µl of substrate mixture into assay plate.
8. Spin plate at 800 RPM for 1 minute, seal, shake plates at 250 RPM for 5 minutes followed by an additional 800 RPM spin.
9. Incubate plates for 40 minutes at room temperature.
10. Mix NADH recycling enzyme with NADH assay buffer from the Elite NADH assay kit and dispense 8 µl into assay plate.
11. Spin plate at 800 RPM for 1 minute, seal, and incubate for 1 hour at room temperature.
12. Read fluorescence intensity with excitation/emission spectra at 540/590 nm per the manufacturer's instructions.

**Measurement of Cellular Glycolysis**

Glycolytic function was assessed by quantifying the rate of lactate formation using the Seahorse Bioscience XF96e platform (Seahorse Bioscience) and the XF Glycolysis Stress Test Assay according to the manufacturer's protocol. Historic studies of cellular function have been performed on monolayer cultures adherent to rigid substrates. Cells within a human tissue, however, are typically encased within a tightly packed mass of cells in which connections with many neighbors and with extracellular matrix components occur. Cells within a 3D environment experience fundamentally different growth conditions compared to those experienced by cells grown in monolayer culture. In order to measure glycolysis under hypoxic, physiologically relevant conditions, a modified hanging drop tissue culture method [72] was used to evaluate 3-dimensional spheroids of PANC-1 HRE cells transduced with shALDOA constructs. On the lid of a 100 mm2 tissue culture dish, 20 10 µl droplets of complete media containing 10,000 +/- 2500 cells (depending on cell line) were arrayed using a multi-channel pipette. The bottom of the dish was filled with 5 ml of PBS to act as a hydration chamber to prevent evaporation of volume from the hanging drop during 3 day incubation times. Three days after seeding cells and 24 hours before running the XF Glycolysis Stress Test, shALDOA expression was induced with 400 ng/ml doxycycline. A final volume of 175 µl of pre-conditioned assay medium containing 18 spheroids was added to each well of a test plate and incubated at 37ºC in a $CO_2$-free incubator until the experiment was initiated. The use of this hanging drop method allowed for the generation of spheroids ranging in size from 300-500 µm which exhibited a hypoxic core based on analysis with a fluorescent LOX-1 hypoxia probe (SCIVAX USA, Inc) without the need for hypoxic gassing conditions.

**Crystallization and Structure Solution**

Screens for the identification of optimized crystallization conditions were performed using a 96-reagent crystallization screen Index (Hampton Research) and a Phoenix robotic drop dispenser (Art Robbins Instruments). Using the sitting drop vapor diffusion method, ALDOA was co-crystallized with inhibitor naphthalene-2,6-diyl bis(dihydrogen phosphate) (NBP). Drops (0.4 µl each) containing 0.2 µl of the protein solution (18 mg/ml ALDOA, 3 mM NBP, 15 mM TRIS buffer pH 7.6, 150 mM NaCl, 0.7 mM TCEP), and 0.2 µl of the crystallization buffer (25% PEG 3350, HEPES buffer pH 7.0), were equilibrated against the crystallization buffer at 23°C. Crystals grew within 2 weeks measuring 0.20x0.06x0.06 $mm^3$. To measure the binding capacity of a lead compound found in high throughput screens of chemical libraries, a 4-benzyl-2-methyl-1,2,4-thiadiazolidine-3,5-dione (TDZD-8) (MedKoo Biosciences) complex was made by soaking preformed NBP co-crystals in PEG 3350 (23% w/v) containing 1.5 mM TDZD-8 for 4 h at 23°C. Crystals were flash-frozen in liquid nitrogen after adding 15% PEG 400 as a cryoprotectant. Diffraction data were collected at the Stanford Synchrotron Radiation Laboratory (SSRL), beamline 12-2, and processed using AUTOXDS [73] and the CCP4i program suite [74]. The structures were solved using the molecular replacement program PHASER [75] and the ALDOA structure (PDB ID: 1ALD) as the search model. Refinement and manual rebuilding were done with REFMAC5 [76] and COOT [77]. The final model is refined at 2.5 Å resolution to an R-factor of 20% ($R_{FREE}$ = 24%).

**The Cancer Genome Atlas Data Analysis**

Comparison of tumor and paired normal tissue samples from 9755 patients for ALDOA, ALDOB and ALDOC mRNA in The Cancer Genome Atlas (TCGA) PANCAN datasets was carried out using publicly available data. Survival data was corrected for tumor type, patient age and patient sex. In this way, TCGA data for mRNA expression as it relates to patient survival

was used to analyze differences between paired samples using the student's t-test in addition to calculation of Pearson's correlation and linear regression analysis.

# Chapter 1: Identification of a Novel Feed Forward Loop

**Glycolytic Enzymes Regulate HIF-1α Activity**

In order to identify genes potentially regulating cellular HIF activity we conducted a genome-wide siRNA screen using MIA PaCa-2 pancreatic cancer cells with a stably integrated 5x HRE/promoter-luciferase (luc) reporter to search for genes that, when silenced would inhibit HIF activity. It is important to note that the reporter cannot distinguish between HIF-1 and HIF-2 activity which was made evident by results that will be discussed later. That screen, which was conducted using a genome wide siRNA library (Dharmacon), identified several glycolysis-related factors. This was an unexpected finding given that while it is known that expression of a number of glycolysis genes are up-regulated by HIF-1 [4, 27], although not by HIF-2 [27], the fact that glycolysis had any regulatory effect on HIF transcriptional activity had not been reported. Identification of various genes in the pathway opened an interesting new avenue in an early novel therapy design effort so the up-regulation of potential targets as a result of HIF-1 activity was confirmed in MIA PaCa-2 cells using small scale, directed mRNA expression profiling. By limiting a typical class discovery experiment in which thousands of possible gene expression levels can be assessed [78] and analyzing only glycolytic genes, a clear pattern of reliance on HIF-1 activity for expression during hypoxic stress was identified (**Table 2**).

| Gene: | Fold change hypoxia: | Fold change siHIF-1α: |
|---|---|---|
| HK1 | 2.611 | 0.491 |
| HK2 | 5.308 | 0.426 |
| HK3 | No Change | No Change |
| GPI | 2.108 | 0.675 |
| PFKM | 0.701 | 1.250 |
| PFKL | No Change | No Change |
| PFKP | No Change | No Change |
| PFKFB1 | No Change | No Change |
| PFKFB2 | No Change | No Change |
| PFKFB3 | No Change | No Change |
| PFKFB4 | No Change | No Change |
| ALDOA | 2.319 | 0.716 |
| ALDOB | No Change | No Change |
| ALDOC | 14.840 | 0.333 |
| TPI1 | 2.299 | 0.533 |
| GAPDH | 2.051 | 0.658 |
| PGK1 | 5.473 | 0.378 |
| PGK2 | 7.947 | 0.259 |
| PGAM1 | 2.287 | 0.649 |
| PGAM2 | No Change | No Change |
| BPGM | 0.588 | 1.505 |
| ENO1 | 2.351 | 0.573 |
| ENO2 | 4.807 | 0.277 |
| ENO3 | 1.115 | 1.750 |
| PKLR | No Change | No Change |
| PKM2 | 1.892 | 0.855 |

**Table 2. HIF-1 Knockdown Inhibits Genes Encoding Glycolytic Enzymes in Hypoxic MIA PaCa-2 Pancreatic Cancer Cells.**

Thirty genes encoding glycolytic enzyme isoforms were selected for validation and investigation based on results from the genome-wide siRNA screen used to identify inhibitors of cellular HIF-1α activity. Through the use of microarray methodologies, we measured fold-change in expression of glycolytic enzymes following control siRNA transfection and exposure to hypoxia (siControl hypoxia/siControl normoxia) or fold-change following HIF-1α knockdown (siHIF-1α hypoxia/siControl hypoxia).

The combination of a clear pattern of HIF-1 activity inhibition with siRNA knockdown of glycolytic gene expression as observed in the primary, genome-wide screen and the heavy reliance on HIF-1 expression and activity for glycolysis gene expression suggested the existence of a previously undescribed glycolysis/HIF-1 feed forward loop. To test this possibility we used an isolated panel of siRNAs specific to 30 glycolysis genes and their isoforms (including pyruvate dehydrogenase, which is responsible for post-glycolytic pyruvate modification in mitochondria) and measured HRE-luciferase activity and cell viability in the same well. Using MIA PaCa-2 pancreatic cancer cells, we found compelling evidence that glycolytic enzyme activity is critical for the normal functionality of HIF-1, further confirming the observations that we made following the primary screen (**Figure 6**). Similar results were obtained using PANC-1 HRE-luc pancreatic, MDA-MB-231 HRE-luc metastatic breast and HT-29 HRE-luc colon cancer cell lines which had been stably transfected with the same HRE-luc reporter used for the MIA PaCa-2 cells in the primary screen (**Figures 7 - 9**). Despite marked changes in HIF-1 activity in gene knockdown events across many of the siRNAs included in the panel, cell growth inhibition was rarely more than 25% except in the case of ALDOA knockdown. The decrease in normalized HRE-luc activity (luciferase activity normalized to effects seen on cell viability to remove cell death or growth inhibition as a possible false positive for inhibition of HIF-1 activity) in all lines followed the same pattern as the greatest decrease was observed following ALDOA inhibition, followed closely by knockdown of PGK1 (phosphoglycerate kinase 1) or its isoform PGK2 (phosphoglycerate kinase 2) depending on the cell line. It is for this reason that ALDOA was selected for further development of novel, dual glycolysis/HIF inhibitors.

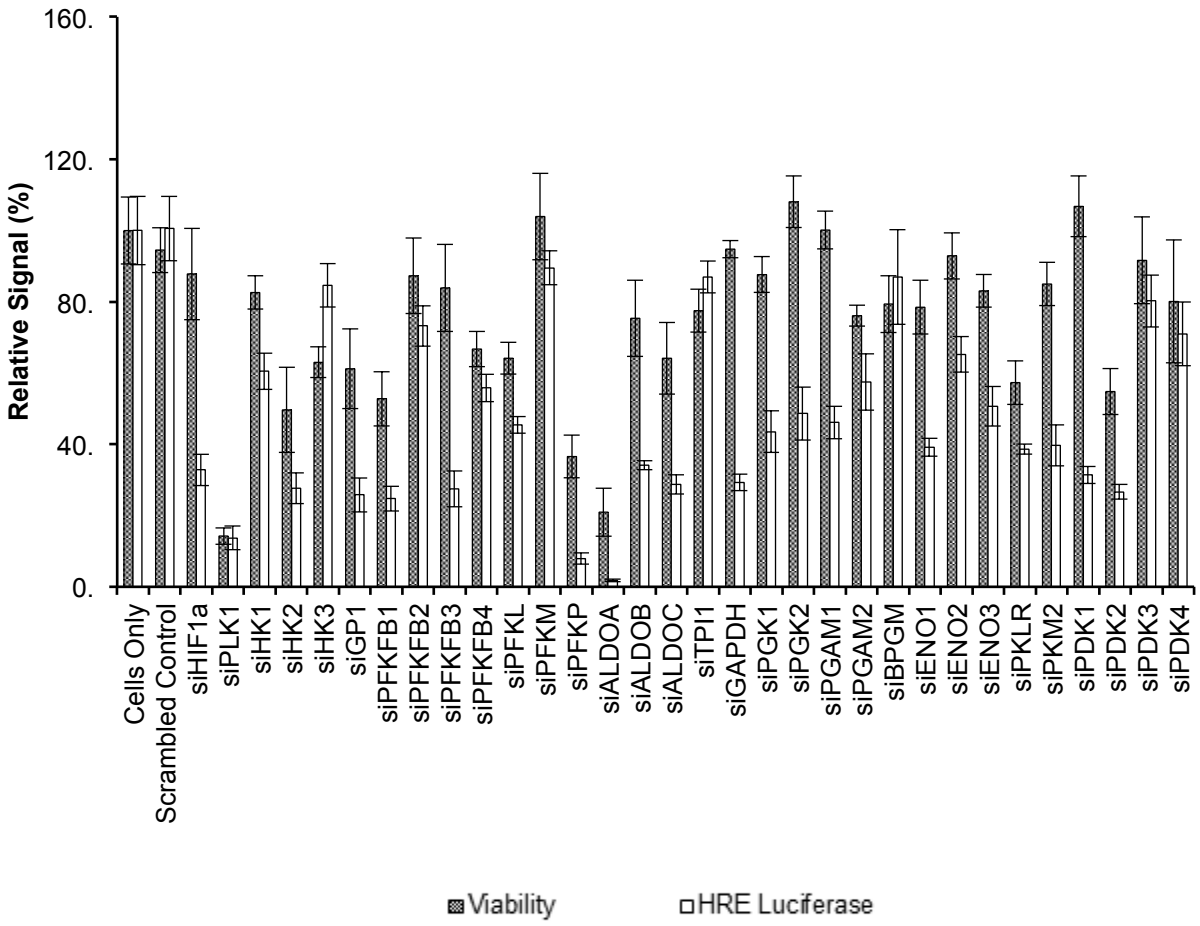


**Figure 6. Changes in Glycolytic Enzyme Expression Alters HIF-1 Activity in MIA PaCa-2 HRE-luc Cells.**

Thirty genes encoding glycolytic enzyme isoforms were selected for validation from a genome-wide siRNA screen for inhibitors of cellular HIF-1 activity. HIF-1 activity was measured using MIA PaCa-2 pancreatic cancer cells stably transfected with a constitutively expressed HRE-luciferase reporter 72 hr after siRNA reverse transfection and after 24 hr hypoxia (1% oxygen). Values were then normalized to cell viability in the same wells following aspiration of viability reagent. Scrambled non-targeting, HIF-1α, and PLK1 (polo like kinase-1 for toxicity) siRNAs served as controls. Bars represent S.D. of 3 studies.

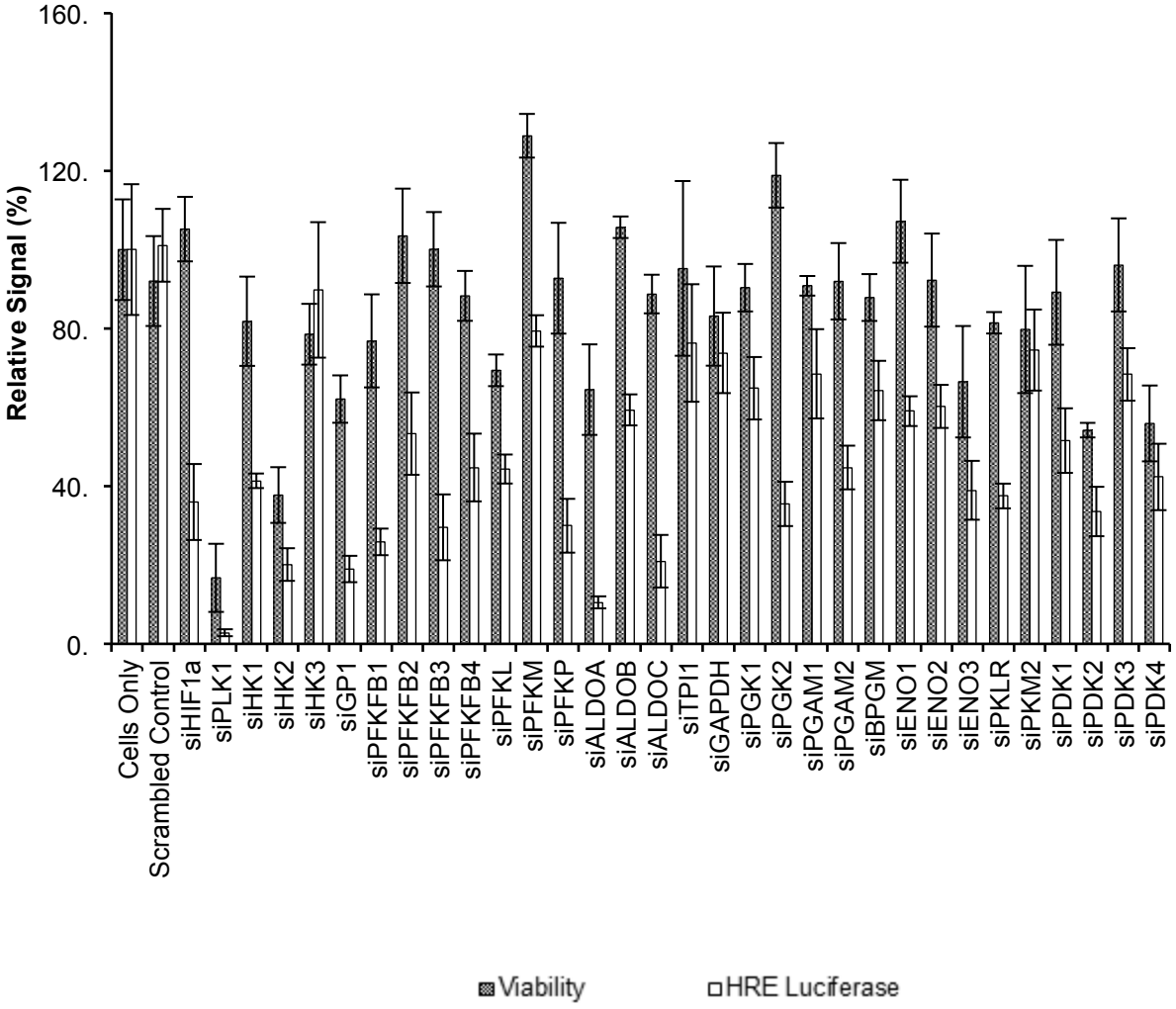


**Figure 7. Changes in Glycolytic Enzyme Expression Alters HIF-1 Activity in PANC-1 HRE-luc Cells.**

Same panel of thirty genes encoding glycolytic enzyme isoforms selected for validation from a genome-wide siRNA screen for inhibitors of cellular HIF-1 activity were used to validate effects as measured in the MIA PaCa-2 line used for primary screening purposes. HIF-1 activity was measured using PANC-1 pancreatic cancer cells stably transfected with a constitutively expressed HRE-luciferase reporter 72 hr after siRNA reverse transfection and after 24 hr hypoxia (1% oxygen). Values were then normalized to cell viability in the same wells following aspiration of viability reagent. Scrambled non-targeting, HIF-1α, and PLK1 (polo like kinase-1 for toxicity) siRNAs served as controls. Bars represent S.D. of 3 studies.

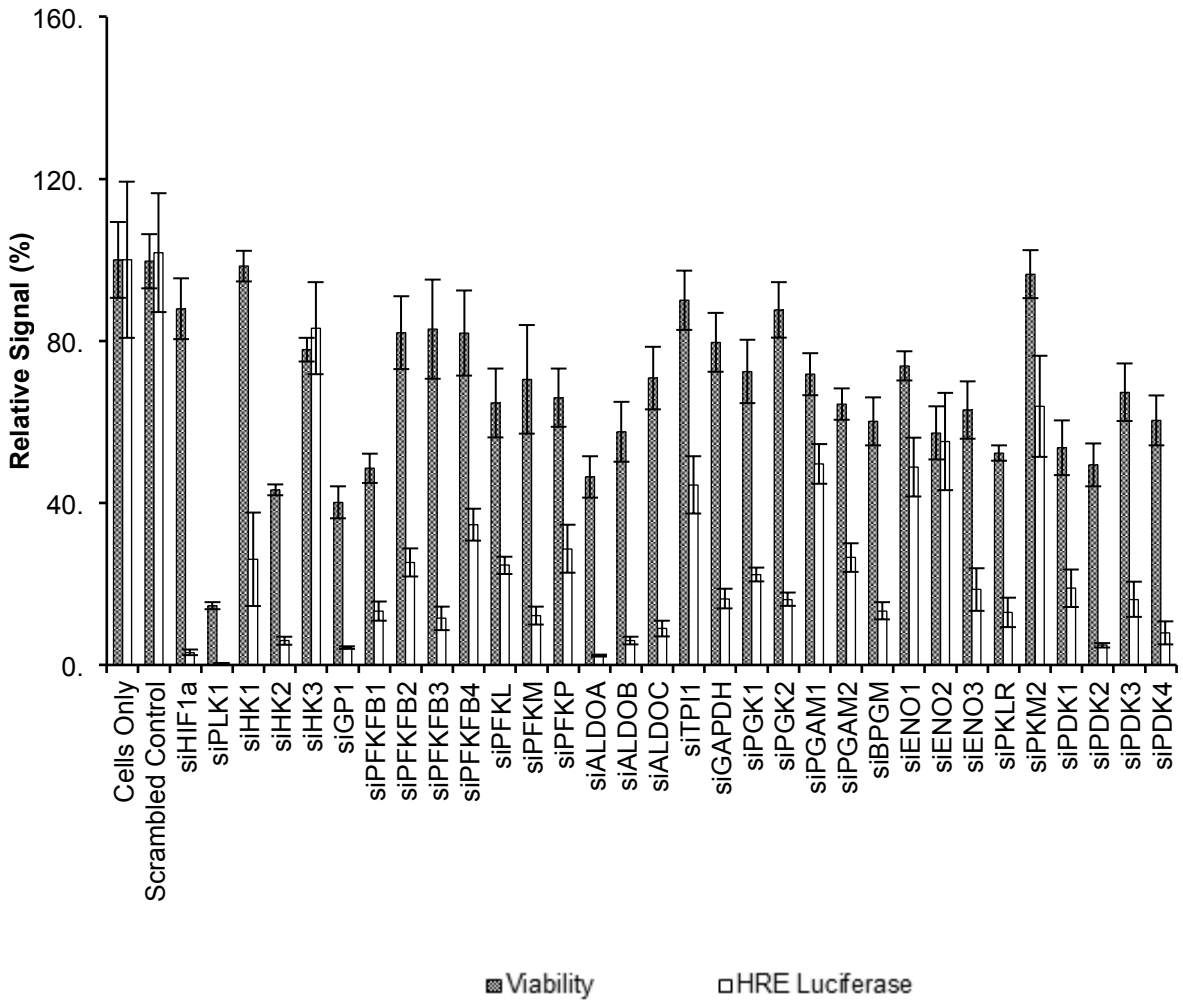


**Figure 8. Changes in Glycolytic Enzyme Expression Alters HIF-1 Activity in MDA-MB-231 HRE-luc Cells.**

Same panel of thirty genes encoding glycolytic enzyme isoforms selected for validation from a genome-wide siRNA screen for inhibitors of cellular HIF-1 activity were used to validate effects as measured in the MIA PaCa-2 line used for primary screening purposes. HIF-1 activity was measured using MDA-MB-231 metastatic breast cancer cells stably transfected with a constitutively expressed HRE-luciferase reporter 72 hr after siRNA reverse transfection and after 24 hr hypoxia (1% oxygen). Values were then normalized to cell viability in the same wells following aspiration of viability reagent. Scrambled non-targeting, HIF-1α, and PLK1 (polo like kinase-1 for toxicity) siRNAs served as controls. Bars represent S.D. of 3 studies.

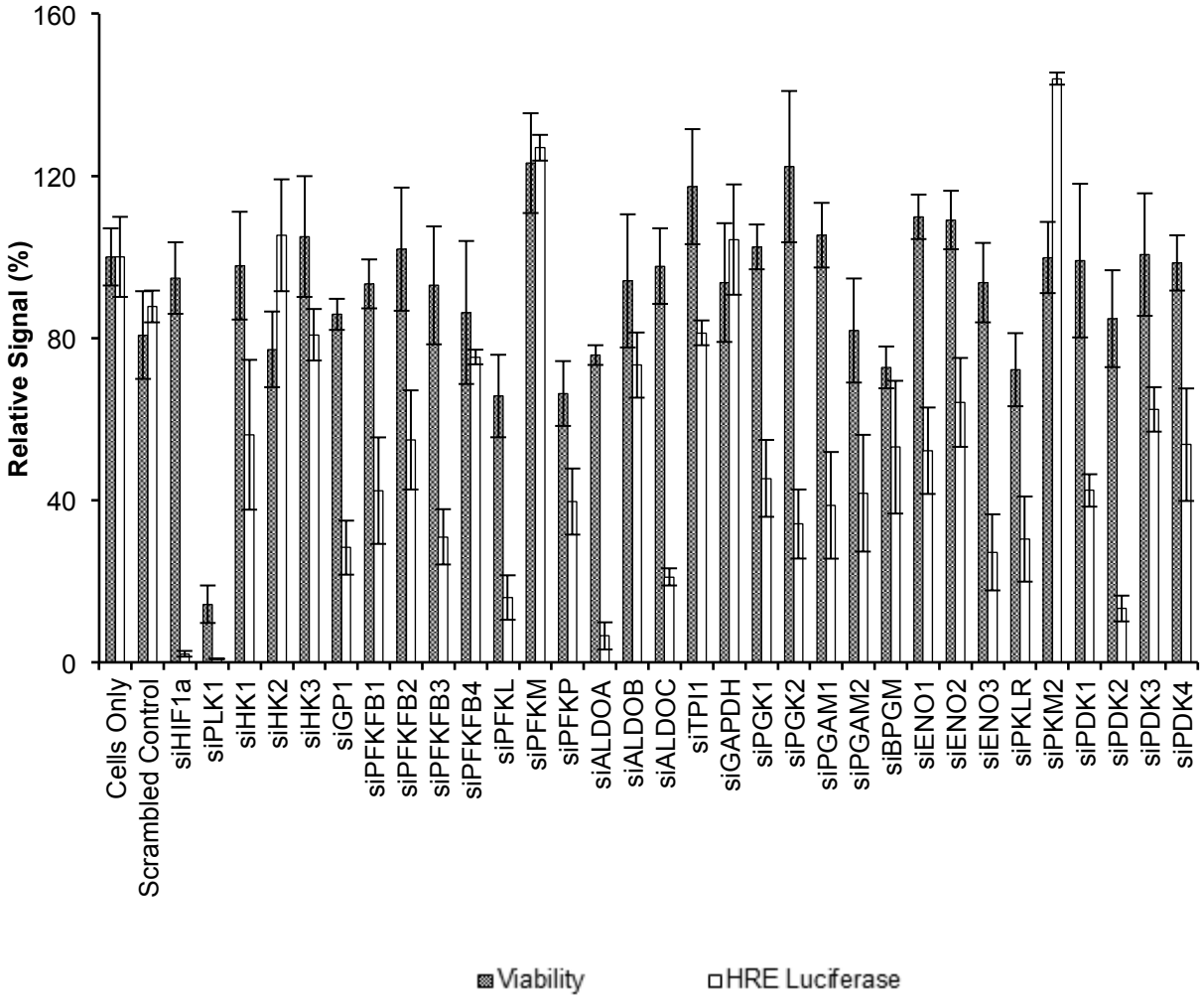


**Figure 9. Changes in Glycolytic Enzyme Expression Alters HIF-1 Activity in HT-29 HRE-luc Cells.**

Same panel of thirty genes encoding glycolytic enzyme isoforms selected for validation from a genome-wide siRNA screen for inhibitors of cellular HIF-1 activity were used to validate effects as measured in the MIA PaCa-2 line used for primary screening purposes. HIF-1 activity was measured using HT-29 colon cancer cells stably transfected with a constitutively expressed HRE-luciferase reporter 72 hr after siRNA reverse transfection and after 24 hr hypoxia (1% oxygen). Values were then normalized to cell viability in the same wells following aspiration of viability reagent. Scrambled non-targeting, HIF-1α, and PLK1 (polo like kinase-1 for toxicity) siRNAs served as controls. Bars represent S.D. of 3 studies.

Similar inhibitory effects were observed in the 786-0 renal adenocarcinoma cell line stably transfected with the same HRE-luciferase promoter, suggesting that regulation of HIF activity is not limited to HIF-1, as these cells express HIF-2 exclusively. Furthermore, differences with this cell line provided additional insight into the fact that siRNA mediated knockdown of glycolytic enzyme expression inhibits HIF-dependent HRE activity in these cells but not the constitutive CMV-luciferase found in a paired cell line which we generated, suggesting that these enzymes are indeed critical for cellular HIF activity rather than solely inhibiting general luciferase activity in our endpoint assays (**Figure 10**).

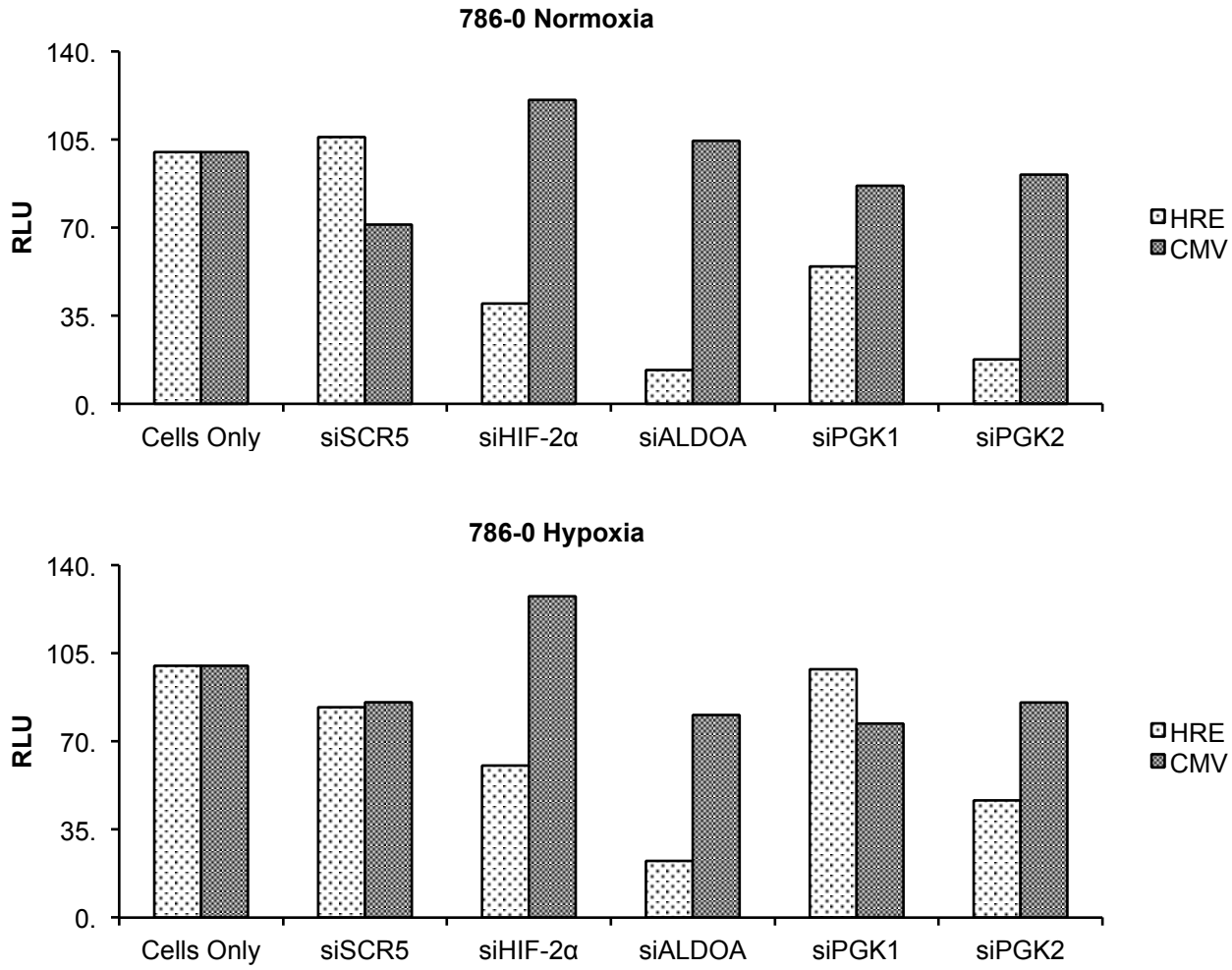


**Figure 10. Glycolytic Enzyme Expression is Critical for Global HIF Activity**

786-0 renal adenocarcinoma cells were used to demonstrate the effect of glycolytic enzyme knockdown on global HIF activity since these cells express no HIF-1α; instead they express only HIF-2α. Additionally, a complimentary 786-0 line was generated with a constitutively active CMV-luciferase reporter and was used to show that siRNA mediated silencing of glycolytic enzymes reduces luciferase activity in a HIF dependent manner rather than global luciferase inhibition. Scrambled non-targeting and HIF-2α siRNAs served as controls.

ALDOA knockdown also resulted in the greatest inhibition of cell proliferation amongst the panel of selected hits from the global siRNA screen. Following identification of the initial hits from the original, pooled library screen, a second siRNA manufacturer was identified (Qiagen) and individual oligos for selected targets were ordered and tested. By selecting sequences from a second manufacturer, the potential for siRNA off-target effects experienced in the primary screen can be overcome by two mechanisms. First, the deconvolution of the original pooled library which contained four sequences targeting a single gene in a single well can be screened independently. Second, by using a sequence different than that found in the original pool, the documented phenomenon of exogenous introduction of siRNA into a cell and subsequent possible downregulation of the expression of a large subset of genes in a microRNA-like manner [79-81] can be overcome. Since only short regions of sequence homology between the siRNA and target sequences are required for this effect, a greater variety in the tested sequences adds confidence during validation steps. Results from the primary screen were validated in this way using all four cancer cell lines previously mentioned for ALDOA, PGK1 and PGK2 with comparable results amongst the lines (**Table 3**).

| | | | Median Relative Luciferase Units (HRE Luciferase/Viability) | | | |
|---|---|---|---|---|---|---|
| **Sequence ID** | **Accession Number** | **Gene ID** | **MIA PaCa-2 HRE** | **PANC-1 HRE** | **MDA-MB-231 HRE** | **HT-29 HRE** |
| **Oligo 1** | NM_000034 | **ALDOA** | 24.41 | 33.07 | 26.70 | 79.85 |
| **Oligo 2** | NM_000034 | **ALDOA** | 23.21 | 23.10 | 23.16 | 20.23 |
| **Oligo 3** | NM_000034 | **ALDOA** | 22.54 | 22.32 | 22.94 | 21.42 |
| **Oligo 1** | NM_000291 | **PGK1** | 50.78 | 38.40 | 25.68 | 30.59 |
| **Oligo 2** | NM_000291 | **PGK1** | 43.60 | 30.83 | 26.01 | 44.54 |
| **Oligo 3** | NM_000291 | **PGK1** | 53.25 | 49.33 | 39.59 | 30.04 |
| **Oligo 1** | NM_138733 | **PGK2** | 92.98 | 64.60 | 49.88 | 56.49 |
| **Oligo 2** | NM_138733 | **PGK2** | 17.49 | 16.81 | 15.34 | 18.71 |
| **Oligo 3** | NM_138733 | **PGK2** | 34.88 | 21.55 | 13.55 | 23.63 |

**Table 3. ALDOA Knockdown Shows Greatest Inhibition of HRE Activity in Secondary Validation**

Using siRNA from a second manufacturer, individual oligos from the original pool are deconvoluted and screened individually. As a result, Aldolase A was again confirmed to have the greatest effect on HRE luciferase activity following siRNA knockdown.

Dual transfection of siRNAs targeting PGK1 and PGK2 suggested overlapping activities as the combined, double knockdown gave at least additive inhibition of HRE-luc activity, without significant inhibition of cell proliferation (**Figure 11**). ALDOA and PGK1 or PGK2 knockdown inhibited cellular glycolysis, as measured by Seahorse® technology, in all lines (**Figure 12**) and, additionally, markedly decreased cellular ATP in hypoxic MIA PaCa-2 and PANC-1 cells (**Figure 13**). HIF-1 knockdown was included as a control and resulted in a similar decrease in ATP level, as expected due to decreased overall glycolysis. The results suggested to us that the effects of ALDOA and PGK1/2 on HIF-1 could be mediated by AMPK that is commonly activated in response to elevated AMP when cell ATP levels are lowered [82, 83].

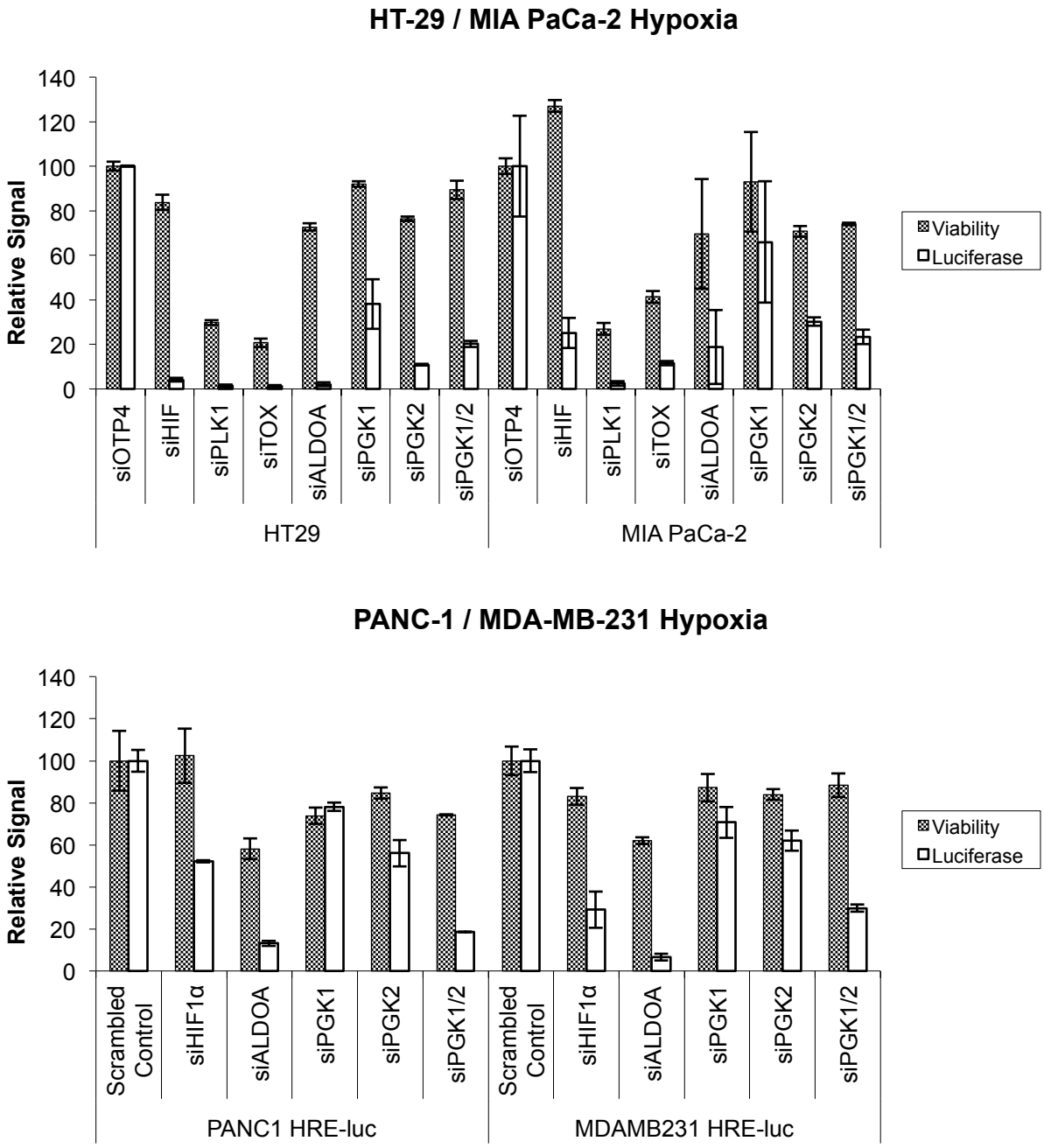


**Figure 11. Dual Transfections of siPGK1 and siPGK2 Suggest Redundant Function**

The additive effect on HRE-luciferase inhibition in dual transfected samples suggests inhibition of both PGK1 and PGK2 isoforms is needed to achieve significant levels of hindrance of HIF activity; further development of PGK inhibitors would require dual action.

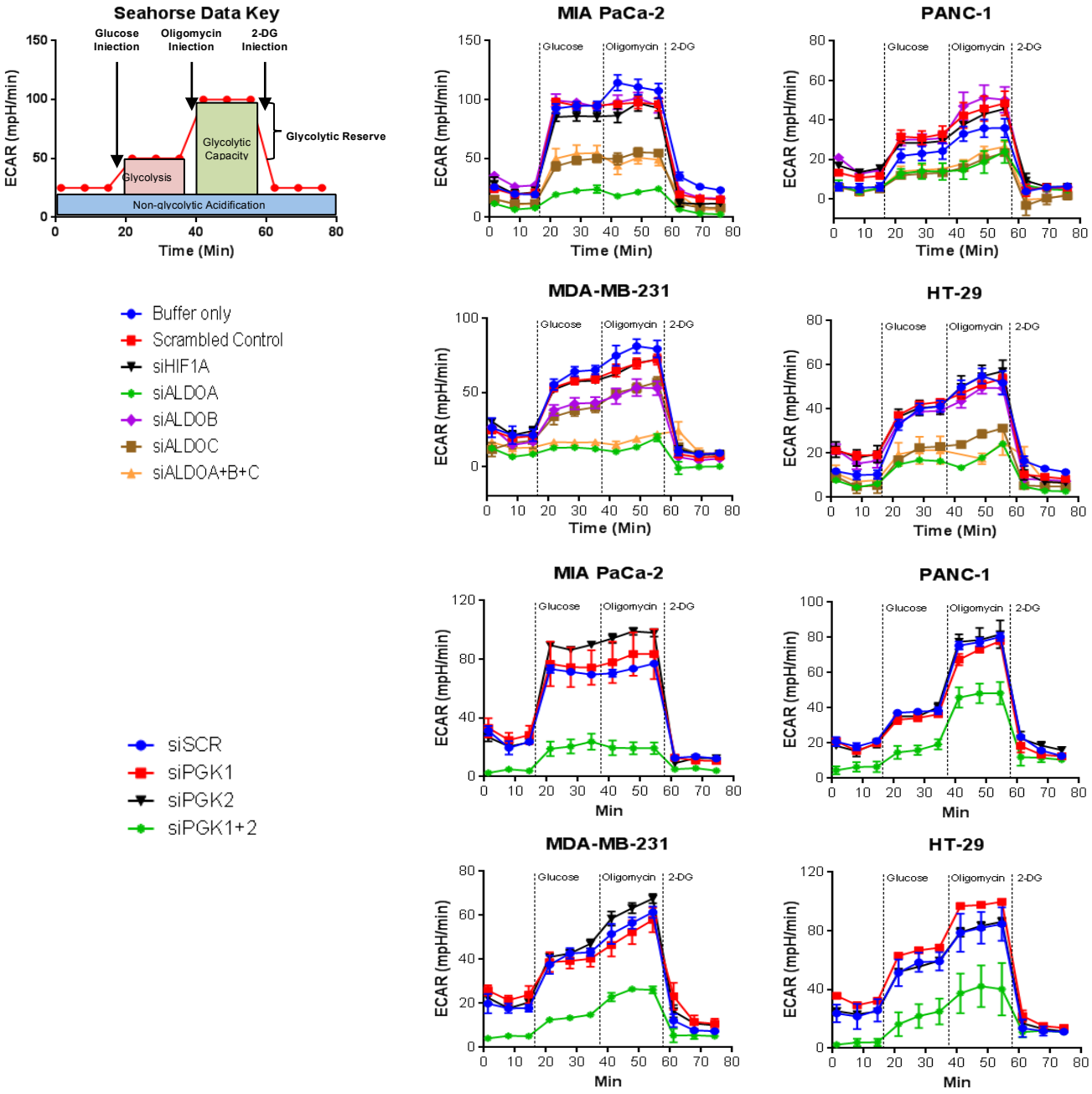


**Figure 12. siRNA Knockdown of Key Glycolytic Enzymes Inhibits Cellular Glycolysis**

The rate of cellular glycolysis and glycolytic reserve (defined as excess glycolytic capacity following Oligomycin-mediated inhibition of mitochondrial oxidative phosphorylation) was measured using Seahorse® technology, as illustrated in the data key at left in all four of the HRE-luciferase lines used throughout various experiments in this work (PANC-1 and MIA PaCa-2 pancreatic, MDA-MB-231 metastatic breast and HT-29 colon cancer lines). Measurements were taken after reverse transfection with siRNA targeting ALDO isoforms A, B and C (either separately or pooled), PGK1 and PGK2 (separately or pooled). Scrambled, non-targeting, and HIF-1α siRNAs served as controls. Bars represent standard deviations from four biological replicates for each sample.

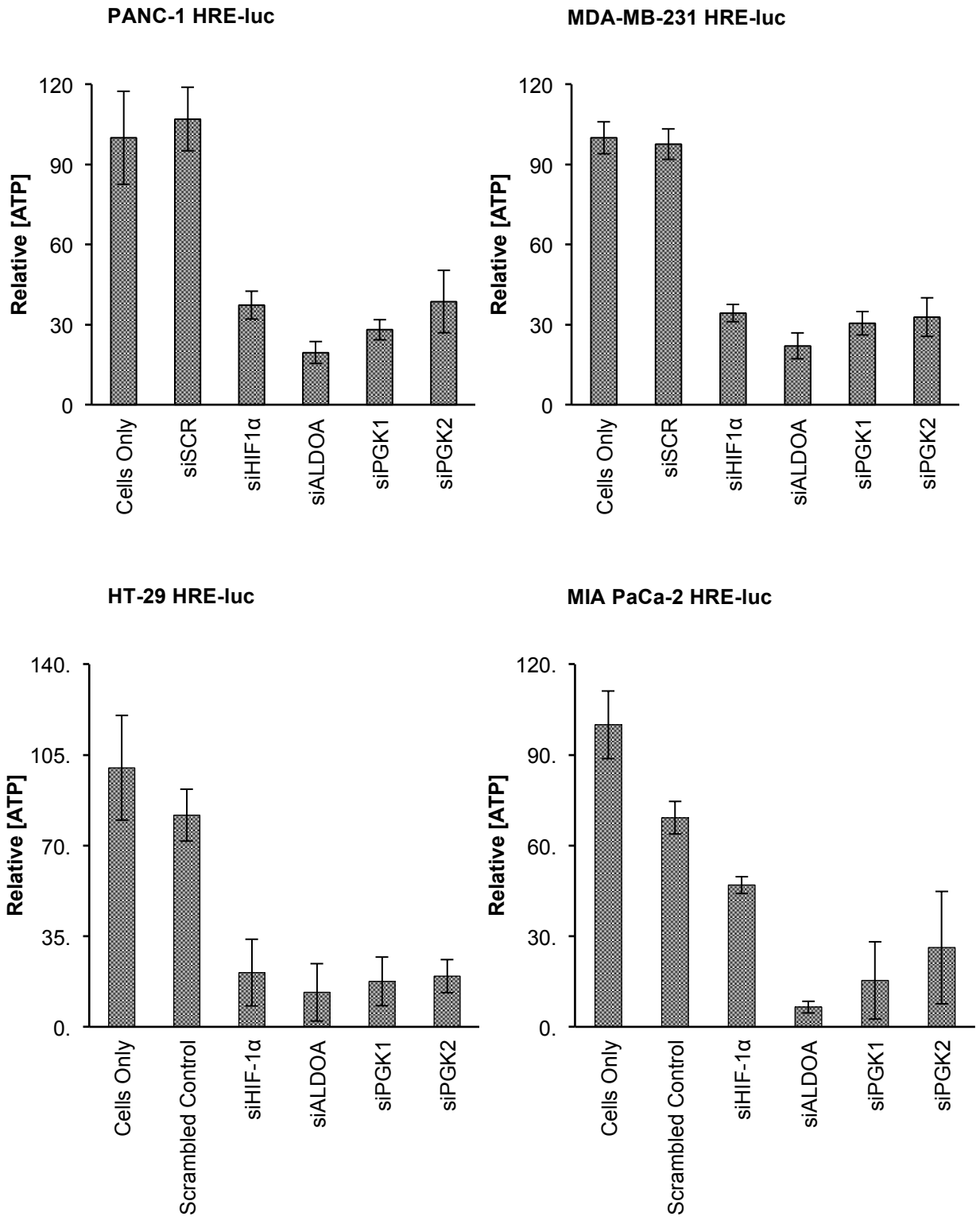


**Figure 13. siRNA Knockdown of Key Glycolytic Enzymes Inhibits Generation of ATP**

Cellular ATP levels 72 hours after transfection with siRNA targeting HIF-1α, ALDOA, and PGK1 or 2 and 16 hours in hypoxia. Bars represent standard deviation from three separate experiments.

**HIF-1α Activity is Mediated by AMPK Activation and EP300 Inactivation**

We first established that, in all cells, decreased HIF-1 activity caused by ALDOA or PGK1 or 2 knockdown occurred without changes in HIF-1 protein levels and was qualitatively similar in normoxia or hypoxia, although an overall greater effect was seen in hypoxia when HIF-1 levels are elevated (**Figure 14**). To evaluate possible mechanisms underlying this activity we co-transfected glycolysis-related siRNAs with siRNAs targeting proteins that are known to regulate HIF-1 activity; [84, 85]. We found that AMPK siRNA rescued the effects of ALDOA or PGK2 knockdown on HIF-1 inhibition, but observed little effect when glycolytic siRNAs were transfected with p300 or PCAF siRNAs (**Figure 15**). FIH siRNA also reversed the effects of ALDOA and PGK1 on HIF-1 activity, likely due to loss of negative regulation of HIF-1. Evidence that the effect is mediated through AMPK regulated actions were further confirmed when the effect of ALDOA or PGK1 or PGK2 knockdown was abolished following treatment with the AMPK inhibitor dorsomorphin (**Figure 16**). Furthermore, western blotting showed that ALDOA knockdown significantly increased phosphorylation of AMPK on Thr172, a marker of AMPK activation in response to cellular stress such as ATP depletion [86-89], in both normoxia and hypoxia (**Figure 17**).

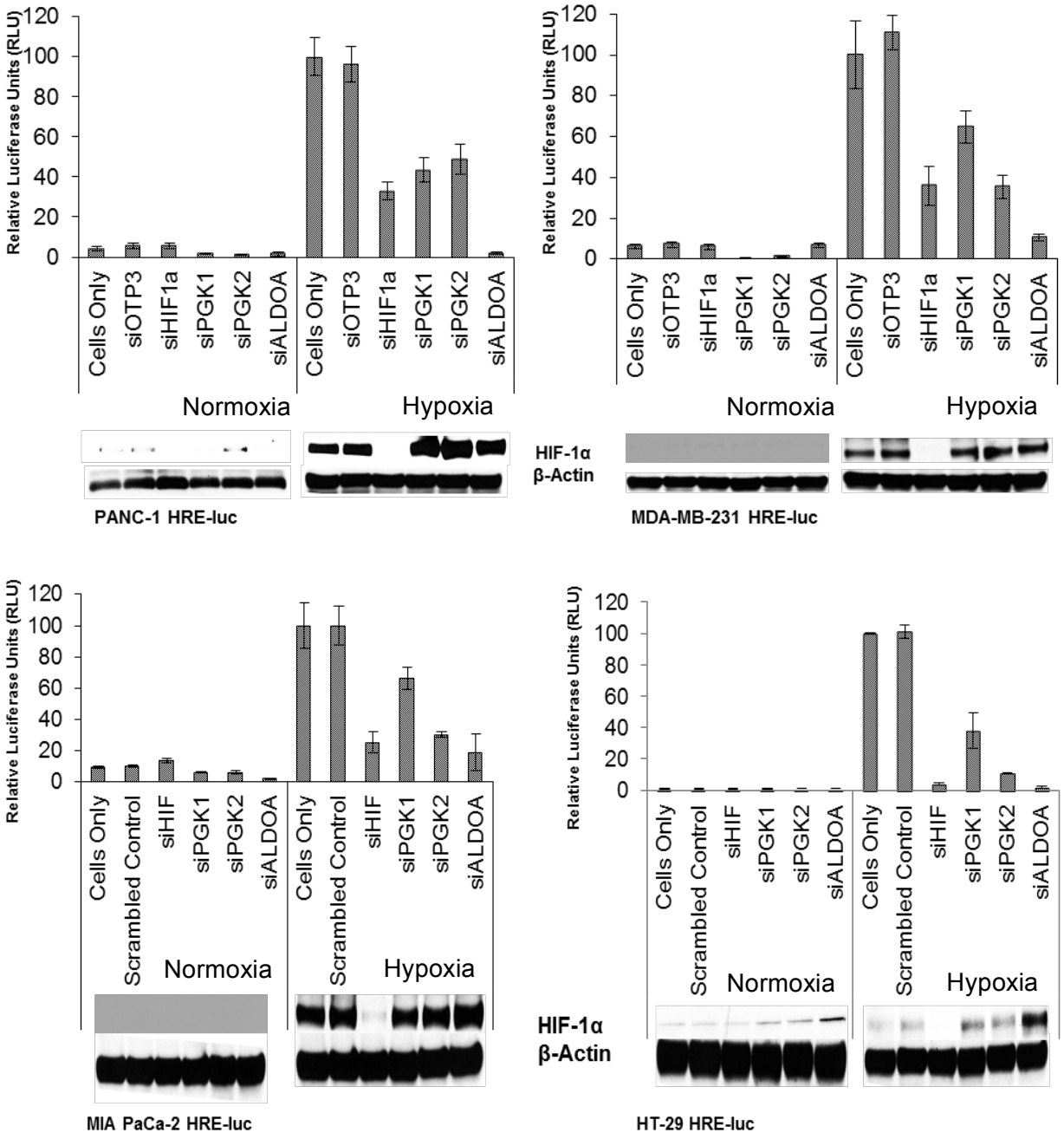


**Figure 14. Knockdown of ALDOA or PGK1 or 2 Inhibits HIF-1 Activity Without Decreasing HIF-1α Protein Levels.**

HIF activity was measured in air (Normoxia) or 1% O2 (Hypoxia) using four cancer cell lines of various types stably transfected with the HRE-luciferase reporter 72 hr after transfection with siRNA targeting ALDOA or PGK1 or 2 and after 24 hr in hypoxia. Bars represent S.D. HIF-1α protein was also measured by Western blotting. Scrambled, non-targeting, and HIF-1α siRNAs served as controls.

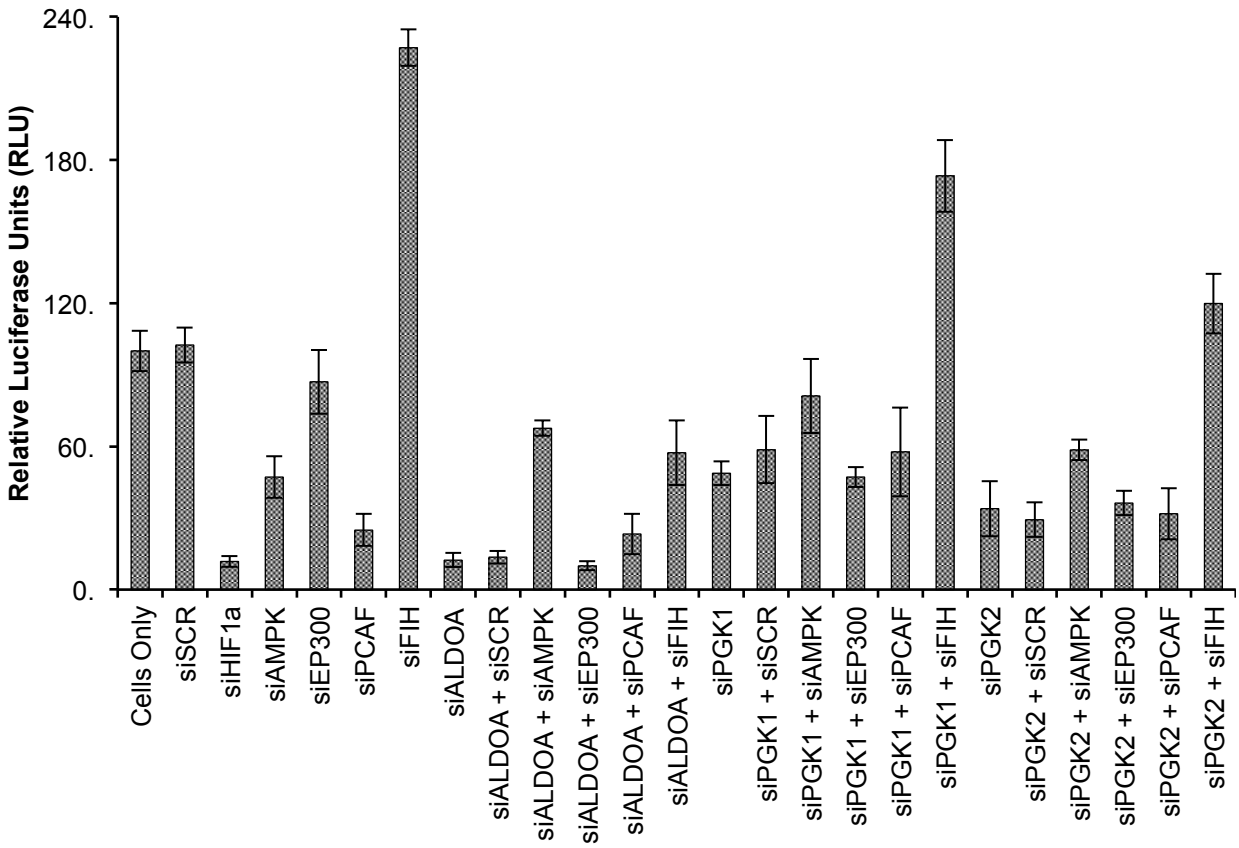


**Figure 15. Dual Transfections Suggest AMPK Responsible for Glycolytic Regulation of HIF Activity**

Dual reverse transfection of siRNAs targeting ALDOA or PGK1 or 2 plus siAMPK (protein kinase, AMP-activated, alpha 2 catalytic subunit), siEP300 (E1A-associated cellular p300 transcriptional co-activator protein), siPCAF (p300/CBP-associated factor), and siFIH (Factor Inhibiting HIF-1). Results indicate that AMPK inhibition mediates the effects of loss of ALDOA or PGK1 or 2 on HIF-1 activity.

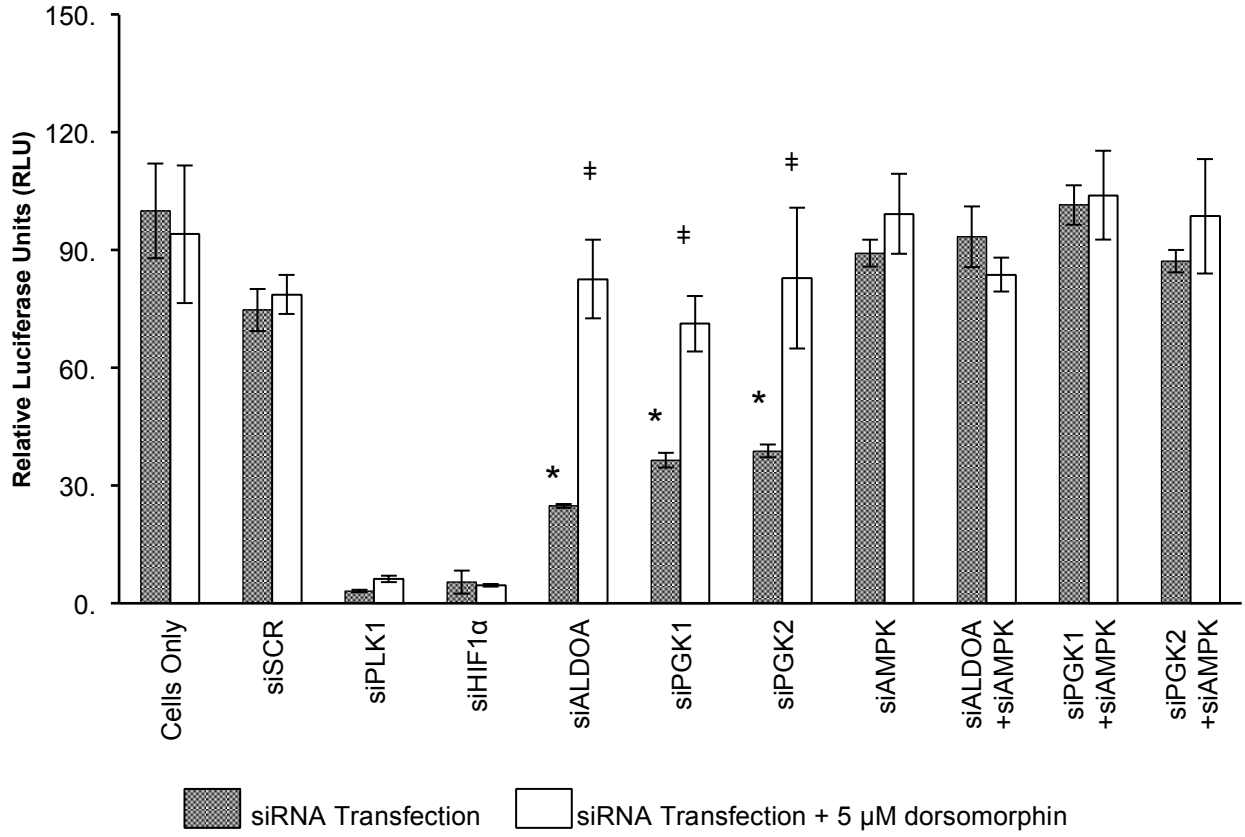


**Figure 16. Inhibition of AMPK Activity by siRNA Knockdown or Treatment with AMPK Inhibitor Leads to HIF Activity Recovery Following Glycolytic Enzyme Knockdown**

HIF-1 activity following knockdown of ALDOA, PGK1, or PGK2 72 hr after transfection and after 24 hr in hypoxia (filled boxes). Effects are rescued following treatment with the AMPK inhibitor dorsomorphin at 5 μM or with siRNA targeting AMPK (open boxes). "*" indicate a p value less than .05 comparing siTarget to dual transfections of siTarget and siAMPK; "ǂ" indicate a p value less than .05 comparing siTarget + DMSO treatment with siTarget + 5 micromolar dorsomorphin treatment

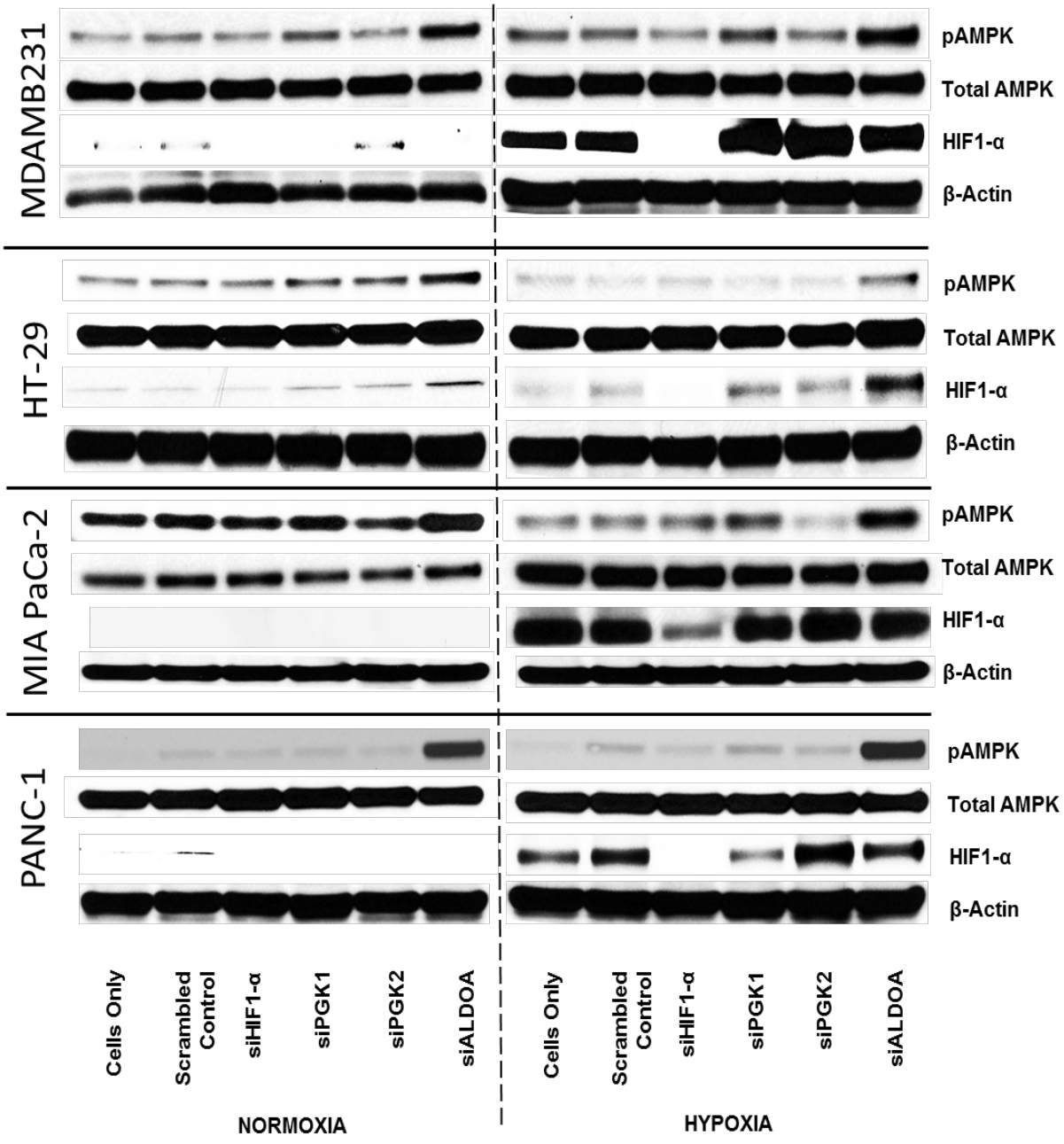


**Figure 17. ALDOA Knockdown Results in Hyper Activation of AMPK**

Western blot showing enhanced phosphorylation of AMPK (at Thr172 following silencing of ALDOA, or PGK1 or PGK2 72 hours after siRNA transfection and after 24 hours in hypoxia in MDA-MB-231, HT-29, MIA PaCa-2 and PANC-1 cells harboring the HRE-luciferase reporter.

We next addressed how activation of AMPK (5'AMP protein kinase) by phosphorylation on its activating loop at Thr172 in response to increased AMP, formed from ADP through adenylate kinase [90], could lead to inhibition of HIF-1 transcriptional activity. AMPK phosphorylates many downstream substrates, one of which is p300/CREB binding protein (p300/CPB) [91] a nuclear transcription factor necessary for HIF-1 transcriptional activity [92]. Unlike other phosphorylations of p300/CPB, phosphorylation on Ser89 by AMPK specifically blocks its transcriptional activity by interfering with its ability to act as a histone acetyltransferase [91]. Phosphorylation of p300 at Ser89, which we observed following knockdown of ALDOA or PGK2 particularly in hypoxic conditions, occurs following AMPK activation, attenuating the interaction of p300 with numerous nuclear receptors *in vitro* and *in vivo* [93] (**Figure 18**). Thus the mechanism we are proposing for the regulation of HIF-1 activity by glycolysis inhibitors is that, in response to lowered ATP, AMPK is activated and phosphorylation of p300/CREB at Ser89 leads to its dissociation from HIF-1 leading to decreased HIF-1 transcriptional activity.

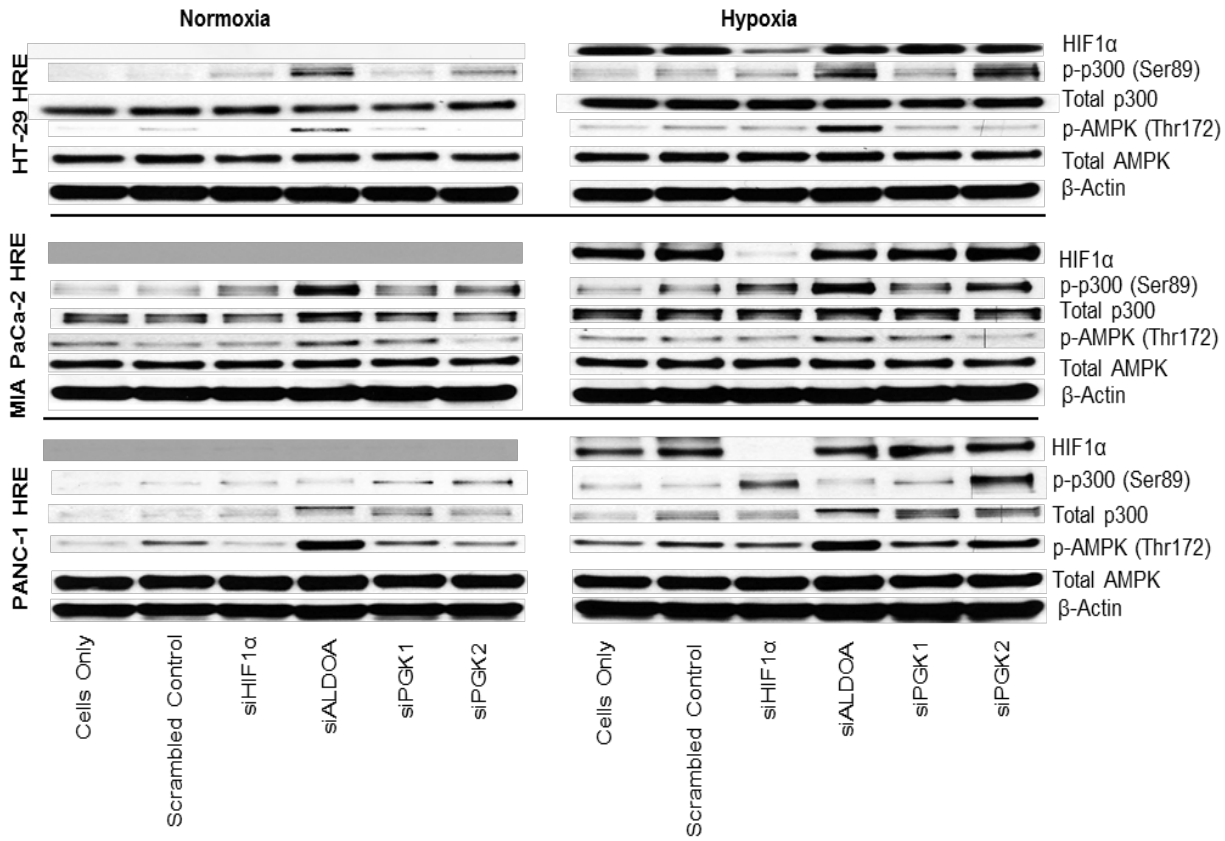


**Figure 18. EP300 Phosphorylation Mediates AMPK Effects on HIF-1 Activity**

Western blot showing enhanced phosphorylation of AMPK (at Thr172) and p300 (at Ser89) following silencing of ALDOA, or PGK1 or PGK2 72 hours after siRNA transfection and after 24 hours in hypoxia in HT-29, MIA PaCa-2 and PANC-1 cells harboring the HRE-luciferase reporter.

To investigate this further, EMSA analysis of MDA-MB-231 HRE luc cells with siRNA mediated knockdown of ALDOA show a complete loss of HIF-1 binding to HRE sequences on DNA. Dual transfection of both siALDOA and siAMPK result in a restoration of HIF-1 binding (**Figure 19**). These results suggest that inhibition of glycolysis and a concomitant decrease in HIF-1α activity are mediated by AMPK activation, possibly in response to low cellular ATP levels, which in turn promotes p300 phosphorylation and terminates its ability to co-activate HIF-1 transcriptional activity (**Figure 20**).

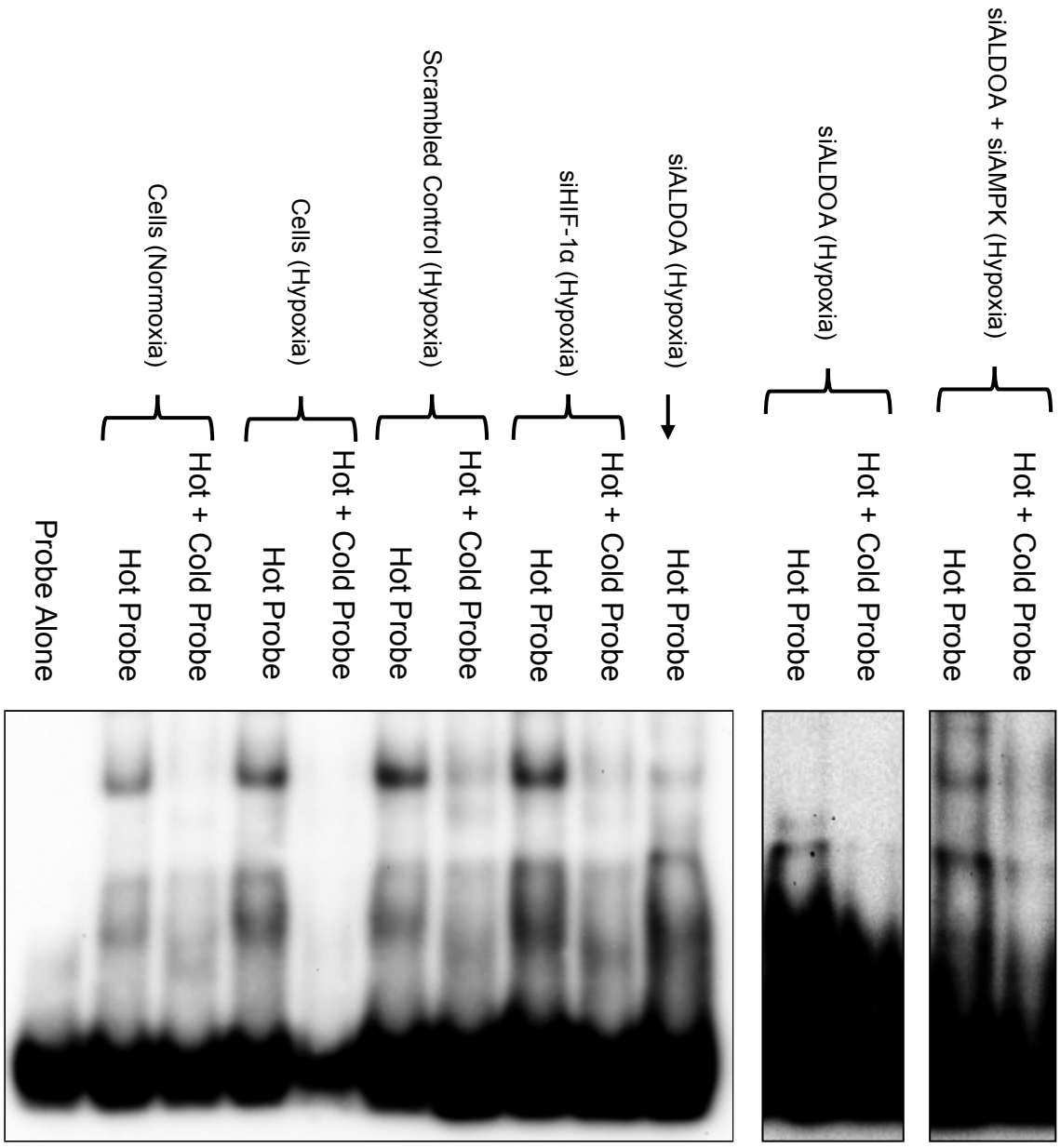


**Figure 19. siRNA Mediated Knockdown of ALDOA in MDA-MB-231 Cells Results in Loss of HIF-1 DNA Binding Ability.**

Electrophoretic Mobility Shift Assay showing complete loss of HIF-1 binding to HRE sequences following knockdown of ALDOA. Binding ability is restored with coincidental knockdown of AMPK.

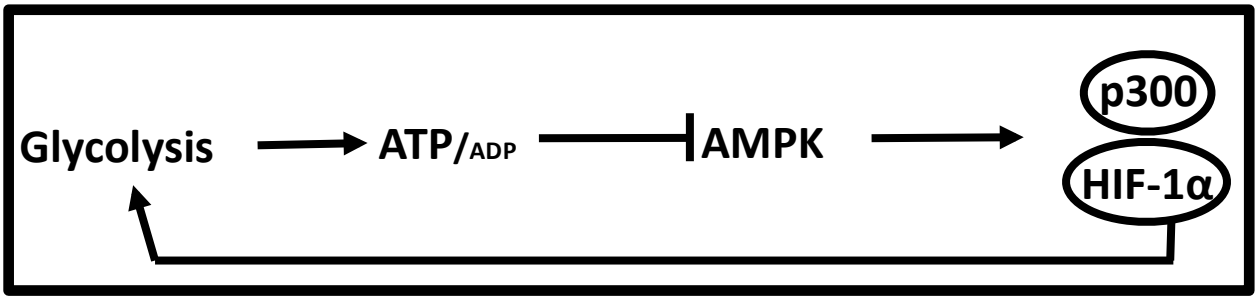


**Figure 20. Proposed Mechanism of Glycolytic Control of Cellular HIF-1 Activity**

**Variable Expression of Aldolase Isoforms Suggest Compensatory Effects on Glycolysis**

To further understand variable effects of ALDOA knockdown on proliferation amongst the four HRE luciferase lines we next conducted immunoblotting to analyze expression of Aldolase B and C isoforms in normoxia and hypoxia to uncover possible compensatory mechanisms when ALDOA is eliminated. Interestingly, we found that the HT-29 HRE line, which shows only minimal decreases in cell viability after ALDOA knockdown, exhibits significantly higher expression of ALDOA compared to MDA-MB-231, MIA PaCa-2 and PANC-1 lines, which show significant decreases in viability following ALDOA knockdown (**Figure 21**). Additionally, high expression of ALDOC in the HT-29 line suggests a possible compensatory effect in the absence of ALDOA at this step of glycolysis. Irregular expression patterns of ALDOA and PGK1 and PGK2 proteins were confirmed by western blot analysis in 12 lung cancer cell lines (**Figure 22**).

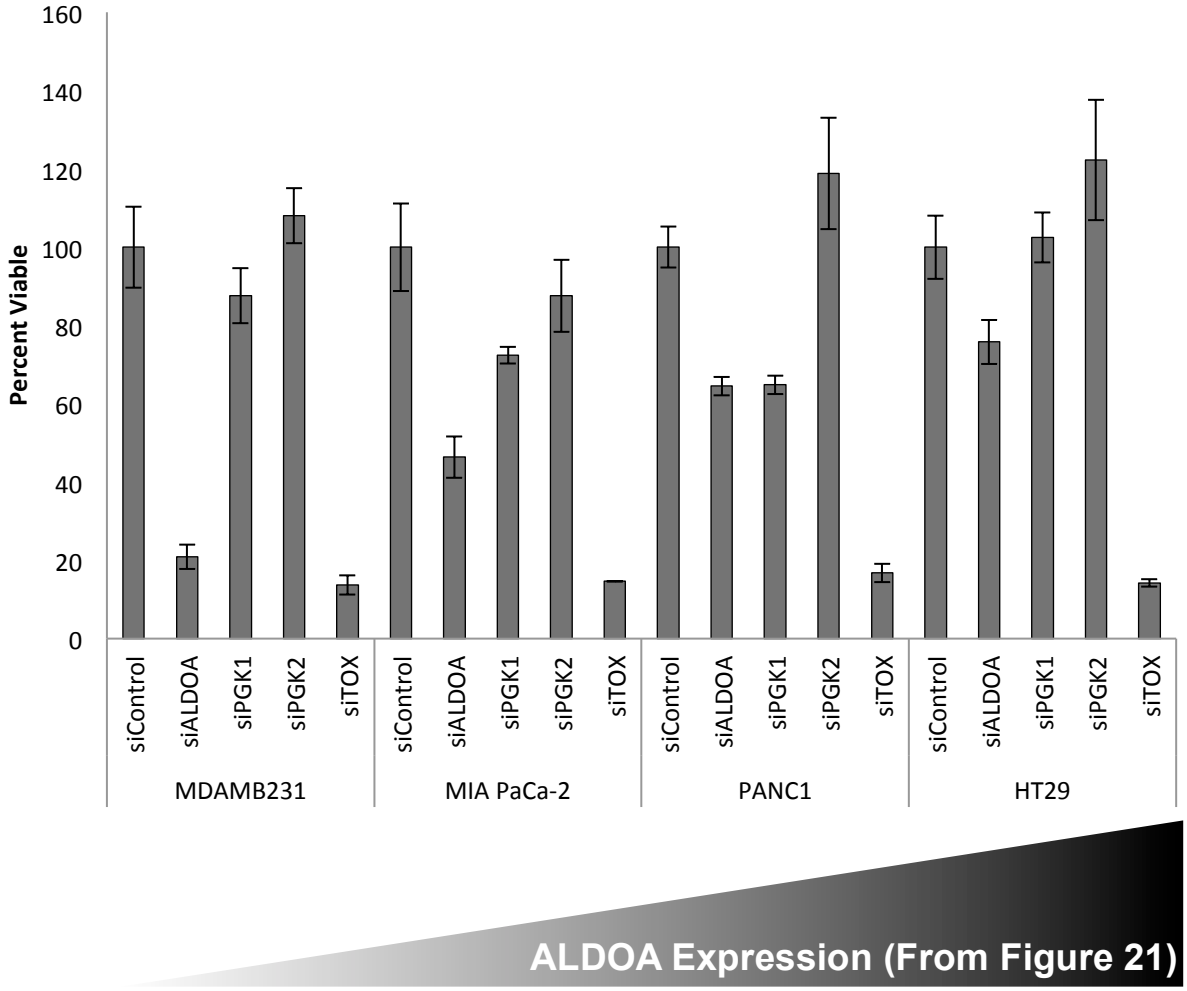


**Figure 21. Aldolase Expression Level Correlates with Sensitivity to siRNA Mediated Knockdown**

Cells expressing low levels of ALDOA are especially sensitive to siALDOA knockdown while cells expressing high levels are less sensitive.

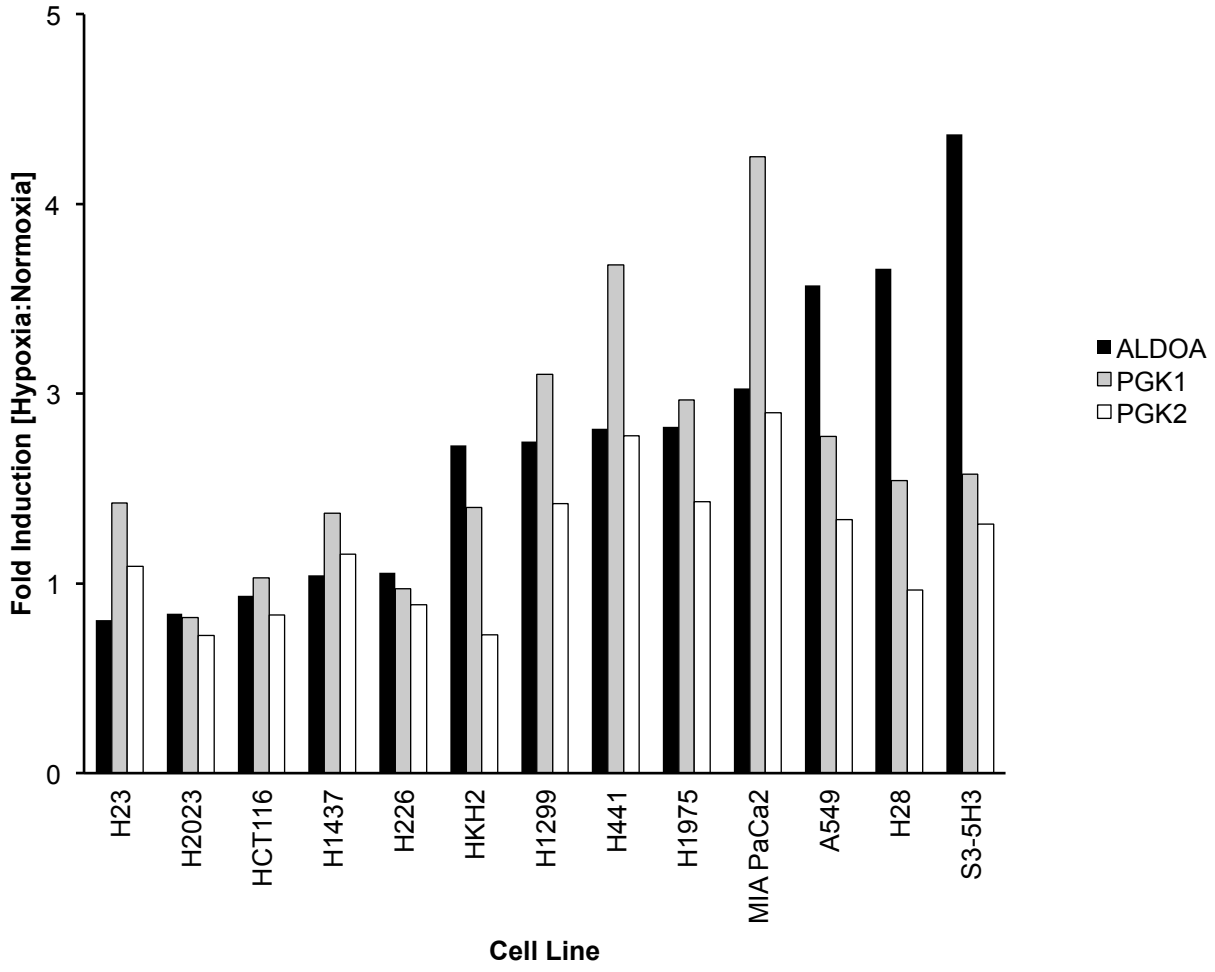


**Figure 22. Differential Expression of ALDO or PGK Isoforms in Cancer Cell Lines**

The panel of cell lines used in Western blot analysis of PGK1, PGK2 and ALDOA was expanded to include cell lines from various tumor types and stage. Densitometry analysis of western blots of lysates from these lines compares the induction measured between normoxia and hypoxia treated samples.

**Inducible ALDOA knockdown Extends Median Survival in an *in vivo* Model of Metastatic Breast Cancer**

To validate ALDOA as a potential therapeutic target and because we have shown that ALDOA knockdown is acutely toxic to cancer cells *in vitro* we expressed a doxycycline-inducible ALDOA shRNA in MDA-MB-231 HRE-luciferase cells, and then used those cells to establish an orthotopic model of metastatic breast cancer in female NOD-SCID mice. Two clonal lines showing complete (clone 8.8) or partial (clone 9.7) ALDOA knockdown and glycolysis inhibition following doxycycline treatment were used (**Figure 23**). Mice fed doxycycline either one week before implantation of cells or when the primary tumor reached approximately 250 $mm^3$ showed increased median lifespan. Mice fed doxycycline a week before implantation showed increases from 37 days in parental, and 41 days in empty vector transfected cells, to 50 and 56 days in two clonal cells lines ($p<0.001$in both cases); mice treated once tumors were established showed increases from 41 days (untreated) to 48 days ($p < 0.001$ compared to control) (**Figure 24**). Since the inducible shALDOA vectors were transduced into HRE-luciferase cells, transdermal fluorescence imaging of the mice was made possible as a measure of HIF activity *in vivo.* With this additional measure, we hypothesize that the extended life expectancy as a result of shALDOA knockdown can be partly attributed to an inhibition of HIF activity since luciferase readings in mice with sh8.8 showed significantly lower mean luciferase readings in both pre-treated and doxycycline treated established tumors compared to tumors established from the parental cell line (**Figure 25**). Postmortem analysis of mice indicated significant metastasis from the primary tumor to the lungs and liver in tumors derived from parental lines but not from tumors derived from the transduced clones.

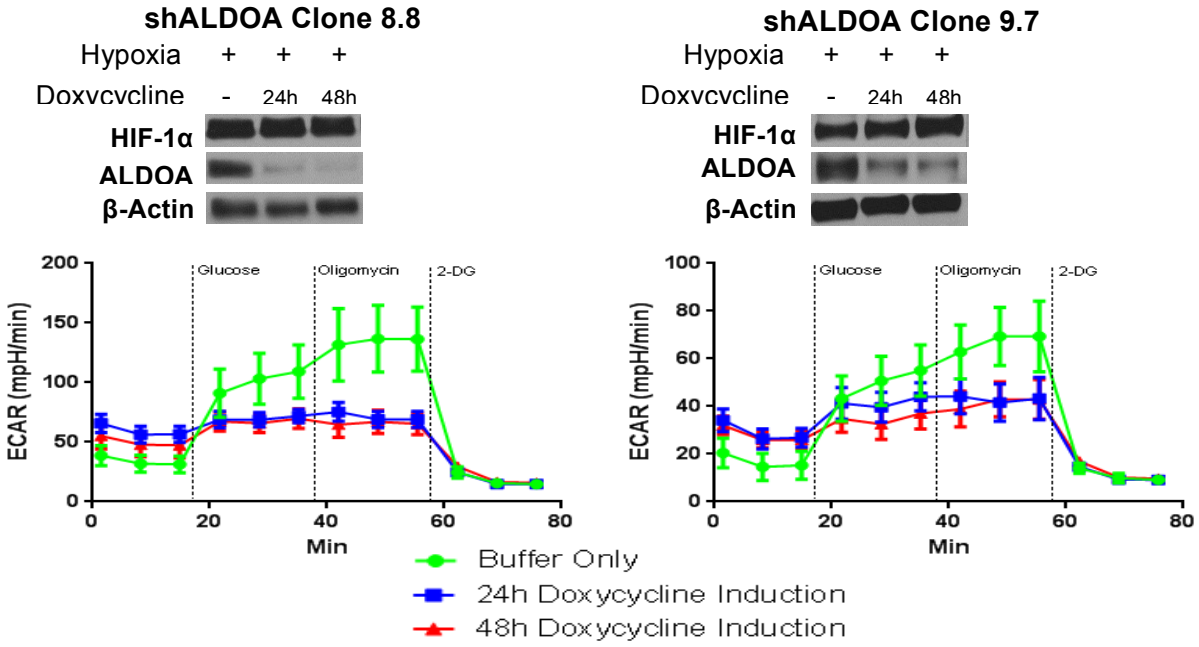


**Figure 23. Inducible shALDOA MDA-MB-231 Breast Cancer Lines Established for Use in *in vivo* Studies.**

Two lentiviral shALDOA doxycycline-inducible clones of MDA-MB-231 metastatic breast cancer cells were established (clones 8.8 and 9.7). Both show doxycycline-inducible ALDOA knockdown together with inhibition of glycolysis (as assessed using Seahorse® technology) and reduced HIF-1α activity, based on activity of the HRE-luciferase reporter measured under hypoxic conditions.

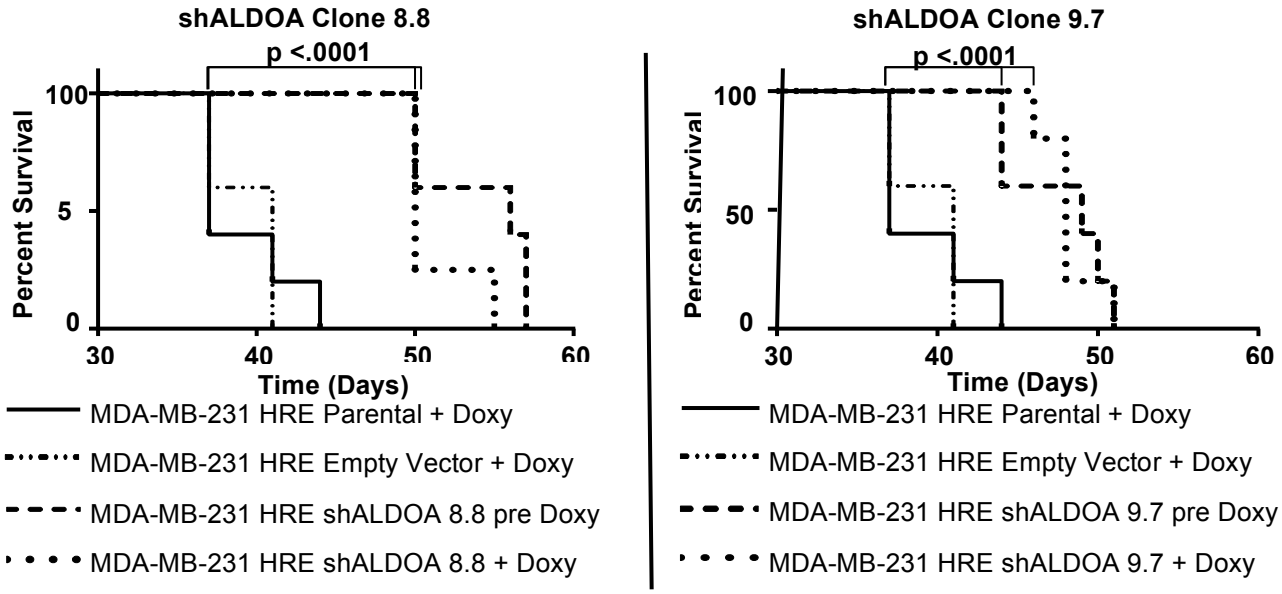


**Figure 24. Inducible ALDOA Knockdown in MDA-MB-231 Breast Cancer Tumors Extends Survival of Xenografted Mice.**

Groups of 5 immunodeficient SCID mice were injected in the breast fat pad with $1x10^6$ MDA-MB-231 parental or vector-only cells, or with clones 8.8 or 9.7. Animals received dietary doxycycline (625 mg/kg) starting 7 days before injection of cells or when tumors reached approximately 250 $mm^3$. Death occurred in all cases associated with metastasis of the MDA-MB-231 cells to the liver and lungs. Median survival of mice with parental MDA-MB-231 tumors was 37 days and with empty vector cells 41 days. Following doxycycline treatment mice injected with clone 8.8 or clone 9.7 cells 7 days before cell injection had a median survival of 56 days and 50 days, respectively ($p<0.001$ relative to combined controls groups in both cases). Animals receiving doxycycline treatment when the tumors reached ~ 250 $mm^3$ had a median survival of 41 and 48 days ($p<0.001$ compared to combined control groups in both cases). At the time of death, lungs and liver of the mice showed extensive metastatic nodules.

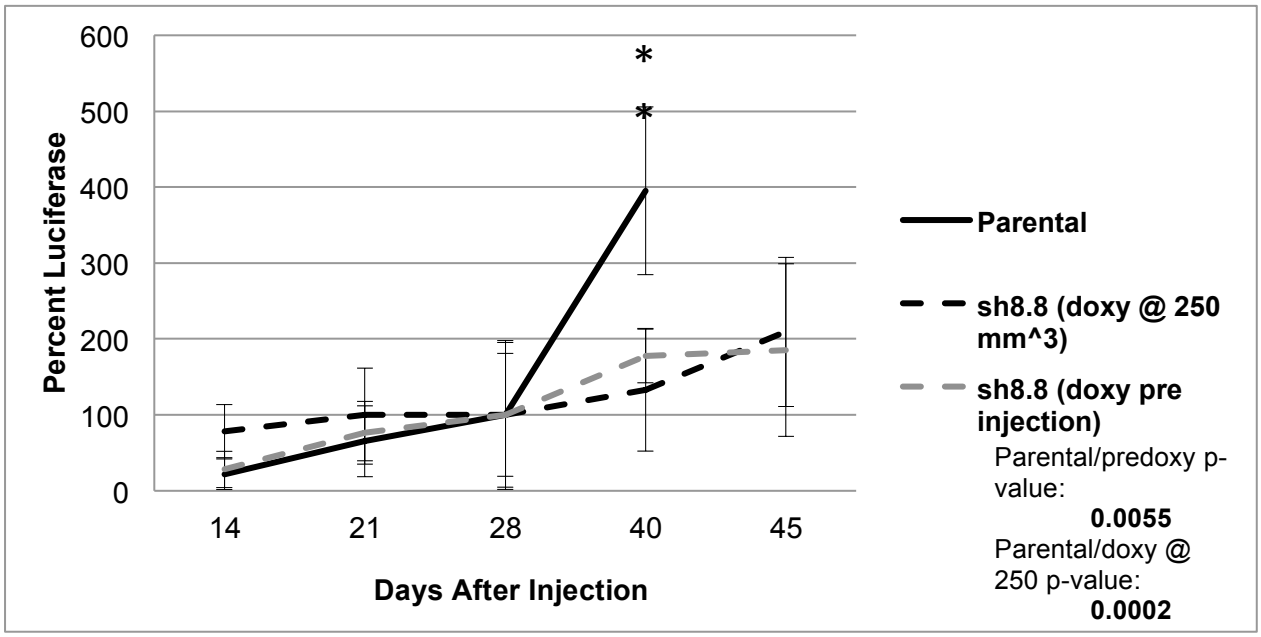


**Figure 25. Inducible ALDOA Knockdown in MDA-MB-231 Breast Cancer Tumors Reduces HIF Activity *in vivo***

*In vivo* HIF-1α activity was determined using the MDA-MB-231 HRE-luc highly metastatic breast cancer cell line after induced silencing of Aldolase A with shRNA. Mice (n=5/group) were measured with Xenogen IVIS imaging system and intraperitoneal injection of luciferin starting 14 days after cell implantation. Silencing of Aldolase A resulted in significant inhibition of HIF-1α activity either in subjects that received doxycycline before cell implantation (doxy pre injection group) or after tumors had grown to 250 cubic millimeters (doxy @ 250 $mm^3$ group). * P<0.01 for both groups relative to non-transduced MDA-MB-231 HRE-luc cells receiving equal doxycycline treatment.

Carrying murine xenograft data forward and in order to determine the clinical relevance and therapeutic implication of novel Aldolase inhibitors for patients with a variety of tumor types, we examined whether expression levels of various Aldolase isoforms correlated with any measureable differences in overall patient survival. Aldolase A, B and C mRNA expression data was obtained from the PANCAN dataset from The Cancer Genome Atlas (TCGA) (n = 9755). Using the TCGA expression data, we found that elevated Aldolase A and C expression was significantly correlated with poor prognosis in regards to survival rates ($p < 0.0001$ in both cases) even when corrected for cancer type and patient age and sex (**Figure 26**). Alternatively, no difference in PFS is observed between high and low level expression of Aldolase B (**Figure 27**), suggesting that A and C isoforms are more significantly associated with progression to advanced disease states. Collectively, this data indicates that Aldolase isozymes are both attractive targets for therapeutic intervention in cancer progression and could also serve as critical diagnostic factors for determining patient response to therapy and overall prognosis. ALDOA expression is clearly associated with poor clinical prognosis of a variety of cancer types, suggesting that its expression patterns could be used in advance to select patients in which Aldolase inhibition would be both beneficial and critical for overall patient health.

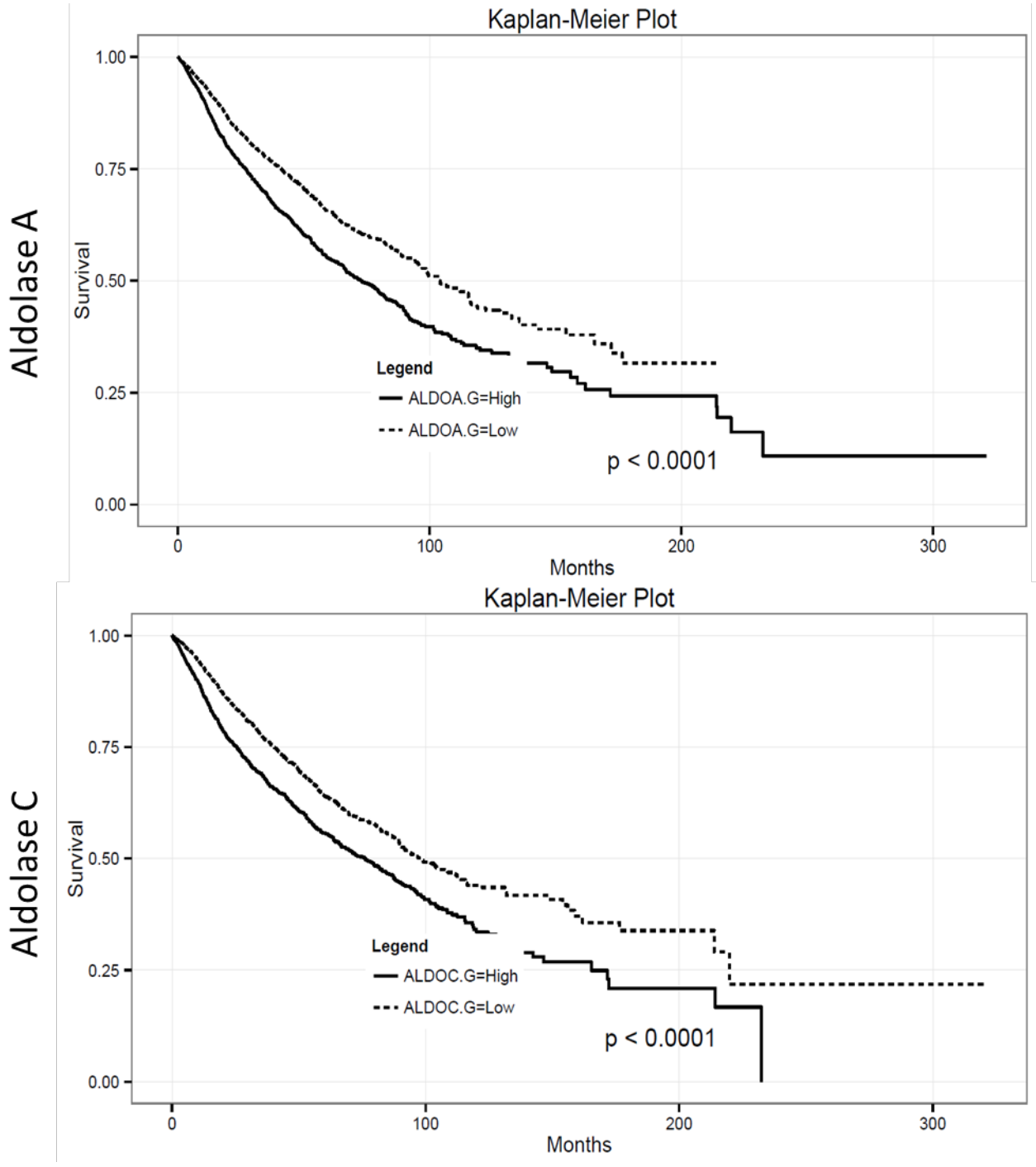


**Figure 26. The Cancer Genome Atlas Data Suggests Aldolase A and C Isoform Expression Data Predicts Overall Patient Survival**

Comparison of tumor and paired normal tissue samples from 9755 patients for ALDOA and ALDOC mRNA suggests high expression of either in patient tumors could be predictor of poor prognosis. Survival data is corrected for tumor type, patient age and patient sex.

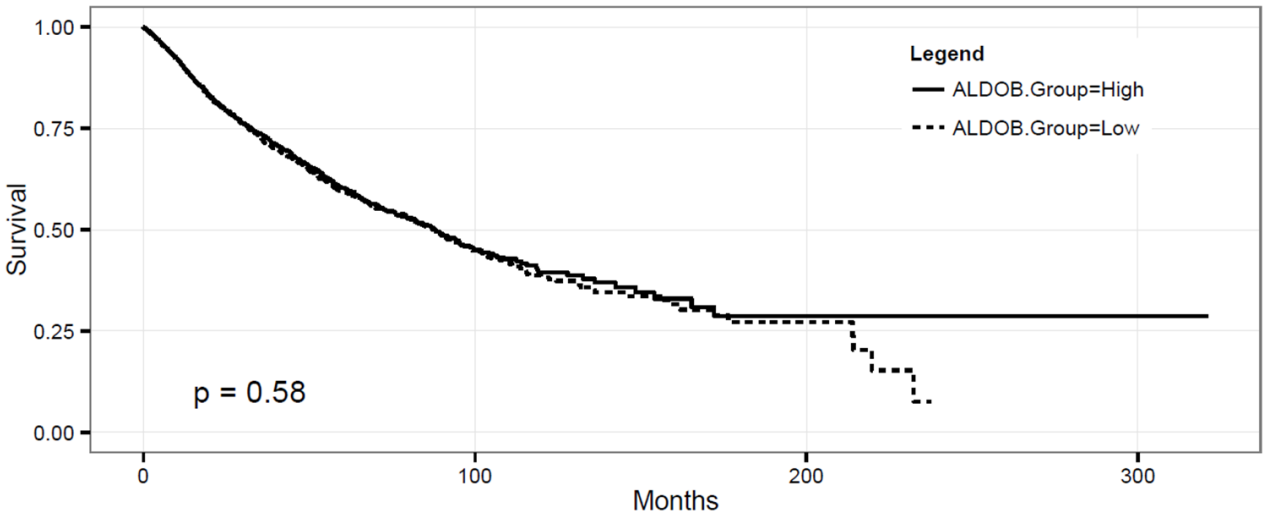


**Figure 27. The Cancer Genome Atlas Data Suggests Aldolase B Isoform Expression Data Cannot be Used as a Predictor of Overall Patient Survival**

Comparison of tumor and paired normal tissue samples from 9755 patients for ALDOB mRNA suggests high expression of the protein in patient tumors has little to no predictive value. Survival data is corrected for tumor type, patient age and patient sex.

Considering the differential expression of ALDOA in cell lines and the correlative pattern that we observed in regards to sensitivity to its knockdown, we next analyzed available TCGA expression data and found, upon initial analysis, that elevated Aldolase A expression was significantly correlated with lower median survival in a variety of cancer types pointing to its potential value as a prognostic factor in the treatment of such diseases with novel inhibitors currently under development (**Figure 28**).

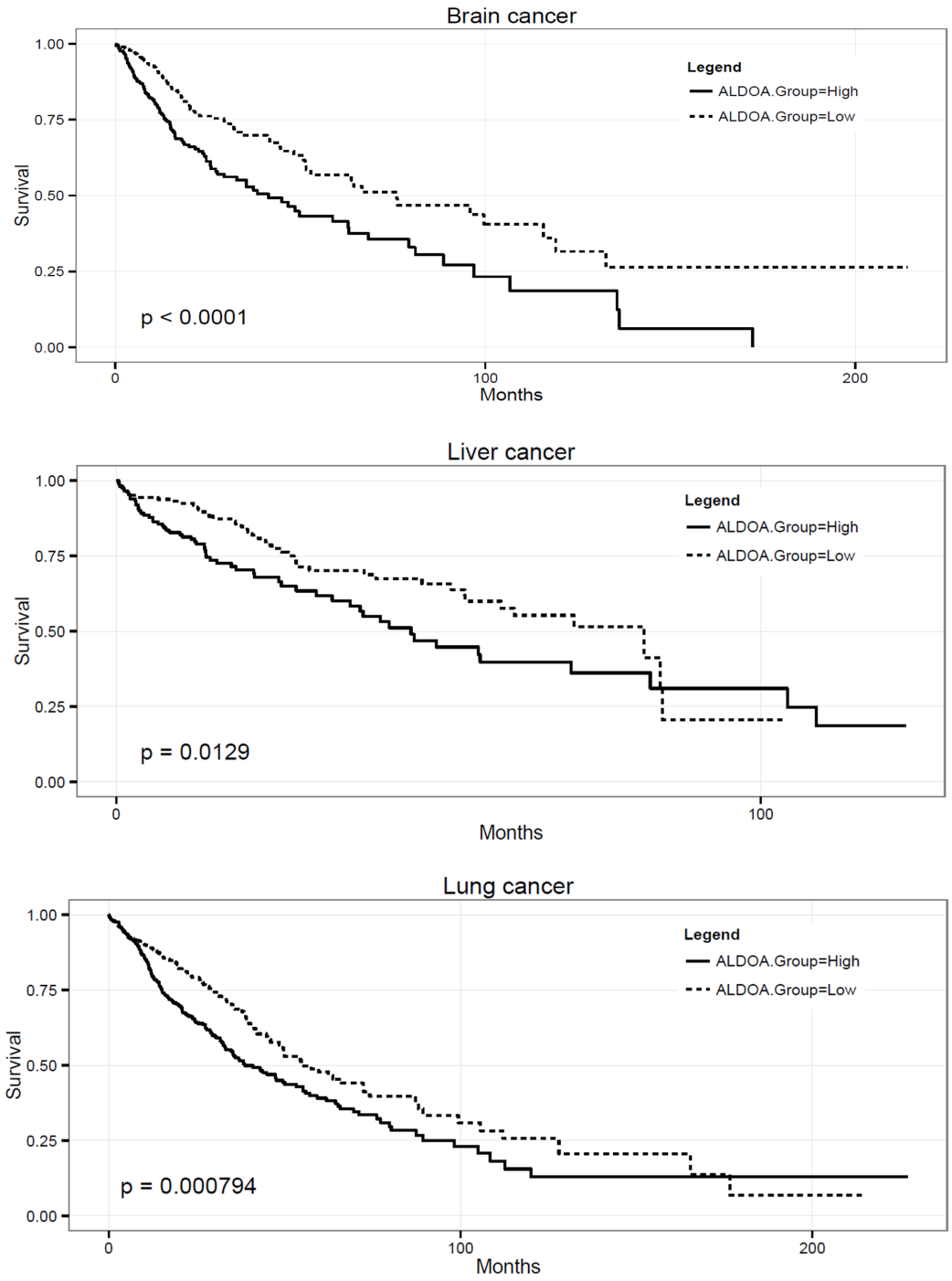


**Figure 28. Variable Expression of ALDOA in Tumors Predicts Median Survival**

Initial consideration of TCGA data following cell line analyses shows a pattern of poor prognosis with high ALDOA expression relative to paired normal tissue.

**Discussion:**

HIF-1α is a key transcription factor that functions in cell survival in stressful hypoxic environments established by many solid tumors due to poor vascularization. Amongst these targets are pro-angiogenic genes such as PDGF and VEGF [23, 26, 28, 94], genes associated with accelerated tumor cell proliferation such as MYC [95, 96], and genes functioning in migration, invasion and remodeling of the extracellular matrix and contributing to increased cell survival and heightened metastatic potential [97-99]. HIF-1 promotes cell survival by up-regulating genes related to cancer cell metabolism and rapid production of ATP and glycolytic metabolites [4, 29, 100]. Increased HIF-1α signaling is observed in many pathophysiological conditions, including pancreatic, colon and breast cancers. However, inhibitors designed to disrupt HIF-1's protective role have thus far been largely ineffective. Thus we took an unbiased approach by utilizing a high-throughput siRNA screen to identify factors that mediate HIF-1α transcriptional activity, in part to reveal novel targets for HIF-1α inhibition. Unexpectedly, several hits in the screen were enzymes functioning in glycolysis. While it was previously known that HIF-1 increases the glycolytic rate in tumors by inducing expression of glycolytic enzymes [4, 5, 27, 29, 100], it has not previously been reported that glycolysis increases HIF-1 activity. We found that 16 of 30 glycolytic enzymes and isoforms were associated with some inhibition of HIF-1 transcriptional activity. Among them, ALDOA and PGK 1/2 knockdown resulted in robust inhibition of HIF-1 activity in all lines tested.

Cellular protein synthesis is energetically expensive; thus protein synthesis rates are tightly regulated in order to couple nutrient availability to signals driving proliferation. It is known that in an energy crisis when glycolysis is inhibited, ATP levels decrease and AMPK is activated subsequently leading to mTOR mediated decreased expression of HIF-1 protein [101]. However, under hypoxic conditions, as found in solid tumors, decreased degradation of HIF-1, at least in the short term, increases levels of HIF-1 protein, which paradoxically obscure potential

decreases in translation. However, we now report that HIF-1 protein is not transcriptionally active when glycolysis is inhibited. The EP300 co-activator is required for numerous signaling pathways governing cellular proliferation and differentiation, processes tightly controlled by p300 phosphorylation status [102]. Specifically, p300 phosphorylation at serine 89 following AMPK activation dramatically reduces p300 interaction *in vitro* and *in vivo* with numerous nuclear receptors but does not alter interaction with non-nuclear receptors [93]. We confirmed these findings in glycolysis inhibition following knockdown of ALDOA, or PGK1 and PGK2, suggesting that control of the transcriptional machinery by activated AMPK is achieved through disruption of normal cancer cell metabolism. Thus, in response to lowered cellular ATP levels, AMPK is activated and p300 phosphorylation at Ser89 promotes dissociation from HIF-1α, decreasing its transcriptional activity.

Interestingly, HIF-2α activity is also subject to inhibition when glycolysis is inhibited as we observed in the case of the 786-O renal line. HIF-1 and HIF-2 upregulate both common and unique downstream targets, and HIF-2 does not upregulate glycolysis genes as does HIF-1. Thus, we conclude that HIF-2 does not participate in the feed forward loop described here, but rather its activity is dependent on HIF-1 stimulation of glycolysis. Most cancer cells express HIF-1 under acute hypoxic conditions, but in prolonged hypoxia HIF-2 is expressed and HIF-1 levels fall [46]. The consequences of HIF-2 inhibition need to be investigated, particularly in clear cell renal cancer cells, which predominantly express HIF-2.

Here we show that ALDOA and PGK1/2 isoforms are the most critical of 40 isoenzymes of the glycolytic pathway in terms of maintenance of normal HIF-1α activity, making both attractive targets to inhibit both cancer cell energy metabolism and survival of stress. The marked extension in median survival time of mice with ALDOA knockdown in the MDA-MB-231 model of metastatic breast cancer confirms this point and opens the possibility of novel drug screening and therapeutic options for cancer subtypes linked to HIF-1α and ALDOA expression. Furthermore, identification of ALDOA as a potential novel regulator of HIF-1 could be clinically

relevant, since ALDOA expression levels are reportedly significantly elevated relative to other glycolytic enzymes in several human tumor types [57, 103], providing a novel means to inhibit HIF-1α function in several solid tumors. Variable expression of Aldolase isoforms in the panel of 4 HRE luciferase lines used here suggests a compensatory mechanism for ALDOC in the absence of ALDOA. In particular, high ALDOC levels seen in HT-29 HRE cells could explain why ALDOA knockdown had minimal impact on this line and demonstrate a need for therapeutic agents targeting both ALDOA and ALDOC. Variability in the pattern of Aldolase isoform expression was further confirmed in a panel of 12 lung cancer cell lines (**Figure 23**). Currently, there are no clinically available inhibitors of these critical steps in glycolysis; establishment of agents targeting crucial components of the pathway could be useful to treat cancers that survive using these mechanisms.

Malignant transformation reportedly shifts cells to a pattern of glycolytic enzyme expression that favors uncontrolled proliferation and facilitates energy production and metabolite production in an oxygen free setting [104, 105] A feed forward loop in tumors promoting increased HIF-1 activity and increased glycolysis provides a target to block tumor energy production pathways and the HIF-1α survival response. Our activity-oriented RNAi screen and subsequent mechanism-based analysis expands our understanding of known and novel regulators of the HIF-1α transcription factor and suggest previously uncharacterized regulation of HIF-1 activity by glycolytic enzyme expression. Moving forward, by designing a therapeutic intervention for ALDOA activity, we hope to inhibit both cancer cell metabolism and the tumor cell's ability to survive hypoxic stress thus exploiting a dual Achilles' heel of the cancer cell.

# Chapter 2: Designing a Chemical Probe

**Virtual High Throughput Screening Quickly Characterizes Potential Lead Compounds**

In the realm of rational drug design, molecular docking programs are frequently used to predict the binding orientation of small molecule pharmacological probe candidates to targets of interest in the form of proteins or, more specifically, enzymes in order to predict the affinity that the small molecule has for the active site of that target [106]. In this way, the use of recursive docking programs in screening operations can play a critically important role in the rational design of new pharmaceutical agents. Given the biological and pharmaceutical potential of these molecular docking systems, considerable efforts have been directed towards the design of new methods and tools that can be used to predict docking [106].

Taking into account the availability of small molecule data bases, these screening methodologies can be focused on drug-like molecules that are either commercially available for testing in biological assays or can be easily generated from already available materials or processes. In this way, the characterization of available chemical compounds, natural products and drugs can be accomplished in such a way as to gain an understanding as to what basic structures stand to give the greatest effect against the target of choice and manipulated later for SAR based studies [107].

GOLD (Genetic Optimization for Ligand Docking) is a program for calculating the likelihood of certain docking conformations of small molecules in specifically outlined protein binding sites as determined by the program's user [108]. The automated ligand docking program uses a genetic algorithm to explore the full range of possible ligand conformations within a specified binding site with partial flexibility of the protein at that site, and satisfies the requirement that the ligand of interest displaces loosely bound water on binding. The software package consists of several programs; the first, for visualization and manipulation of the unadulterated protein structure as input from the protein databank, a second for the calculation based protein-ligand docking screening algorithm and a third for post-processing and visualization of the docking

results from high-throughput virtual screening. An extensive review of literature outlining information regarding both the crystal structure of the Aldolase A isozyme and studies of the effect of mutation of specific residues on the functionality of the enzyme yielded a set of six critical residues to be included in the specifically outlined protein flexibility algorithm: Asp33, Ser38, Lys146, Arg148, Glu187, and Lys229. The program, by including protein side chain and backbone flexibility in this user defined list of residues within the protein of interest, takes into account the wide range of possible conformations of not only individual substrates but also the enzyme itself during the virtual docking mechanisms. The results of the survey of the literature were visualized and manipulated in PyMOL, a molecular visualization system capable of translating Protein Data Bank files into high quality 3D images [109] (**Figure 29**).

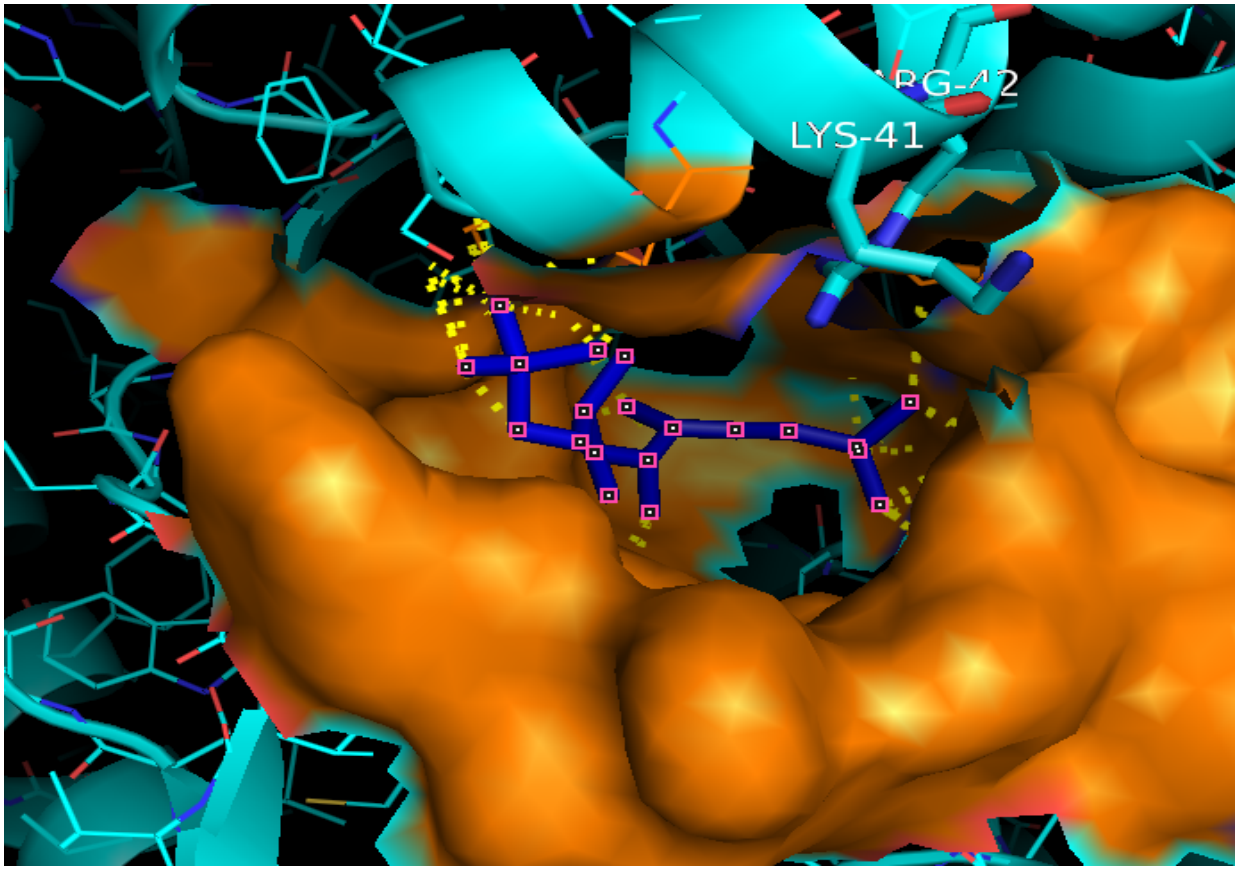


**Figure 29: Computer model of active binding site of Aldolase A isozyme**

Using the published available crystal structure for Aldolase A (4ALD in PDB), PyMOL was used to visualize the surface of the active binding site of the enzyme (orange) to contrast the cartoon version of the enzyme as a whole (teal) and Fructose-1,6-bis(phosphate), the enzyme's natural substrate (shown in dark blue). Using this method, key residues in the binding site were identified for virtual screening methodologies.

**Virtual High Throughput Sigma TimTec Myria Screen Uncovers Novel Tool Compounds**

For the purposes of this study, GoldScore, the original scoring function within a range of possible criteria sets for assessment of ligand binding, was selected as it has been optimized for the prediction of ligand binding positions and takes into account factors such as H-bonding energy, van der Waals forces and strain on the ligand itself given specific conformational changes [110]. Additional features that made this scoring function ideally suited for this particular project were alluded to earlier, as GoldScore is the only scoring function that takes into account flexible residues within the targeted binding site - in cases where program users are docking a ligand into a binding site known to contain a flexible side chain (such as the Aldolase isozymes), it is possible to specify that these residues be allowed to undergo automatic rotation around one or more of its acyclic bonds. Since it was determined from literature review that there were at least six critical residues that were capable of torsional rotation, this was the clear choice for appropriate scoring functions [111-113]. In this way, the conformations of the flexible motifs were altered during docking in order to optimize the hydrogen bonding interactions of the residue with the ligand, improving the final indication of likelihood of binding affinity.

Using the solved crystal structure (4ALD from Protein Data Bank) and the parameters as outlined above, the Sigma TimTec Myria library of 10,000 compounds was selected for initial screening. The value of this library was the careful consideration of several physical and chemical properties by the library's designers at both Sigma and TimTec including the diversity of molecular weight, cLogP (measure of relative hydrophobicity), hydrogen bond acceptors, hydrogen bond donors, and rotatable bonds. Further, the collection is largely drug like according to Lipinski's Rule of 5 [114] which was useful for this screening operation in that we were interested in identifying novel inhibitors that could be made into pharmacological probes for further drug design efforts. Each of the 10,000 compounds was docked in five possible

conformations in order to yield a range of scores for each compound taking into account several possible docking scenarios within the active site.

If the system were perfect, the calculated binding energy of a specific substrate would correlate perfectly with an experimental binding energy, so that the pose with the lowest predicted binding free energy would correspond directly to the experimentally determined structure. Since the process of free energy calculation is confounded by many factors surrounding the interaction between the substrate and specific residues within the binding site, this is not always the case; for this reason, it is often found that the lowest energy structure predicted by docking will not be the closest to the experimentally determined crystal structure of the protein. Molecular docking processes are generally used to simply identify a set of compounds to be used in further development experiments rather than to select a single compound on which to base all future research. Taking this into account, it was important to include a system of checks and balances in the original experimental design in order to measure the effectiveness of residue selection. As a validation of the effectiveness of the screening procedure, fructose 1,6-bisphosphate was included with the Myria compound library to be included in the list of possible compounds; this natural substrate ranked among the top ten compounds according to its binding affinity relative to the compounds found in the screened library initially verifying the validity of residue selection for use during the screen.

Upon completion of the screening operation that considered over 50,000 possible permutations of potential small molecule inhibitors and their binding to the active site of ALDOA, GOLD fitness was used as a parameter to describe the interaction between the ligand and the binding site. In order to further refine the selection process, several parameters were considered:

1. The number of times that each of the five iterations of each compound's conformational changes appear amongst the top ranked hits was taken into account.

Logically, a compound that appeared four times in top 20 compounds was more likely a worthwhile hit than one that only appears once in the top 100.

2. Compounds were removed from the list if the cLogP was over 2 since this would neither be easy to test in cell models, nor a useful therapeutic agent if *in vitro* work proved the agent was effective at silencing the action of Aldolase A.
3. For the most part, chemicals that were symmetrical were taken out of the ranks; however, there was one compound in the top ten that consistently ranked highly according to its GOLD score that was not removed.
4. The diversity of chemical structures was also considered in the selection process since the likelihood that even after early *in vitro* work each of the chosen structures would have to be modified for purposes of SAR studies at a later time was considerable.

After cropping the list of top hits from 50,000 to just 100, the top hits were then rescreened in GOLD with 20 iterations of possible conformations using a fully flexible binding site model. As expected, this process did not have a significant effect on the ranking of each compound.

Finally, these top 100 compounds were visually inspected in PyMOL relative to the natural substrate to make sure that there were not significant changes in the structure of the docked complex relative to the proven crystal structure. This also was effective in showing how each of the potential probes fit into the binding site relative to critical residues and the natural substrate itself. During this procedure the list of 100 compounds was again reduced to the top 22 which were chosen for *in vitro* experiments. Since Aldolase is found at a critical point in glycolysis in which NADH is oxidized, a simple spectrophotometric assay was employed for this function. Optimization experiments to determine the ideal concentration of Aldolase protein for use per well in a 96 well plate format gave proof that the assay was robust enough for testing of inhibitors from the virtual screen (**Figure 30**).

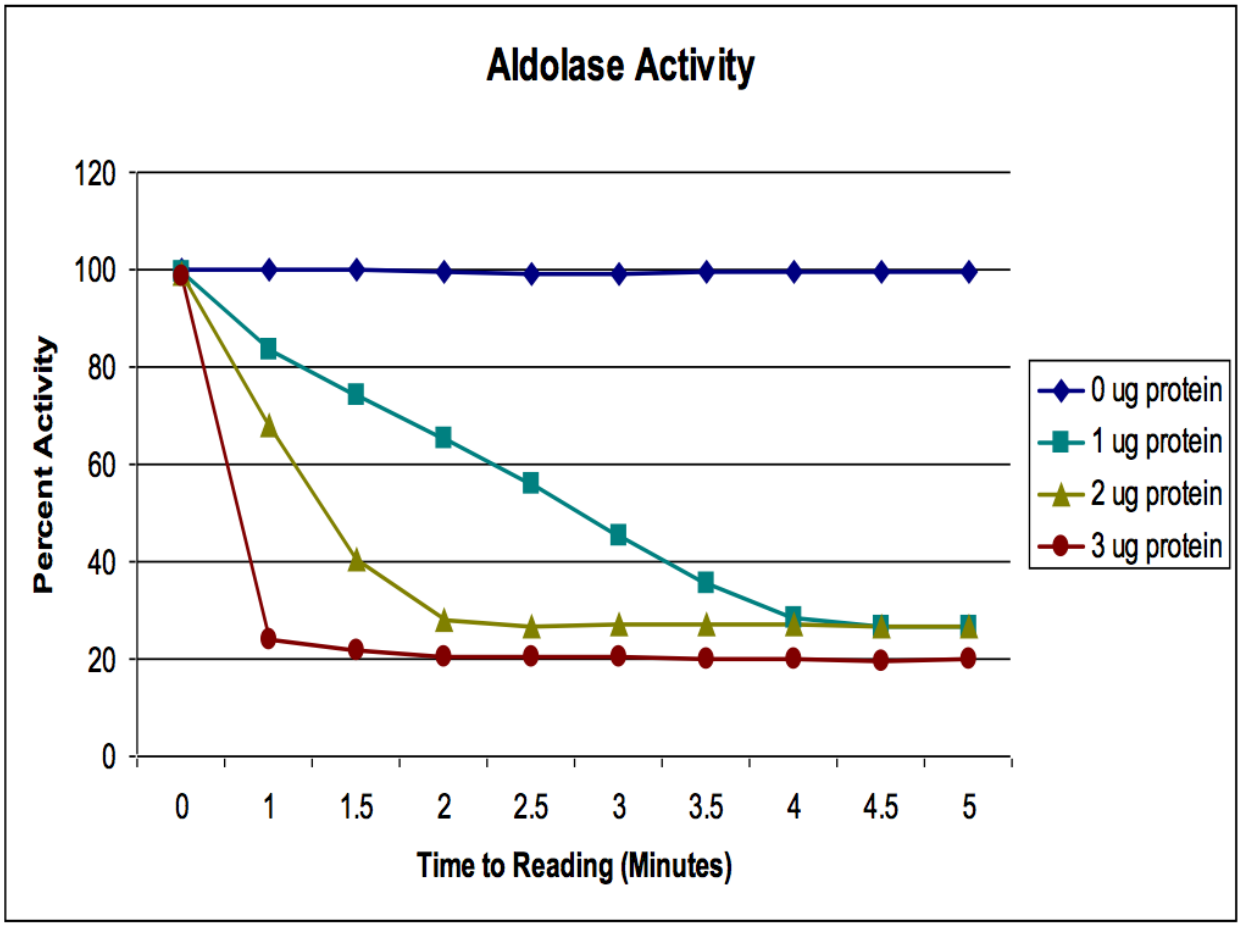


**Figure 30. Optimization of NADH Oxidation Mediated Aldolase Activity Assay**

Initial work in the development of a multi-well plate assay to measure the activity of ALDOA has used a 96 well plate assay based on conversion of fructose 1,6-bisphosphate (F-1,6-BP) into glyceraldehyde 3-phosphate (GAP) and dihydroxyacetone phosphate (DHAP) measured in a coupled reaction with GAP dehydrogenase by the oxidation of NADH to NAD at 364 nm.. This reaction can be easily manipulated by altering initial ALDOA protein concentration in the reaction well to produce changes in the velocity of the reaction which are proportional to the amount of active ALDOA added.

Of the tested compounds, 3-hydroxy-5-(4-isopropylphenyl)-1-(1,3,4-thiadiazol-2-yl)-4-(2-thienylcarbonyl)-1,5-dihydro-2H-pyrrol-2-one (referred to as “Compound 6” due to its rank as the 6$^{th}$ best hit from the GOLD screen) gave the best results in the biochemical assay; however, the non- Michaelis-Menten nature of the kinetic profile made the calculation of critical values used in the description of an agents effect on enzymatic activity impossible. In order to understand these effects on enzyme function, a kinetic description of their activity as measured as the rate of catalysis of the natural substrate (described as the rate of product formation) is needed and, typically, will vary proportionally with the concentration of the substrate – similar to the profile seen in Figure 4. In this case, however, a lag phase in which inhibitory effects of the compound are basically absent is observed prior to an immediate drop off (**Figure 31**).

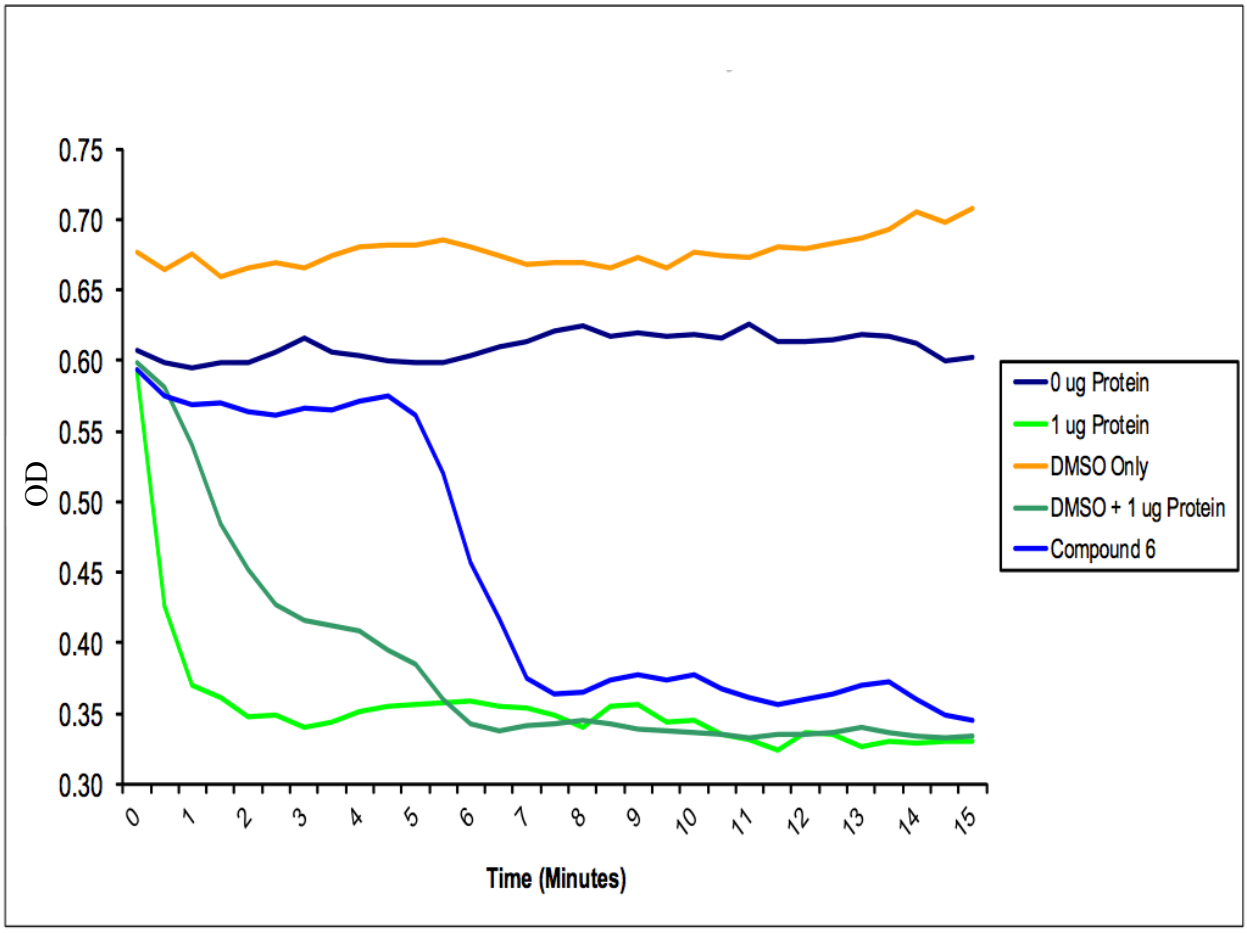


**Figure 31. Non-Michaelis-Menten Enzyme Kinetics Observed Using 'Compound 6'**

They typical hyperbolic plot that is found in Michaelis-Menten kinetics is missing with the use of Compound 6 in recombinant protein based biochemical assessment of the proposed Aldolase A inhibitor. The 5 minute lag phase followed by abrupt loss of Aldolase activity defies traditional enzymatic activity patterns and raises questions regarding its activity as an Aldolase inhibitor.

**High Throughput Small Molecule Screen *in vitro* Uncovers Novel Pharmacological Probes**

Previous work suggests a modification of residues on the C-terminal tail of Aldolase which is known to overlay the catalytic site might be responsible for inhibition of activity of the enzyme [115]. Since residues in the portion of the target were not considered in the initial GOLD screen, it is possible that the results, while initially interesting, did not provide the robust effects that were expected and inclusion of these residues in future screening efforts would be needed.

Considering the effectiveness of the biochemical assay used for the initial assessment of hits from the virtual screen, large scale, high-throughput screening of small molecule libraries using the assay was a logical next step. Typical assessment of Aldolase activity *in vitro* was achieved through the use of a coupled enzymatic reaction with α-Glycerophosphate Dehydrogenase (GAPDH). Since this step of glycolysis causes the conversion of NADH to NAD in the presence of the natural products of Aldolase, the absorbance based quantification of remaining NADH in solution could indirectly measure Aldolase activity [70]. However, since the sensitivity of NADH absorbance is low, and since interference of small molecules with absorbance less than the 400 nm wavelength required for the assay could result in high rates of false positive identification, an alternative, first of kind, fluorescent based assay was developed by medicinal chemists at the University of Texas at Austin (Ashwini Devkota, Eun Jeong Cho and Kevin Dalby) in order to swiftly identify lead compounds for therapeutic development of Aldolase A inhibitors (**Figure 4, 5**). The Elite NADH assay, which is marketed as a method to measure the levels of NADH/NAD+ in various sample types, was repurposed for use in a highly sensitive, high throughput function. The kit's enzyme reduces a chromophore into a highly fluorescent product in states of NADH dehydrogenation. Glyceraldehyde-3-phosphate dehydrogenase converts glyceraldehyde-3-phosphate (G-3-P) to 1,3-bisphosphoglycerate (1,3-BGP) through oxidative phosphorylation. NAD+ is oxidized to NADH when a phosphate group is exchanged for a hydrogen on the carbonyl carbon of G-3-P thus converting G-3-P to 1,3-BGP.

This assay uses glycerophosphate dehydrogenase to catalyze the conversion of dihydroxyacetone phosphate (the product of the ALDOA catalyzed reaction) to glyceraldehyde-3 phosphate in an NADH-dependent manner. Thus, the rate of change of fluorescence intensity is used to indirectly calculate the activity of ALDOA. After identifying and manipulating this system to fit our needs, robustness and reproducibility of the assay was validated through the use of Z'-factor calculation in the comparison of positive control (all assay components in the absence of ALDOA corresponding to complete enzymatic activity inhibition and, therefore, highest fluorescence intensity) and negative control (all assay components in the presence of excess ALDOA corresponding to full enzymatic activity of Aldolase and, therefore, lowest fluorescence intensity) wells in the presence of an optimized concentration of Aldolase A recombinant protein (**Figure 32**) and Fructose-1,6-bisphosphate substrate (**Figure 33**) per well.

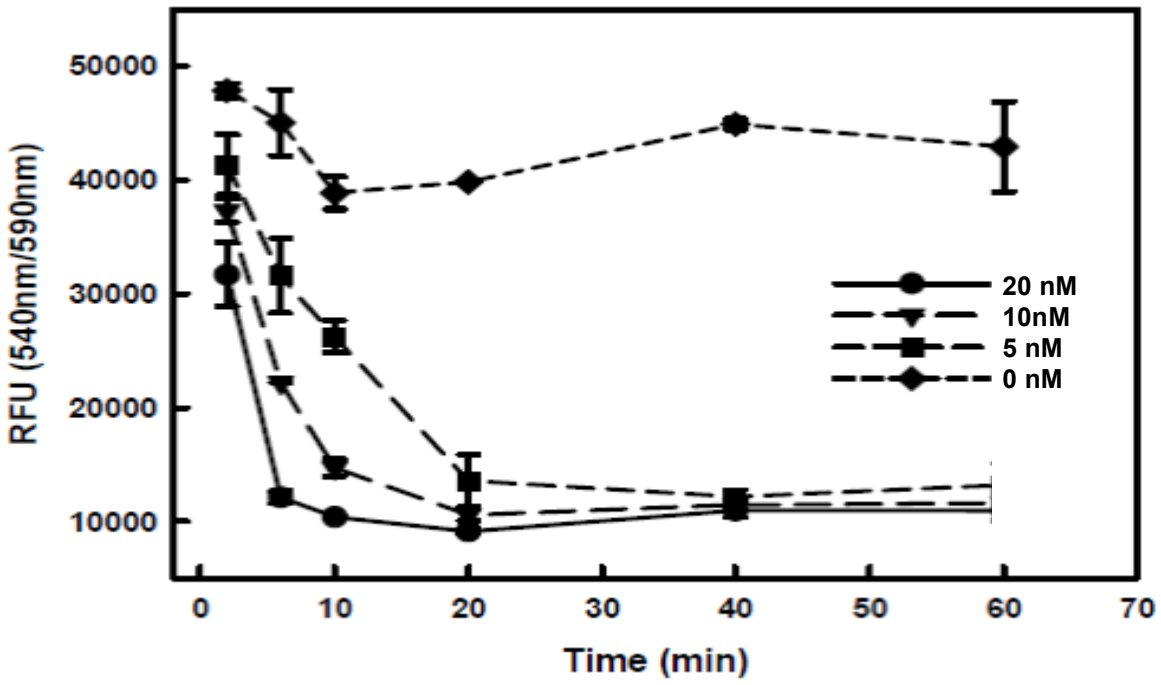


**Figure 32. Assay Optimization: Enzyme Dose Response Versus Time**

Preliminary optimization experiments included the identification of appropriate Aldolase A concentration per well – 0, 5, 10, and 20 nM recombinant protein were evaluated against standard concentrations of substrate and reaction mixture (including glyceraldehyde dehydrogenase). With a reaction completion time of ~30 minutes, 5 nM Aldolase was chosen for use in further optimization experiments.

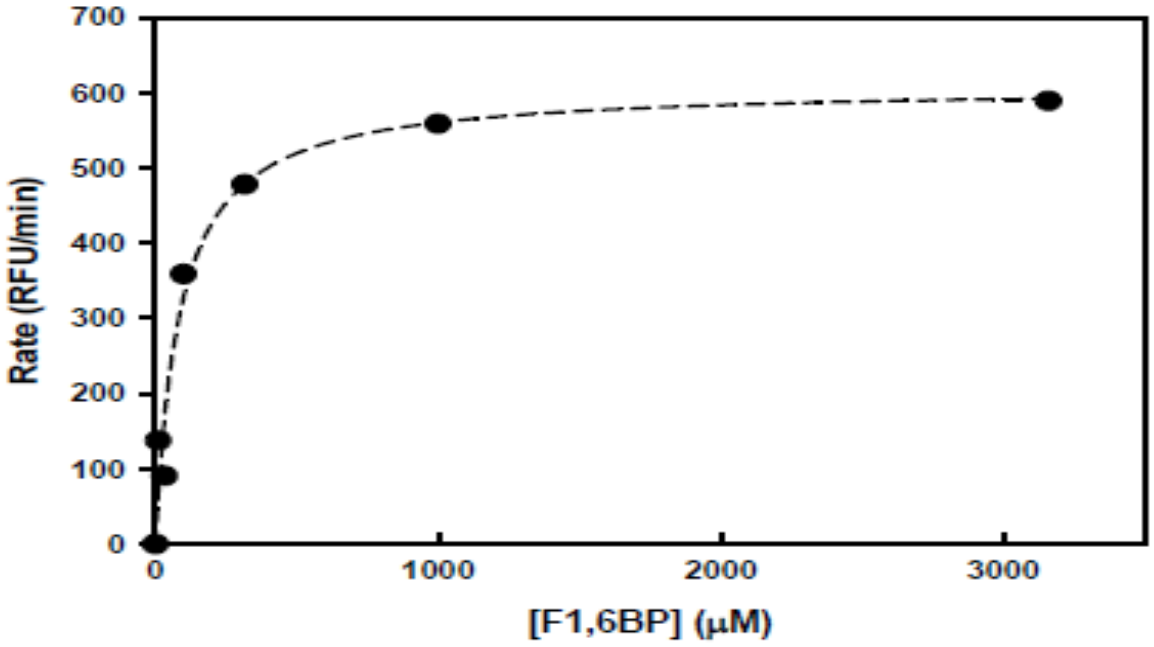


**Figure 33. Assay Optimization: Substrate Concentration**

Following the optimization of Aldolase A concentration per well, F(1,6)BP concentration was optimized against 5 nM protein and standard NADH and GDH per well. Falling in the linear range of the kinetic profile generated during this optimization, 100 µm F(1,6)BP was chosen for the finalized assay parameters.

Using this assay, characterization of over 65,000 chemical agents obtained from both commercial and academic suppliers was made possible while limiting the likelihood of false positives due to interference caused by absorbance inherent to the small molecules alone. Similar to the Myria screen used for virtual screening methods described earlier, collections of these agents which were selected for functional screening were compiled based on structural diversity amongst available biologically active known drugs or natural products and hits were selected based on the criteria of 25% inhibition of Aldolase activity following the execution of the assay.

**Discussion**

By using an unbiased, large scale, small molecule library screen in a recombinant protein assay, the typical challenges associated with cell based small molecule screens can be overcome. While many of the compounds found in these libraries have either undetermined targets or have been previously identified as inhibitors of proteins other than those that we are trying to exploit in this study, early results suggest a promising panel of pharmacological probes for the inhibition of normal Aldolase function. Despite this fact, there are a wide range of cellular functions, components of the extracellular space and physiological confounders that can hinder the clear efficacy that we observed in the initial screen and further work both *in vitro* and *in vivo* is required.

By carrying 'hit' compounds into cell based assays a number of parameters could be satisfied in an ongoing attempt to design an effective therapy for the ubiquitous processes associated with tumor cell metabolism and stress survival. First, identification of compounds which are effective in both biochemical and cell based *in vitro* experiments can provide novel insight about differences between cell types and, in the case of normoxic versus hypoxic cells, the inherent variability between different cellular states. Second, after identifying molecules that

are most effective in the cell based assays, new compounds can be designed and generated for use in SAR studies in order to optimize analogues with molecular structures that, although similar, may have a greater efficacy in target inhibition. And third, the eventual FDA approval of any compound will be almost impossible without a clear understanding of its cellular target and the effect that it has in order to achieve its inhibition even if the effect on cancer cell death, HIF activity, and energetics is profound.

While initial findings from our large scale small molecule screen were promising, the understanding that physiological components can act as hindrances to a compound's efficacy highlight the need to optimize the pharmacokinetic and pharmacodynamic parameters of our early lead compounds. Delivery of an active compound to the target after escape from vasculature, penetration into tumor cells which are distal to the convoluted vasculature of a tumor and maintenance of its biologically active form after traveling throughout the body are all considerations to be made and overcome in the steps following initial identification of a promising hit compound.

# Chapter 3: Developing a Novel ALDOA Inhibitor

**Identification of Lead Compound for Testing Based on Time Dependent Inhibition of ALDOA in Biochemical Assay**

In order to confirm that ALDOA is a target with potential for cancer therapy we sought to test small molecule probes initially identified as inhibitors of recombinant human ALDOA first in the chemical library screen in cell based, biological assays. Identified in the biochemical assay, amongst other compounds, was TDZD-8, a previously described, selective, non-ATP competitive GSK-3β inhibitor [116]. In this initial screening assay, this compound showed a time dependent inhibition of protein function suggesting a direct interaction with the ALDO protein used in the assay (**Figure 34**). Pointing again to the value and flexibility of small molecule library screening, we felt that the identification of a compound with previously described use in cancer as an inhibitor of a target other than ALDOA could have value later on in the drug development process if proof of this protein interaction could be realized. To that end, a combination of *in vitro* and *in vivo* experiments investigating this interaction and the effect that it had on cancer cells and subsequent xenograft tumors was initiated.

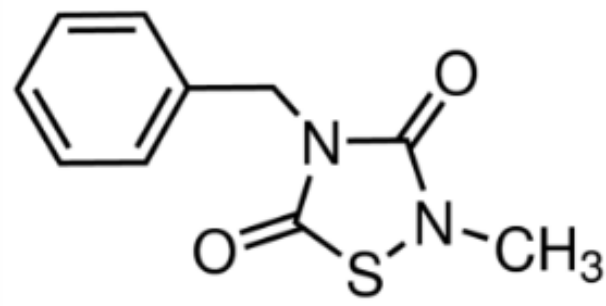


**TDZD-8**

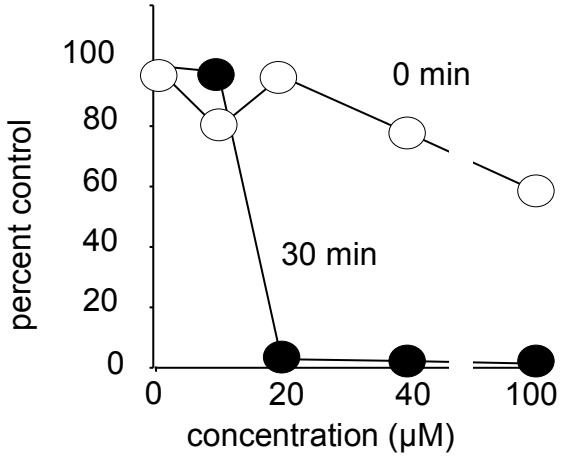


**Figure 34. Time Dependent Inhibition of ALDOA Function Suggests Direct Protein Binding**

The small molecule TDZD-8 was discovered as an inhibitor of recombinant human ALDOA activity through a chemical library high throughput screen. Varying concentrations of TDZD-8 were either pre-incubated for 30 minutes with recombinant ALDOA or introduced into assay wells at the initiation of the enzymatic assay. In this way, inhibition of ALDOA was shown to be time dependent suggesting that TDZD-8 could be interacting directly with the protein.

**X-ray Crystallography Implies Cysteine Residues Distal to Active Site are Critical for Normal ALDO Function**

To address the matter of TDZD-8 interaction with the ALDOA protein, X-ray crystallography studies were initiated in which ALDOA crystals were soaked with the inhibitor to measure residues which might be responsible for the inhibitory effects that we observed in the primary screen. Human ALDOA is found as a tetramer [68, 117], and our X-ray crystallographic studies showed that TDZD-8 bound with full occupancy to Cys289 in each of the four ALDOA subunits of the tetramer, and with partial occupancy at Cys239. Both Cys residues are on the surface of the tetramer and distal to the catalytic site (**Figure 35**), so their mechanism of inhibition is currently unclear. Interestingly, the literature survey that lead up to virtual high throughput screening methodologies used at the start of this drug discovery effort did not include residues outside of the substrate binding site; that said, the results from this study came as a surprise. The reaction of 1,2,4-thiadiazoles with the Cys sulfur leads to opening of the thiadiazole ring between the nitrogen and sulfur and formation of an irreversible disulfide bond. This is a relatively slow reaction that is dependent on the nucleophilicity of the cysteine sulfur [118], which may account for the slow reaction in the ALDOA inhibition studies that we observed previously (**Figure 34**). The S-S bond may also be stabilized by a hydrogen bond between the carbonyl oxygen at the 3-position in the ring, designated as the "recognition arm" [119] and an H-bond donor in the protein. The electron density is fully consistent with disulfide bond formation and ring-opening. It is significant that there was marked loss of inhibition by TDZD-8 when ALDOA Cys289 was mutated to Ala further implicating this residue in inhibitory effect of the agent on ALDOA functionality.

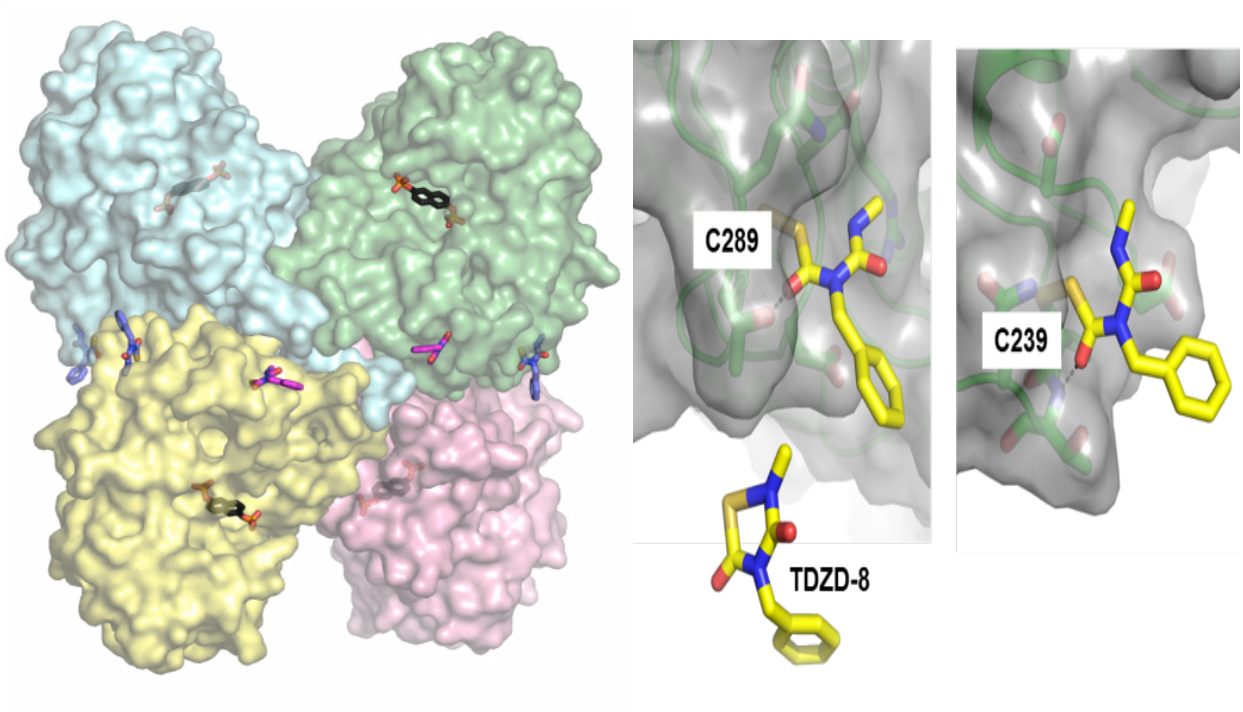


**Figure 35. Cys239 and Cys289 Binding Appear Critical for Inhibition of ALDOA Function**

Human recombinant ALDOA crystals were soaked with TDZD-8 and refined at 2.5 Å resolution to an R-factor of 20% (RFREE = 24%). The crystal structure showing TDZD-8 (blue and red stick structure) bound specifically to Cys-289 of each monomer in the tetrameric ALDOA complex; and to a much lesser extent to Cys-239. The electron density supports the formation of an S-S bond between protein and inhibitor and concomitant breaking of the S-N bond within the 1,2,4-thiadiazole ring. In general, density for the terminal Phe group is weak or non-existent, consistent with its flexibility. There is no evidence for modification of any other Cys residues. Both modified Cys residues are located distal to the catalytic pocket of ALDOA, (shown by a black and red stick structure of a partial substrate analog) and their mechanism of ALDOA inhibition is currently unclear. It is noteworthy that TDZD-8 bound better to ALDOA crystals when they were co-crystallized (i.e., prebound) with the substrate analog.

**Assessment of Glycolytic Substrates, Intermediates, and Products Suggests Aldolase Inhibition**

The YSI 7100 Multiparameter Bioanalytical System Analyzer allows for focused analysis of specific metabolites in biological samples. To measure a substrate of interest, one or more enzymes are immobilized between two membrane layers in the instrument's sensor. YSI membranes contain three layers. The first layer limits the diffusion of the specific substrate into the enzyme layer and prevents the reaction from becoming enzyme-limited. The third layer excludes nearly all electrochemical compounds from interfering with the measurement of hydrogen peroxide as the endpoint product. Using this robust system, the swift quantification of various substrates, intermediates, and products of the glycolytic process can be carried out. In addition to the XTT and luciferase assays used to show its inhibition of cancer cell proliferation and HIF-1 activity (**Figure 36**) and the reduction in ECAR observed when using the Seahorse BioScience® XF96e platform that is consistent with glycolysis inhibition, we were also able to show that TDZD-8 inhibited glycolytic activity at low μM concentrations by quantifying the ratio of lactate and glucose using the YSI platform (**Figure 37**). Lastly, GC-MS technology was employed for metabolic flux analysis using stable isotope labeling in which the absolute quantities of critical intermediates were assessed. Most notably affected were dihydroxyacetone phosphate (DHAP) and pyruvate suggesting that Aldolase was being inhibited following treatment with TDZD-8 (**Figure 38**). Despite not seeing overall inhibition of glycolysis (i.e. relatively constant levels of 3PG, PEP and lactate) we suspect that the inhibitor is still having an overall negative effect on the cell's ability to conduct glycolysis and that this is only a reflection of intracellular pool sizes of specific glycolytic intermediates, especially considering the significant reduction in DHAP concentration per sample following treatment.

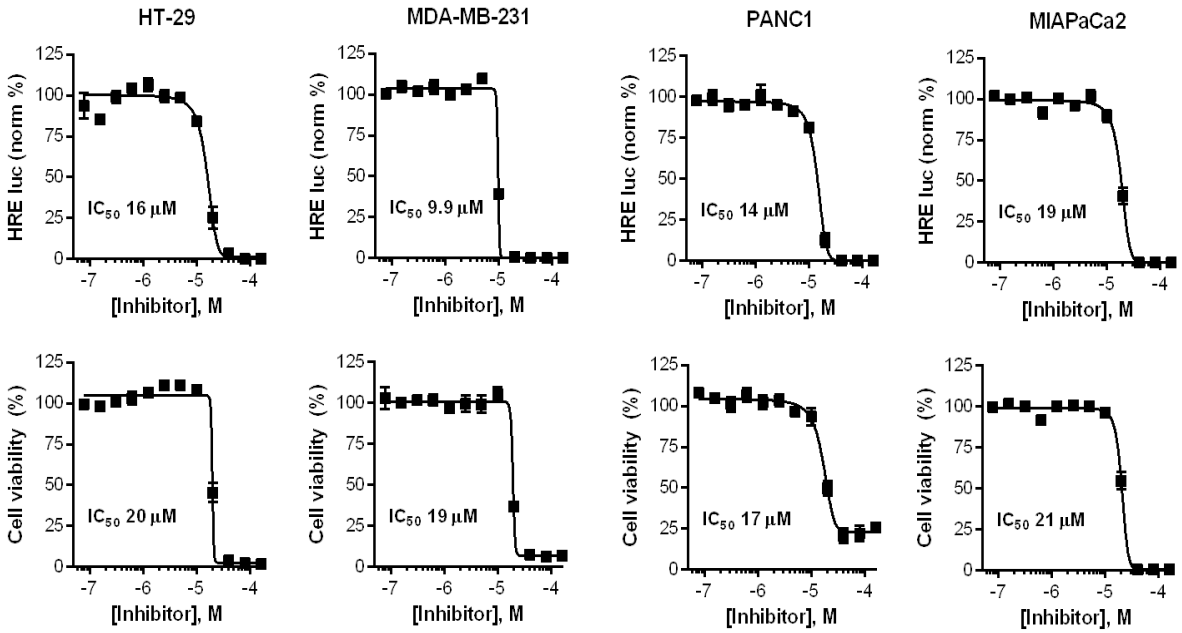


**Figure 36. TDZD-8 Inhibits Cancer Cell Proliferation and HIF-1 Activity *in vitro***

Panel showing *in vitro* TDZD-8 inhibition at low micromolar IC50 concentrations of cellular HIF-1 activity (as measured with the HRE luciferase reporter) and cancer cell proliferation.

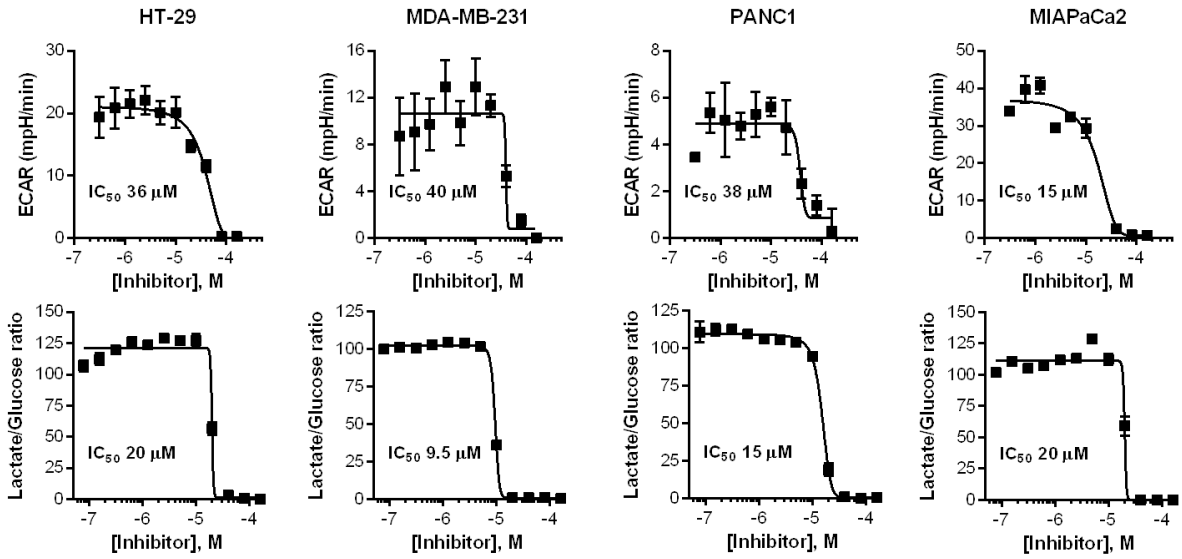


**Figure 37. TDZD-8 Inhibits Glycolytic Activity *in vitro***

Panel showing *in vitro* TDZD-8 inhibition at low micromolar IC50 concentrations of cellular glycolytic activity as a function of both the Extra Cellular Acidification Rate (ECAR) as measured by Seahorse® Technology and the ratio of lactate to glucose in the medium as measured by YSI technology.

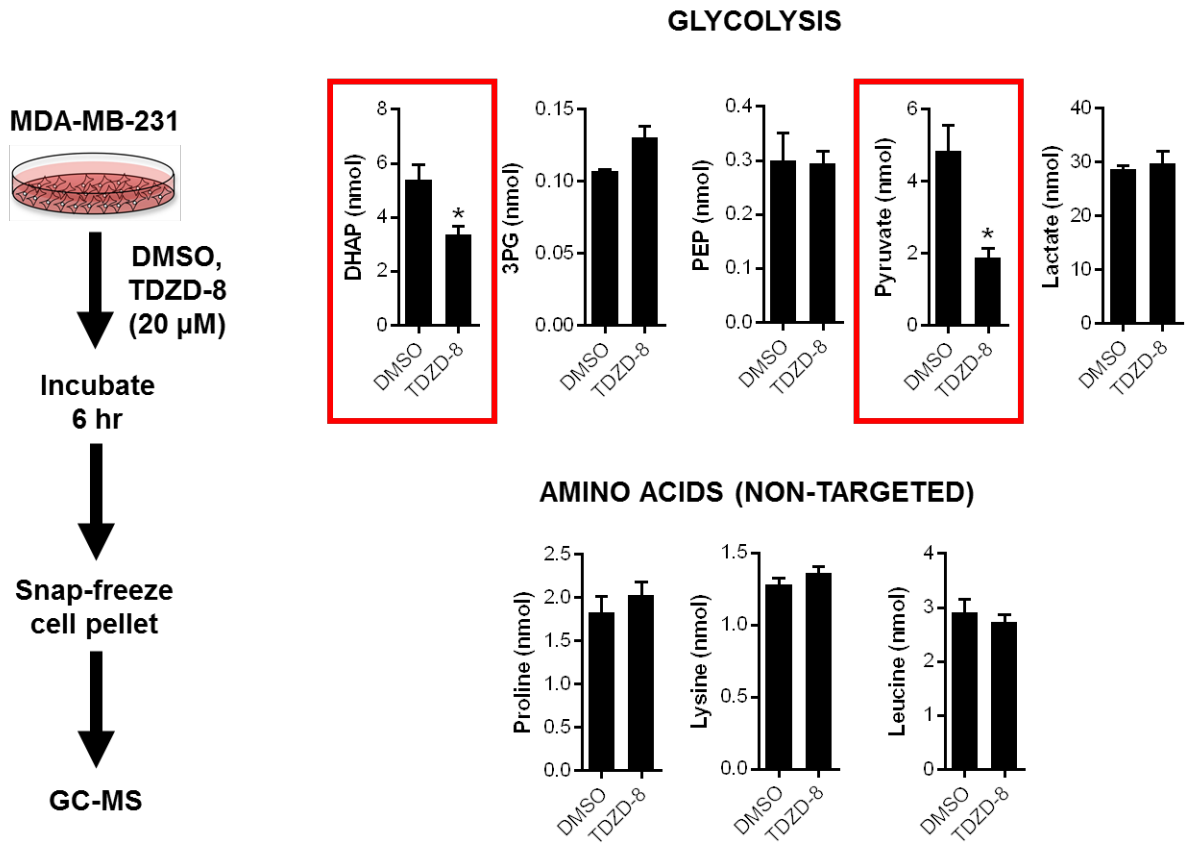


**Figure 38. GC/MS Analysis Shows TDZD-8 Inhibition of Glycolysis *in vitro***

GC-MS analysis of cell lysates after 6 hours of treatment with TDZD-8 (20 µM) of MDA-MB-231 cells shows a reduction of DHAP, the direct product of Aldolase, and pyruvate suggesting an inhibition of cellular glycolysis. Amino acids whose levels are not known to be affected by glycolysis were included as assay controls.

**TDZD-8 Inhibits Tumor Growth and Glycolysis *in vivo***

Although TDZD-8 is a reactive molecule, our results support a significant level of specificity and we used it as a pharmacological probe to see if we could inhibit ALDOA *in vivo* and solicit an antitumor effect. When administered intraperitoneally daily for 20 days at a dose of 12 mg/kg/day to mice with MDA-MB-231 orthotopic breast cancer tumors, TDZD-8 caused significant slowing of tumor growth by about 60% by day 32. Pharmacokinetic studies showed no detectable parent compound in the mouse plasma, but pharmacodynamic studies after a single dose of TDZD-8 showed about a 50% decrease in tumor lactate levels within 4 h, a 40% decrease in dihydroxyacetone phosphate (a product of the cleavage of fructose-1,6-bisphosphate by ALDOA), and a slower decrease over a period of days in downstream phosphoenolpyruvate (**Figure 38**). Thus, TDZD-8 itself at low levels or an active metabolite appears to reach the tumor to inhibit tumor glycolysis and is associated with measureable antitumor activity.

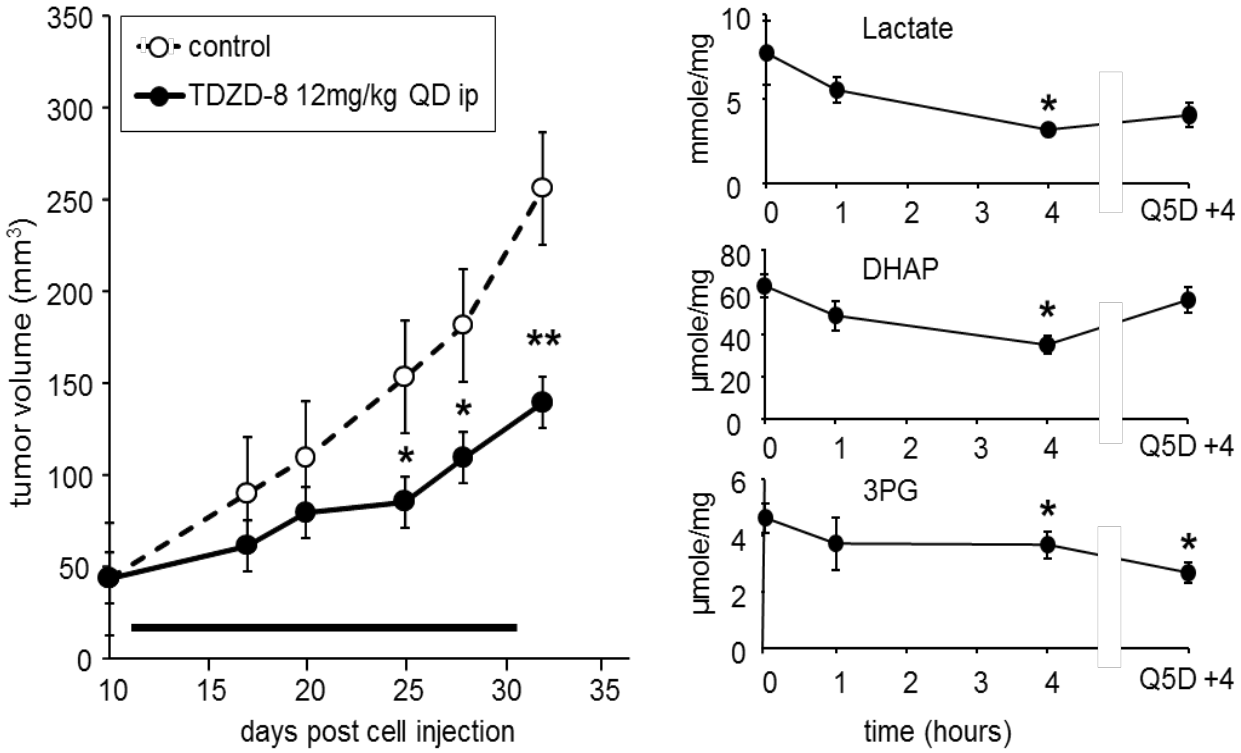


**Figure 39. TDZD-8 Inhibits Tumor Growth and Glycolysis *in vivo***

TDZD-8 at daily doses of 12 mg/kg by intraperitoneal injection daily for 20 days to immunodeficient SCID mice with MDA-MB-231 tumor xenografts shows significant inhibition of tumor growth. There were 10 mice per group and bars are S.E. of the mean. * p = < 0.05 and ** p = <0.01 compared to control mice. MDA-MB-231 xenografts (~ 250 $mm^3$) were also collected at 1 and 4 hr after a single intraperitoneal dose of TDZD-8 of 12 mg/kg, or 4 hr after the last of 5 daily doses (Q5D + 4), and tumor levels of lactic acid, dihydroxyacetone phosphate (DHAP) and 3 phosphoglycerate were measured. Values are the mean of 4 mice each and bars are S.E. * p = < 0.05 compared to non-treated control tumors.

**Discussion**

We initially identified a link between glycolytic gene expression and HIF-1 as a promising target with potential for development of selective inhibitors of both cancer energetics and stress survival. Of the key enzymes found in the glycolytic pathway that came out as interesting genes in the primary screen, ALDOA was selected as a gene that had a high level of selectivity for the inhibition of global HIF activity in the cell and a drug discovery effort was initiated in order to identify novel pharmacological probes of the enzyme. Combining both virtual and biochemical based high throughput screening methodologies, a putative small molecule inhibitor was identified and found to be effective in the inhibition of glycolysis, HIF activity and cell viability.

Measurement of extracellular flux and the corresponding ECAR by Seahorse ® technology was used as a proxy for lactate production was a key first glimpse into TDZD-8's activity as a potent inhibitor of both the basal and maximal glycolytic rates in cancer cells. Taking the analysis of glycolysis inhibition a step further, GC/MS was employed to investigate the effect that TDZD-8 treatment had on pool sizes of key glycolytic intermediates (like DHAP, the main product of Aldolase activity) relative to untreated cells and found evidence that the small molecule inhibitor was indeed interfering with cellular glycolytic function.

Much like the effects that were observed in siRNA mediated functional genomics studies putative small molecule inhibitors identified in the high throughput screen were also tested for their ability to inhibit cell viability and global HIF activity. The combination of the XTT viability assay and in-house HRE luciferase activity was again used to identify inhibitors of these key cellular processes and, as suspected based on the profound level of glycolysis inhibition observed in a range of assays, TDZD-8 was identified as a key inhibitor; these results confirmed the findings discussed previously regarding the interplay between Aldolase and normal HIF function and, through validation of the findings in a panel of cell lines, this small molecule was selected as a useful tool compound for future studies.

Finally, the validation of the overall findings in each of the *in vitro* experiments mentioned above was carried forward into the same murine model used for shALDOA studies mentioned earlier. Intraperitoneal administration of TDZD-8 into these mice had the clear effect of recapitulating the anti-tumor activity of ALDOA knockdown by induced shRNA with the added evidence of 3PG, DHAP and lactate production inhibition following GC/MS analysis.

Taken together, these findings suggest that the careful design of high throughput screening methodologies through the use of either virtual or *in vitro* platforms followed by selection of promising inhibitors identified using these assays has yielded a promising small molecule inhibitor of cancer cell metabolism, stress survival mechanisms, and ultimately tumor development and progression.

# Chapter 4: Summary and Future Directions

Solid tumors present researchers with a very unique set of hurdles during the drug development process which must be encountered and navigated when considering the specific needs in the design of a targeted therapy. Normal glycolytic function is a critical means for tumors to generate much needed energy in the form of ATP for the development of new biomass as the rapidly dividing cells found within the tumor microenvironment expand [5, 120]. Because of this rapid expansion of the cells which form them, solid tumors typically outgrow a normal vasculature and, therefore, possess poorly organized blood vessels that are often described as having erratic and chaotic branching structures [121]. This results in the possible separation from functional blood vessels and, subsequently, a hypoxic environment which is inherently stressful to normal cells while heavily favoring tumor growth [21-23]. Unlike normal cells, a cancer cell's ability to survive the stress associated with a hypoxic environment is ultimately attributed to the expression of the hypoxia inducible transcription factors HIF-1 and 2 [24, 25] and the cascade of enhanced expression of a range of survival genes which are associated with their activity. Because of their critical functions, both have been extensively studied as possible therapeutic targets as means to inhibit tumor growth and cancer cell survival [7, 56, 60, 92, 122-125]. Although many attempts have been made to identify HIF specific inhibitors through a variety of mechanisms (inhibition of HIF-1 protein synthesis [126] and stabilization [127], the transactivation of HIF target genes [128] and even its translocation into the nucleus [129]), drug development attempts in this realm have ultimately fallen short. Through the execution of this work we are now able to report that because of the previously unknown feed forward relationship between glycolysis and HIF activity as a transcription factor, we have uncovered a novel target for the inhibition of tumor growth.

**Future Directions: Glycolytic Regulation of HIF Activity**

While the finding that there is a clear relationship between ALDOA inhibition and the reduction in cellular glycolysis and HIF activity is an interesting one, there are additional

experiments that could be conducted in order to further solidify the proposed mechanism of this regulation and further understand the molecular basis for this regulation.

First, in **Chapter 1** I outline the fact that AMPK activation following ALDOA knockdown leads to the phosphorylation of the p300/CREB binding protein [91]. The subsequent deactivation of its transcriptional activity can be attributed to the loss of HIF function without the loss of HIF protein expression, a result which we saw in a number of cell lines. As a possible confirmatory study, site directed mutagenesis could be employed to investigate the relationship between p300 phosphorylation and the ALDOA/HIF feed forward loop. Since we argue here that phosphorylation at Ser89 is a critical step in the dissociation of HIF and its critical co-activator, mutation of this key residue and overexpression in various cell lines would confirm this finding following knockdown of glycolytic enzymes as previously described. Following ALDOA inhibition using this model, Ser89 mutation should result in a rescue of HIF activity in the cell and could be measured using a number of the assays described here including HRE-luciferase activity and loss of HIF binding in the EMSA assay.

Second, although we see very little effect of glycolytic enzyme knockdown in cancer cells following treatment with normoxic conditions, it would be interesting to investigate the effects with both siRNA mediated and putative small molecule inhibitor mediated inhibition of ALDOA activity in normal cells. That said, through the use of available cell lines such as mouse embryonic fibroblasts (3T3) or immortalized human fibroblasts, for instance, the effect of ALDOA inhibition could be further investigated as a means to selectively disrupt cancer cell proliferation while also generating only minimal toxicity in otherwise normal cells and minimal side effects compared to traditional therapies in patients. We assume that because of the profound differences between cancer and normal cell metabolic pathways of choice that the use of normoxic cancer cells in these assays would be proof enough that this kind of novel therapy would avoid such toxicity to healthy tissue but the presence of additional genetic confounders between the cell populations may warrant additional consideration.

**Future Directions: TDZD-8 and Analogs' Mechanism of Action**

In chapter 3, the effects of siRNA mediated ALDOA deletion were recapitulated with a small molecule inhibitor identified from a high throughput *in vitro* small molecule screen with clear effects on the inhibition of cellular glycolysis and HIF function as well as antitumor activity in mice.

Despite this fact, the experiments with TDZD-8 do not necessarily point to a clear inhibition of ALDOA activity *in vivo*. As noted, TDZD-8 was initially marketed as a GSK-3β inhibitor [116] so a clear demonstration of ALDOA inhibition in tumors may be critical. In order to accomplish this, it would be interesting to again employ site directed mutagenesis studies at the two key cysteine residues mentioned previously (Cys239 and Cys289). Generation of Cys289Ala mutants and the more conservative mutant, Cys289Ser, for comparison will allow for multifaceted follow-up work; while the substitution of cysteine by alanine would offer a non-polar alternative thus eliminating the possible interaction with TDZD-8, the serine substitution and possible participation of this residue in hydrogen bonding would be preserved. Establishing cell lines which express these mutated proteins will provide the tools to carry out several forms of confirmatory studies. First, the *in vitro* treatment of several cell lines harboring these mutant ALDOA proteins with TDZD-8 will provide an early assessment of the drug's activity as it specifically relates to this suspected critical residue. Additionally, the broader applicability of the inhibitor in tumors could be established by using several cell lines both with and without the ALDOA mutations by painting a more complete picture using orthotopic models with other cancer cell lines.

Carrying this exciting new inhibitor forward, SAR studies with analogs could provide additional insight into its mechanism of action and possible ways to improve the efficacy. This will also require these agents to acceptable pharmacokinetic and pharmacodynamic properties thus requiring additional modifications to this tool compound's structure. Should these initial challenges be overcome, however, the inhibition of Aldolase activity could emerge as an

exciting novel therapeutic option for patients without the typical side effects associated with traditional chemotherapeutic agents.

**Summary**

The overarching goal for modern translational research efforts is the design of new agents and therapeutic strategies for the inhibition of cancer specific targets in order to spare healthy tissue and avoid toxicities associated with a lower quality of life for patients undergoing treatment. Despite years of ongoing research surrounding gene and protein expression similarities and differences between cancers and normal tissue, the wide range of targets and the heterogeneity found from one individual to the next has confounded even the best attempts at new inhibitors and therapies. As I have discussed here, the use of high throughput screening methodologies in carefully designed assays has led to the identification of a novel interplay between cancer cell metabolism and the transcriptional activity of the hypoxia inducible factor and, as a result, a new therapeutic target has been identified. With a new small molecule inhibitor currently in preclinical investigation, the value of the combination of basic research, computational biology, chemistry and pharmaceutical design found within an experimental therapeutics program is clear. The collective knowledge from each of these realms contributed to the development of a novel tool compound with great potential for an eventual impactful clinical therapy.

## References


1. Kim, J.W., K.I. Zeller, Y. Wang, A.G. Jegga, B.J. Aronow, K.A. O'Donnell and C.V. Dang, *Evaluation of myc E-box phylogenetic footprints in glycolytic genes by chromatin immunoprecipitation assays.* Mol Cell Biol, 2004. **24**(13): p. 5923-36.
2. Vander Heiden, M.G., L.C. Cantley and C.B. Thompson, *Understanding the Warburg effect: the metabolic requirements of cell proliferation.* Science, 2009. **324**(5930): p. 1029-33.
3. Yeung, S.J., J. Pan and M.H. Lee, *Roles of p53, MYC and HIF-1 in regulating glycolysis - the seventh hallmark of cancer.* Cell Mol Life Sci, 2008. **65**(24): p. 3981-99.
4. Lum, J.J., T. Bui, M. Gruber, J.D. Gordan, R.J. DeBerardinis, K.L. Covello, M.C. Simon and C.B. Thompson, *The transcription factor HIF-1alpha plays a critical role in the growth factor-dependent regulation of both aerobic and anaerobic glycolysis.* Genes Dev, 2007. **21**(9): p. 1037-49.
5. Garber, K., *Energy deregulation: licensing tumors to grow.* Science, 2006. **312**(5777): p. 1158-9.
6. Warburg, O., *On the origin of cancer cells.* Science, 1956. **123**(3191): p. 309-14.
7. Jang, M., S.S. Kim and J. Lee, *Cancer cell metabolism: implications for therapeutic targets.* Exp Mol Med, 2013. **45**: p. e45.
8. Fantin, V.R., J. St-Pierre and P. Leder, *Attenuation of LDH-A expression uncovers a link between glycolysis, mitochondrial physiology, and tumor maintenance.* Cancer Cell, 2006. **9**(6): p. 425-34.
9. Zheng, J., *Energy metabolism of cancer: Glycolysis versus oxidative phosphorylation (Review).* Oncol Lett, 2012. **4**(6): p. 1151-1157.
10. Wood, I.S., B. Wang, S. Lorente-Cebrian and P. Trayhurn, *Hypoxia increases expression of selective facilitative glucose transporters (GLUT) and 2-deoxy-D-glucose uptake in human adipocytes.* Biochem Biophys Res Commun, 2007. **361**(2): p. 468-73.
11. Calvo, M.B., A. Figueroa, E.G. Pulido, R.G. Campelo and L.A. Aparicio, *Potential role of sugar transporters in cancer and their relationship with anticancer therapy.* Int J Endocrinol, 2010. **2010**.
12. Kinahan, P.E., R.K. Doot, M. Wanner-Roybal, L.M. Bidaut, S.G. Armato, C.R. Meyer and G. McLennan, *PET/CT Assessment of Response to Therapy: Tumor Change Measurement, Truth Data, and Error.* Transl Oncol, 2009. **2**(4): p. 223-30.
13. Zhu, A., D. Lee and H. Shim, *Metabolic positron emission tomography imaging in cancer detection and therapy response.* Semin Oncol, 2011. **38**(1): p. 55-69.
14. Quon, M.J., H. Chen, B.L. Ing, M.L. Liu, M.J. Zarnowski, K. Yonezawa, M. Kasuga, S.W. Cushman and S.I. Taylor, *Roles of 1-phosphatidylinositol 3-kinase and ras in regulating translocation of GLUT4 in transfected rat adipose cells.* Mol Cell Biol, 1995. **15**(10): p. 5403-11.
15. Morani, F., L. Pagano, F. Prodam, G. Aimaretti and C. Isidoro, *Loss of expression of the oncosuppressor PTEN in thyroid incidentalomas associates with GLUT1 plasmamembrane expression.* Panminerva Med, 2012. **54**(2): p. 59-63.
16. Shim, H., C. Dolde, B.C. Lewis, C.S. Wu, G. Dang, R.A. Jungmann, R. Dalla-Favera and C.V. Dang, *c-Myc transactivation of LDH-A: implications for tumor metabolism and growth.* Proc Natl Acad Sci U S A, 1997. **94**(13): p. 6658-63.

17. Gordan, J.D., C.B. Thompson and M.C. Simon, *HIF and c-Myc: sibling rivals for control of cancer cell metabolism and proliferation.* Cancer Cell, 2007. **12**(2): p. 108-13.
18. Ying, H., A.C. Kimmelman, C.A. Lyssiotis, S. Hua, G.C. Chu, E. Fletcher-Sananikone, J.W. Locasale, J. Son, H. Zhang, J.L. Coloff, H. Yan, W. Wang, S. Chen, A. Viale, H. Zheng, J.H. Paik, C. Lim, A.R. Guimaraes, E.S. Martin, J. Chang, A.F. Hezel, S.R. Perry, J. Hu, B. Gan, Y. Xiao, J.M. Asara, R. Weissleder, Y.A. Wang, L. Chin, L.C. Cantley and R.A. DePinho, *Oncogenic Kras maintains pancreatic tumors through regulation of anabolic glucose metabolism.* Cell, 2012. **149**(3): p. 656-70.
19. Bryant, K.L., J.D. Mancias, A.C. Kimmelman and C.J. Der, *KRAS: feeding pancreatic cancer proliferation.* Trends Biochem Sci, 2014. **39**(2): p. 91-100.
20. Matoba, S., J.G. Kang, W.D. Patino, A. Wragg, M. Boehm, O. Gavrilova, P.J. Hurley, F. Bunz and P.M. Hwang, *p53 regulates mitochondrial respiration.* Science, 2006. **312**(5780): p. 1650-3.
21. Vaupel, P., *Tumor microenvironmental physiology and its implications for radiation oncology.* Semin Radiat Oncol, 2004. **14**(3): p. 198-206.
22. Kumagai, Y., M. Toi and H. Inoue, *Dynamism of tumour vasculature in the early phase of cancer progression: outcomes from oesophageal cancer research.* Lancet Oncol, 2002. **3**(10): p. 604-10.
23. Dewhirst, M.W., H. Kimura, S.W. Rehmus, R.D. Braun, D. Papahadjopoulos, K. Hong and T.W. Secomb, *Microvascular studies on the origins of perfusion-limited hypoxia.* Br J Cancer Suppl, 1996. **27**: p. S247-51.
24. Semenza, G.L., *HIF-1 mediates metabolic responses to intratumoral hypoxia and oncogenic mutations.* J Clin Invest, 2013. **123**(9): p. 3664-71.
25. Wang, G.L., B.H. Jiang, E.A. Rue and G.L. Semenza, *Hypoxia-inducible factor 1 is a basic-helix-loop-helix-PAS heterodimer regulated by cellular O2 tension.* Proc Natl Acad Sci U S A, 1995. **92**(12): p. 5510-4.
26. Kelly, B.D., S.F. Hackett, K. Hirota, Y. Oshima, Z. Cai, S. Berg-Dixon, A. Rowan, Z. Yan, P.A. Campochiaro and G.L. Semenza, *Cell type-specific regulation of angiogenic growth factor gene expression and induction of angiogenesis in nonischemic tissue by a constitutively active form of hypoxia-inducible factor 1.* Circ Res, 2003. **93**(11): p. 1074-81.
27. Hu, C.J., L.Y. Wang, L.A. Chodosh, B. Keith and M.C. Simon, *Differential roles of hypoxia-inducible factor 1alpha (HIF-1alpha) and HIF-2alpha in hypoxic gene regulation.* Mol Cell Biol, 2003. **23**(24): p. 9361-74.
28. Manalo, D.J., A. Rowan, T. Lavoie, L. Natarajan, B.D. Kelly, S.Q. Ye, J.G. Garcia and G.L. Semenza, *Transcriptional regulation of vascular endothelial cell responses to hypoxia by HIF-1.* Blood, 2005. **105**(2): p. 659-69.
29. Marin-Hernandez, A., J.C. Gallardo-Perez, S.J. Ralph, S. Rodriguez-Enriquez and R. Moreno-Sanchez, *HIF-1alpha modulates energy metabolism in cancer cells by inducing over-expression of specific glycolytic isoforms.* Mini Rev Med Chem, 2009. **9**(9): p. 1084-101.
30. Lu, C.W., S.C. Lin, K.F. Chen, Y.Y. Lai and S.J. Tsai, *Induction of pyruvate dehydrogenase kinase-3 by hypoxia-inducible factor-1 promotes metabolic switch and drug resistance.* J Biol Chem, 2008. **283**(42): p. 28106-14.
31. Hingorani, S.R., L. Wang, A.S. Multani, C. Combs, T.B. Deramaudt, R.H. Hruban, A.K. Rustgi, S. Chang and D.A. Tuveson, *Trp53R172H and KrasG12D cooperate to promote*

*chromosomal instability and widely metastatic pancreatic ductal adenocarcinoma in mice.* Cancer Cell, 2005. **7**(5): p. 469-83.
32. Pelicano, H., D.S. Martin, R.H. Xu and P. Huang, *Glycolysis inhibition for anticancer treatment.* Oncogene, 2006. **25**(34): p. 4633-46.
33. Ganapathy-Kanniappan, S. and J.F. Geschwind, *Tumor glycolysis as a target for cancer therapy: progress and prospects.* Mol Cancer, 2013. **12**: p. 152.
34. Neuzil, J., M. Tomasetti, Y. Zhao, L.F. Dong, M. Birringer, X.F. Wang, P. Low, K. Wu, B.A. Salvatore and S.J. Ralph, *Vitamin E analogs, a novel group of "mitocans," as anticancer agents: the importance of being redox-silent.* Mol Pharmacol, 2007. **71**(5): p. 1185-99.
35. Kim, W., J.H. Yoon, J.M. Jeong, G.J. Cheon, T.S. Lee, J.I. Yang, S.C. Park and H.S. Lee, *Apoptosis-inducing antitumor efficacy of hexokinase II inhibitor in hepatocellular carcinoma.* Mol Cancer Ther, 2007. **6**(9): p. 2554-62.
36. Clem, B., S. Telang, A. Clem, A. Yalcin, J. Meier, A. Simmons, M.A. Rasku, S. Arumugam, W.L. Dean, J. Eaton, A. Lane, J.O. Trent and J. Chesney, *Small-molecule inhibition of 6-phosphofructo-2-kinase activity suppresses glycolytic flux and tumor growth.* Mol Cancer Ther, 2008. **7**(1): p. 110-20.
37. Cao, X., M. Bloomston, T. Zhang, W.L. Frankel, G. Jia, B. Wang, N.C. Hall, R.M. Koch, H. Cheng, M.V. Knopp and D. Sun, *Synergistic antipancreatic tumor effect by simultaneously targeting hypoxic cancer cells with HSP90 inhibitor and glycolysis inhibitor.* Clin Cancer Res, 2008. **14**(6): p. 1831-9.
38. Barban, S. and H.O. Schulze, *The effects of 2-deoxyglucose on the growth and metabolism of cultured human cells.* J Biol Chem, 1961. **236**: p. 1887-90.
39. Aghaee, F., J. Pirayesh Islamian and B. Baradaran, *Enhanced radiosensitivity and chemosensitivity of breast cancer cells by 2-deoxy-d-glucose in combination therapy.* J Breast Cancer, 2012. **15**(2): p. 141-7.
40. Dwarakanath, B. and V. Jain, *Targeting glucose metabolism with 2-deoxy-D-glucose for improving cancer therapy.* Future Oncol, 2009. **5**(5): p. 581-5.
41. Nakano, A., H. Miki, S. Nakamura, T. Harada, A. Oda, H. Amou, S. Fujii, K. Kagawa, K. Takeuchi, S. Ozaki, T. Matsumoto and M. Abe, *Up-regulation of hexokinaseII in myeloma cells: targeting myeloma cells with 3-bromopyruvate.* J Bioenerg Biomembr, 2012. **44**(1): p. 31-8.
42. Cardaci, S., E. Desideri and M.R. Ciriolo, *Targeting aerobic glycolysis: 3-bromopyruvate as a promising anticancer drug.* J Bioenerg Biomembr, 2012. **44**(1): p. 17-29.
43. Jae, H.J., J.W. Chung, H.S. Park, M.J. Lee, K.C. Lee, H.C. Kim, J.H. Yoon, H. Chung and J.H. Park, *The antitumor effect and hepatotoxicity of a hexokinase II inhibitor 3-bromopyruvate: in vivo investigation of intraarterial administration in a rabbit VX2 hepatoma model.* Korean J Radiol, 2009. **10**(6): p. 596-603.
44. Madhok, B.M., S. Yeluri, S.L. Perry, T.A. Hughes and D.G. Jayne, *Dichloroacetate induces apoptosis and cell-cycle arrest in colorectal cancer cells.* Br J Cancer, 2010. **102**(12): p. 1746-52.
45. Kaufmann, P., K. Engelstad, Y. Wei, S. Jhung, M.C. Sano, D.C. Shungu, W.S. Millar, X. Hong, C.L. Gooch, X. Mao, J.M. Pascual, M. Hirano, P.W. Stacpoole, S. DiMauro and D.C. De Vivo, *Dichloroacetate causes toxic neuropathy in MELAS: a randomized, controlled clinical trial.* Neurology, 2006. **66**(3): p. 324-30.

46. Koh, M.Y. and G. Powis, *Passing the baton: the HIF switch.* Trends Biochem Sci, 2012. **37**(9): p. 364-72.
47. Ohh, M., C.W. Park, M. Ivan, M.A. Hoffman, T.Y. Kim, L.E. Huang, N. Pavletich, V. Chau and W.G. Kaelin, *Ubiquitination of hypoxia-inducible factor requires direct binding to the beta-domain of the von Hippel-Lindau protein.* Nat Cell Biol, 2000. **2**(7): p. 423-7.
48. Maxwell, P.H., C.W. Pugh and P.J. Ratcliffe, *Activation of the HIF pathway in cancer.* Curr Opin Genet Dev, 2001. **11**(3): p. 293-9.
49. Zhong, H., A.M. De Marzo, E. Laughner, M. Lim, D.A. Hilton, D. Zagzag, P. Buechler, W.B. Isaacs, G.L. Semenza and J.W. Simons, *Overexpression of hypoxia-inducible factor 1alpha in common human cancers and their metastases.* Cancer Res, 1999. **59**(22): p. 5830-5.
50. Seeber, L.M., R.P. Zweemer, R.H. Verheijen and P.J. van Diest, *Hypoxia-inducible factor-1 as a therapeutic target in endometrial cancer management.* Obstet Gynecol Int, 2010. **2010**: p. 580971.
51. Welsh, S., R. Williams, L. Kirkpatrick, G. Paine-Murrieta and G. Powis, *Antitumor activity and pharmacodynamic properties of PX-478, an inhibitor of hypoxia-inducible factor-1alpha.* Mol Cancer Ther, 2004. **3**(3): p. 233-44.
52. Kajita, E., J. Moriwaki, H. Yatsuki, K. Hori, K. Miura, M. Hirai and K. Shiokawa, *Quantitative expression studies of aldolase A, B and C genes in developing embryos and adult tissues of Xenopus laevis.* Mech Dev, 2001. **102**(1-2): p. 283-7.
53. Asaka, M., T. Kimura, T. Meguro, M. Kato, M. Kudo, T. Miyazaki and E. Alpert, *Alteration of aldolase isozymes in serum and tissues of patients with cancer and other diseases.* J Clin Lab Anal, 1994. **8**(3): p. 144-8.
54. Hu, J., J.W. Locasale, J.H. Bielas, J. O'Sullivan, K. Sheahan, L.C. Cantley, M.G. Vander Heiden and D. Vitkup, *Heterogeneity of tumor-induced gene expression changes in the human metabolic network.* Nat Biotechnol, 2013. **31**(6): p. 522-9.
55. Kusakabe, T., K. Motoki and K. Hori, *Human aldolase C: characterization of the recombinant enzyme expressed in Escherichia coli.* J Biochem, 1994. **115**(6): p. 1172-7.
56. Zhao, Y., E.B. Butler and M. Tan, *Targeting cellular metabolism to improve cancer therapeutics.* Cell Death Dis, 2013. **4**: p. e532.
57. Du, S., Z. Guan, L. Hao, Y. Song, L. Wang, L. Gong, L. Liu, X. Qi, Z. Hou and S. Shao, *Fructose-bisphosphate aldolase a is a potential metastasis-associated marker of lung squamous cell carcinoma and promotes lung cell tumorigenesis and migration.* PLoS One, 2014. **9**(1): p. e85804.
58. Ritterson Lew, C. and D.R. Tolan, *Aldolase sequesters WASP and affects WASP/Arp2/3-stimulated actin dynamics.* J Cell Biochem, 2013. **114**(8): p. 1928-39.
59. Kim, J.H., S. Lee, J.H. Kim, T.G. Lee, M. Hirata, P.G. Suh and S.H. Ryu, *Phospholipase D2 directly interacts with aldolase via Its PH domain.* Biochemistry, 2002. **41**(10): p. 3414-21.
60. Granchi, C. and F. Minutolo, *Anticancer agents that counteract tumor glycolysis.* ChemMedChem, 2012. **7**(8): p. 1318-50.
61. Blum, R. and Y. Kloog, *Metabolism addiction in pancreatic cancer.* Cell Death Dis, 2014. **5**: p. e1065.
62. di Magliano, M.P. and C.D. Logsdon, *Roles for KRAS in pancreatic tumor development and progression.* Gastroenterology, 2013. **144**(6): p. 1220-9.

63. van Vugt, M.A., A.K. Gardino, R. Linding, G.J. Ostheimer, H.C. Reinhardt, S.E. Ong, C.S. Tan, H. Miao, S.M. Keezer, J. Li, T. Pawson, T.A. Lewis, S.A. Carr, S.J. Smerdon, T.R. Brummelkamp and M.B. Yaffe, *A mitotic phosphorylation feedback network connects Cdk1, Plk1, 53BP1, and Chk2 to inactivate the G(2)/M DNA damage checkpoint.* PLoS Biol, 2010. **8**(1): p. e1000287.
64. Reynolds, A., E.M. Anderson, A. Vermeulen, Y. Fedorov, K. Robinson, D. Leake, J. Karpilow, W.S. Marshall and A. Khvorova, *Induction of the interferon response by siRNA is cell type- and duplex length-dependent.* RNA, 2006. **12**(6): p. 988-93.
65. Claerhout, S., B. Dutta, W. Bossuyt, F. Zhang, C. Nguyen-Charles, J.B. Dennison, Q. Yu, S. Yu, G. Balazsi, Y. Lu and G.B. Mills, *Abortive autophagy induces endoplasmic reticulum stress and cell death in cancer cells.* PLoS One, 2012. **7**(6): p. e39400.
66. Sharp, D.J., K.L. McDonald, H.M. Brown, H.J. Matthies, C. Walczak, R.D. Vale, T.J. Mitchison and J.M. Scholey, *The bipolar kinesin, KLP61F, cross-links microtubules within interpolar microtubule bundles of Drosophila embryonic mitotic spindles.* J Cell Biol, 1999. **144**(1): p. 125-38.
67. Sussman, J.L., D. Lin, J. Jiang, N.O. Manning, J. Prilusky, O. Ritter and E.E. Abola, *Protein Data Bank (PDB): database of three-dimensional structural information of biological macromolecules.* Acta Crystallogr D Biol Crystallogr, 1998. **54**(Pt 6 Pt 1): p. 1078-84.
68. Dalby, A., Z. Dauter and J.A. Littlechild, *Crystal structure of human muscle aldolase complexed with fructose 1,6-bisphosphate: mechanistic implications.* Protein Sci, 1999. **8**(2): p. 291-7.
69. Verdonk, M.L., J.C. Cole, M.J. Hartshorn, C.W. Murray and R.D. Taylor, *Improved protein-ligand docking using GOLD.* Proteins, 2003. **52**(4): p. 609-23.
70. Racker, E., *Spectrophotometric measurement of hexokinase and phosphohexokinase activity.* J Biol Chem, 1947. **167**(3): p. 843-54.
71. Congreve, M., R. Carr, C. Murray and H. Jhoti, *A 'rule of three' for fragment-based lead discovery?* Drug Discov Today, 2003. **8**(19): p. 876-7.
72. Foty, R., *A simple hanging drop cell culture protocol for generation of 3D spheroids.* J Vis Exp, 2011(51).
73. Kabsch, W., *Xds.* Acta Crystallogr D Biol Crystallogr, 2010. **66**(Pt 2): p. 125-32.
74. Collaborative Computational Project, N., *The CCP4 suite: programs for protein crystallography.* Acta Crystallogr D Biol Crystallogr, 1994. **50**(Pt 5): p. 760-3.
75. McCoy, A.J., R.W. Grosse-Kunstleve, P.D. Adams, M.D. Winn, L.C. Storoni and R.J. Read, *Phaser crystallographic software.* J Appl Crystallogr, 2007. **40**(Pt 4): p. 658-674.
76. Murshudov, G.N., A.A. Vagin and E.J. Dodson, *Refinement of macromolecular structures by the maximum-likelihood method.* Acta Crystallogr D Biol Crystallogr, 1997. **53**(Pt 3): p. 240-55.
77. Emsley, P. and K. Cowtan, *Coot: model-building tools for molecular graphics.* Acta Crystallogr D Biol Crystallogr, 2004. **60**(Pt 12 Pt 1): p. 2126-32.
78. Chen, J.J., *Key aspects of analyzing microarray gene-expression data.* Pharmacogenomics, 2007. **8**(5): p. 473-82.
79. Carthew, R.W. and E.J. Sontheimer, *Origins and Mechanisms of miRNAs and siRNAs.* Cell, 2009. **136**(4): p. 642-55.
80. Hammond, S.M., *Dicing and slicing: the core machinery of the RNA interference pathway.* FEBS Lett, 2005. **579**(26): p. 5822-9.

81. Doench, J.G., C.P. Petersen and P.A. Sharp, *siRNAs can function as miRNAs.* Genes Dev, 2003. **17**(4): p. 438-42.
82. Lee, M., J.T. Hwang, H.J. Lee, S.N. Jung, I. Kang, S.G. Chi, S.S. Kim and J. Ha, *AMP-activated protein kinase activity is critical for hypoxia-inducible factor-1 transcriptional activity and its target gene expression under hypoxic conditions in DU145 cells.* J Biol Chem, 2003. **278**(41): p. 39653-61.
83. Laderoute, K.R., K. Amin, J.M. Calaoagan, M. Knapp, T. Le, J. Orduna, M. Foretz and B. Viollet, *5'-AMP-activated protein kinase (AMPK) is induced by low-oxygen and glucose deprivation conditions found in solid-tumor microenvironments.* Mol Cell Biol, 2006. **26**(14): p. 5336-47.
84. Lando, D., D.J. Peet, J.J. Gorman, D.A. Whelan, M.L. Whitelaw and R.K. Bruick, *FIH-1 is an asparaginyl hydroxylase enzyme that regulates the transcriptional activity of hypoxia-inducible factor.* Genes Dev, 2002. **16**(12): p. 1466-71.
85. Mahon, P.C., K. Hirota and G.L. Semenza, *FIH-1: a novel protein that interacts with HIF-1alpha and VHL to mediate repression of HIF-1 transcriptional activity.* Genes Dev, 2001. **15**(20): p. 2675-86.
86. Shaw, R.J., M. Kosmatka, N. Bardeesy, R.L. Hurley, L.A. Witters, R.A. DePinho and L.C. Cantley, *The tumor suppressor LKB1 kinase directly activates AMP-activated kinase and regulates apoptosis in response to energy stress.* Proc Natl Acad Sci U S A, 2004. **101**(10): p. 3329-35.
87. Woods, A., S.R. Johnstone, K. Dickerson, F.C. Leiper, L.G. Fryer, D. Neumann, U. Schlattner, T. Wallimann, M. Carlson and D. Carling, *LKB1 is the upstream kinase in the AMP-activated protein kinase cascade.* Curr Biol, 2003. **13**(22): p. 2004-8.
88. Hawley, S.A., M. Davison, A. Woods, S.P. Davies, R.K. Beri, D. Carling and D.G. Hardie, *Characterization of the AMP-activated protein kinase kinase from rat liver and identification of threonine 172 as the major site at which it phosphorylates AMP-activated protein kinase.* J Biol Chem, 1996. **271**(44): p. 27879-87.
89. Hawley, S.A., J. Boudeau, J.L. Reid, K.J. Mustard, L. Udd, T.P. Makela, D.R. Alessi and D.G. Hardie, *Complexes between the LKB1 tumor suppressor, STRAD alpha/beta and MO25 alpha/beta are upstream kinases in the AMP-activated protein kinase cascade.* J Biol, 2003. **2**(4): p. 28.
90. Hardie, D.G., *AMP-activated protein kinase: an energy sensor that regulates all aspects of cell function.* Genes Dev, 2011. **25**(18): p. 1895-908.
91. Zhang, Y., J. Qiu, X. Wang, Y. Zhang and M. Xia, *AMP-activated protein kinase suppresses endothelial cell inflammation through phosphorylation of transcriptional coactivator p300.* Arterioscler Thromb Vasc Biol, 2011. **31**(12): p. 2897-908.
92. Ziello, J.E., I.S. Jovin and Y. Huang, *Hypoxia-Inducible Factor (HIF)-1 regulatory pathway and its potential for therapeutic intervention in malignancy and ischemia.* Yale J Biol Med, 2007. **80**(2): p. 51-60.
93. Yang, W., Y.H. Hong, X.Q. Shen, C. Frankowski, H.S. Camp and T. Leff, *Regulation of transcription by AMP-activated protein kinase: phosphorylation of p300 blocks its interaction with nuclear receptors.* J Biol Chem, 2001. **276**(42): p. 38341-4.
94. Yamakawa, M., L.X. Liu, T. Date, A.J. Belanger, K.A. Vincent, G.Y. Akita, T. Kuriyama, S.H. Cheng, R.J. Gregory and C. Jiang, *Hypoxia-inducible factor-1 mediates activation of cultured vascular endothelial cells by inducing multiple angiogenic factors.* Circ Res, 2003. **93**(7): p. 664-73.

95. Dang, C.V., K.A. O'Donnell, K.I. Zeller, T. Nguyen, R.C. Osthus and F. Li, *The c-Myc target gene network.* Semin Cancer Biol, 2006. **16**(4): p. 253-64.
96. Lawlor, E.R., L. Soucek, L. Brown-Swigart, K. Shchors, C.U. Bialucha and G.I. Evan, *Reversible kinetic analysis of Myc targets in vivo provides novel insights into Myc-mediated tumorigenesis.* Cancer Res, 2006. **66**(9): p. 4591-601.
97. Staller, P., J. Sulitkova, J. Lisztwan, H. Moch, E.J. Oakeley and W. Krek, *Chemokine receptor CXCR4 downregulated by von Hippel-Lindau tumour suppressor pVHL.* Nature, 2003. **425**(6955): p. 307-11.
98. Zagzag, D., B. Krishnamachary, H. Yee, H. Okuyama, L. Chiriboga, M.A. Ali, J. Melamed and G.L. Semenza, *Stromal cell-derived factor-1alpha and CXCR4 expression in hemangioblastoma and clear cell-renal cell carcinoma: von Hippel-Lindau loss-of-function induces expression of a ligand and its receptor.* Cancer Res, 2005. **65**(14): p. 6178-88.
99. Franovic, A., L. Gunaratnam, K. Smith, I. Robert, D. Patten and S. Lee, *Translational up-regulation of the EGFR by tumor hypoxia provides a nonmutational explanation for its overexpression in human cancer.* Proc Natl Acad Sci U S A, 2007. **104**(32): p. 13092-7.
100. Lu, H., R.A. Forbes and A. Verma, *Hypoxia-inducible factor 1 activation by aerobic glycolysis implicates the Warburg effect in carcinogenesis.* J Biol Chem, 2002. **277**(26): p. 23111-5.
101. Hsieh, A.C., Y. Liu, M.P. Edlind, N.T. Ingolia, M.R. Janes, A. Sher, E.Y. Shi, C.R. Stumpf, C. Christensen, M.J. Bonham, S. Wang, P. Ren, M. Martin, K. Jessen, M.E. Feldman, J.S. Weissman, K.M. Shokat, C. Rommel and D. Ruggero, *The translational landscape of mTOR signalling steers cancer initiation and metastasis.* Nature, 2012. **485**(7396): p. 55-61.
102. Janknecht, R. and T. Hunter, *Versatile molecular glue. Transcriptional control.* Curr Biol, 1996. **6**(8): p. 951-4.
103. Oparina, N.Y., A.V. Snezhkina, A.F. Sadritdinova, V.A. Veselovskii, A.A. Dmitriev, V.N. Senchenko, N.V. Mel'nikova, A.S. Speranskaya, M.V. Darii, O.A. Stepanov, I.M. Barkhatov and A.V. Kudryavtseva, *[Differential expression of genes that encode glycolysis enzymes in kidney and lung cancer in humans].* Genetika, 2013. **49**(7): p. 814-23.
104. Szutowicz, A., J. Kwiatkowski and S. Angielski, *Lipogenetic and glycolytic enzyme activities in carcinoma and nonmalignant diseases of the human breast.* Br J Cancer, 1979. **39**(6): p. 681-7.
105. Hennipman, A., J. Smits, B. van Oirschot, J.C. van Houwelingen, G. Rijksen, J.P. Neyt, J.A. Van Unnik and G.E. Staal, *Glycolytic enzymes in breast cancer, benign breast disease and normal breast tissue.* Tumour Biol, 1987. **8**(5): p. 251-63.
106. Song, C.M., S.J. Lim and J.C. Tong, *Recent advances in computer-aided drug design.* Brief Bioinform, 2009. **10**(5): p. 579-91.
107. Ortholand, J.Y. and A. Ganesan, *Natural products and combinatorial chemistry: back to the future.* Curr Opin Chem Biol, 2004. **8**(3): p. 271-80.
108. Jones, G., P. Willett, R.C. Glen, A.R. Leach and R. Taylor, *Development and validation of a genetic algorithm for flexible docking.* J Mol Biol, 1997. **267**(3): p. 727-48.
109. Pan, L. and S.G. Aller, *Tools and procedures for visualization of proteins and other biomolecules.* Curr Protoc Mol Biol, 2015. **110**: p. 19 12 1-19 12 47.

110. Xu, W., A.J. Lucke and D.P. Fairlie, *Comparing sixteen scoring functions for predicting biological activities of ligands for protein targets.* J Mol Graph Model, 2015. **57**: p. 76-88.
111. St-Jean, M. and J. Sygusch, *Stereospecific proton transfer by a mobile catalyst in mammalian fructose-1,6-bisphosphate aldolase.* J Biol Chem, 2007. **282**(42): p. 31028-37.
112. Lorentzen, E., B. Siebers, R. Hensel and E. Pohl, *Mechanism of the Schiff base forming fructose-1,6-bisphosphate aldolase: structural analysis of reaction intermediates.* Biochemistry, 2005. **44**(11): p. 4222-9.
113. Schneider, M.L. and C.B. Post, *Solution structure of a band 3 peptide inhibitor bound to aldolase: a proposed mechanism for regulating binding by tyrosine phosphorylation.* Biochemistry, 1995. **34**(51): p. 16574-84.
114. Lipinski, C.A., F. Lombardo, B.W. Dominy and P.J. Feeney, *Experimental and computational approaches to estimate solubility and permeability in drug discovery and development settings.* Adv Drug Deliv Rev, 2001. **46**(1-3): p. 3-26.
115. Heyduk, T., R. Michalczyk and M. Kochman, *Long-range effects and conformational flexibility of aldolase.* J Biol Chem, 1991. **266**(24): p. 15650-5.
116. Collino, M., C. Thiemermann, R. Mastrocola, M. Gallicchio, E. Benetti, G. Miglio, S. Castiglia, O. Danni, O. Murch, C. Dianzani, M. Aragno and R. Fantozzi, *Treatment with the glycogen synthase kinase-3beta inhibitor, TDZD-8, affects transient cerebral ischemia/reperfusion injury in the rat hippocampus.* Shock, 2008. **30**(3): p. 299-307.
117. Dalby, A.R., D.R. Tolan and J.A. Littlechild, *The structure of human liver fructose-1,6-bisphosphate aldolase.* Acta Crystallogr D Biol Crystallogr, 2001. **57**(Pt 11): p. 1526-33.
118. Tam, T.F., R. Leung-Toung, W. Li, M. Spino and K. Karimian, *Medicinal chemistry and properties of 1,2,4-thiadiazoles.* Mini Rev Med Chem, 2005. **5**(4): p. 367-79.
119. Leung-Toung, R., J. Wodzinska, W. Li, J. Lowrie, R. Kukreja, D. Desilets, K. Karimian and T.F. Tam, *1,2,4-thiadiazole: a novel Cathepsin B inhibitor.* Bioorg Med Chem, 2003. **11**(24): p. 5529-37.
120. Guppy, M., E. Greiner and K. Brand, *The role of the Crabtree effect and an endogenous fuel in the energy metabolism of resting and proliferating thymocytes.* Eur J Biochem, 1993. **212**(1): p. 95-9.
121. Belozerov, V.E. and E.G. Van Meir, *Hypoxia inducible factor-1: a novel target for cancer therapy.* Anticancer Drugs, 2005. **16**(9): p. 901-9.
122. Cuperlovic-Culf, M., A.S. Culf, M. Touaibia and N. Lefort, *Targeting the latest hallmark of cancer: another attempt at 'magic bullet' drugs targeting cancers' metabolic phenotype.* Future Oncol, 2012. **8**(10): p. 1315-30.
123. Pili, R. and R.C. Donehower, *Is HIF-1 alpha a valid therapeutic target?* J Natl Cancer Inst, 2003. **95**(7): p. 498-9.
124. Hewitson, K.S. and C.J. Schofield, *The HIF pathway as a therapeutic target.* Drug Discov Today, 2004. **9**(16): p. 704-11.
125. Scatena, R., P. Bottoni, A. Pontoglio, L. Mastrototaro and B. Giardina, *Glycolytic enzyme inhibitors in cancer treatment.* Expert Opin Investig Drugs, 2008. **17**(10): p. 1533-45.
126. Li, J., C. Mi, J. Ma, K.S. Wang, J.J. Lee and X. Jin, *Dihydrotanshinone I inhibits the translational expression of hypoxia-inducible factor-1alpha.* Chem Biol Interact, 2015. **240**: p. 48-58.

127. Sceneay, J., M.C. Liu, A. Chen, C.S. Wong, D.D. Bowtell and A. Moller, *The antioxidant N-acetylcysteine prevents HIF-1 stabilization under hypoxia in vitro but does not affect tumorigenesis in multiple breast cancer models in vivo.* PLoS One, 2013. **8**(6): p. e66388.
128. Masoud, G.N., J. Wang, J. Chen, D. Miller and W. Li, *Design, Synthesis and Biological Evaluation of Novel HIF1alpha Inhibitors.* Anticancer Res, 2015. **35**(7): p. 3849-59.
129. Kosyna, F.K., M. Nagel, L. Kluxen, K. Kraushaar and R. Depping, *The importin alpha/beta-specific inhibitor Ivermectin affects HIF-dependent hypoxia response pathways.* Biol Chem, 2015.

## Vita

Geoffrey Voss Grandjean was born in Lake Jackson, Texas on December 15, 1984, the son of Cynthia Diane Grandjean and Brett Grandjean. After completing his work at H.H. Dow High School, Midland, Michigan in 2003, he entered Michigan State University in East Lansing, Michigan. He received the degree of Bachelor of Science with a major in medical technology and biomedical laboratory operations from Michigan State in May, 2007. For the next five years, he worked as a research technician in the Department of Experimental Therapeutics at the University of Texas MD Anderson Cancer Center. In August of 2012 he entered The University of Texas Graduate School of Biomedical Sciences at Houston to earn a degree in Experimental Therapeutics.

Permanent address:

1435 India Street, #411

San Diego, California 92101